



**CENTRO DE INVESTIGACIÓN Y DE ESTUDIOS
AVANZADOS DEL INSTITUTO POLITÉCNICO
NACIONAL**

UNIDAD ZACATENCO

DEPARTAMENTO DE BIOMEDICINA MOLECULAR

**“Participación de la proteína de unión a actina, cortactina, en la activación
de células T: implicaciones para la leucemia linfoblástica aguda tipo T”**

TESIS

Que presenta

M. en C. Ramón Castellanos Martínez

Para obtener el grado de
DOCTOR EN CIENCIAS

**EN LA ESPECIALIDAD DE
BIOMEDICINA MOLECULAR**

Director de Tesis:
Dr. Michael Schnoor

Ciudad de México

Agosto, 2022



**CENTER FOR RESEARCH AND ADVANCED
STUDIES OF THE NATIONAL POLYTECHNIC
INSTITUTE (CINVESTAV)**

ZACATENCO UNIT

DEPARTMENT OF MOLECULAR BIOMEDICINE

**“The role of the actin-binding protein cortactin in the activation of T cells:
implications for T-cell acute lymphoblastic leukemia”**

THESIS

Presented by

MSc Ramón Castellanos Martínez

To obtain the degree of

PHYLOSOPHY DOCTOR

IN THE SPECIALTY OF

MOLECULAR BIOMEDICINE

Thesis Director:

Dr. Michael Schnoor

Mexico City

August, 2022

ACKNOWLEDGEMENTS

To National Council for Science and Technology (CONACYT), for the scholarship during the period comprised 2018-2022.

To Dr. Michael Schnoor for being an excellent mentor during my PhD formation.

To my committee Dr. Rosana Pelayo, Dr. Leopoldo Santos, Dr. Vianey Ortíz, and Dr. Oscar Medina for your input to this work and all the good advice and help.

To the MVZ Ricardo Gaxiola Centeno and MVZ Benjamin Emmanuel Chávez Álvarez, and technicians Victor Manuel García Gómez and Felipe Cruz Martínez for their assistance in animal care and handling.

To my dear friends from Schnoor Lab, MSc Idaira Guerrero, MSc Karina Jimenez, MSc Iliana Leon, MSc Armando Montoya, Dr. Salvador Valle, MSc Belén, Dr. Hilda Vargas and Augusto, for your friendship and support.

To my beloved friends David, Perla, Cynthia, Karla, Tania, Valeria, Noel, Perla G., for your good vibes and wishes, even in the distance.

To my family, specially to my parents, Ramón and Olivia, for always supporting me throughout my career, thanks to them I am who I am now.

To my wife, my everything, Gabriela Osuna, for always having my back.

INDEX

ABBREVIATIONS	iv
LIST OF FIGURES	x
LIST OF TABLES	xiii
1. RESUMEN	1
1. ABSTRACT	2
2. INTRODUCTION	3
2.1 T cell lymphocytes	3
2.2 T cell lymphopoiesis	3
2.2.1 T cell progenitors in the BM	5
2.2.2 Thymic seeding of early T cell progenitors and T cell maturation	6
2.2.3 T cell maturation in the thymus	6
2.3 T cell migration	11
2.3.1 Tethering and rolling	12
2.3.2 Adhesion	13
2.3.3 Diapedesis	15
2.4 Activation in secondary lymphoid organs and differentiation	16
2.4.1 T cell activation and formation of the immunological synapse	17
2.4.2 The proximal signaling complex	18
2.4.3 Downstream transcription factors	19
2.4.3 T cell differentiation	21
2.5 The actin cytoskeleton in T cell activation and migration	24
2.5.1 The actin-binding protein cortactin	27
2.5.2 Cortactin expression in hematopoietic cells	30
2.5.3 HS1 and cortactin in T cell activation and migration	31
2.6 Pathophysiological relevance of T cell activation in T-ALL	32
3. JUSTIFICATION	36
4. HYPOTHESIS AND AIMS	37
4.1 Hypothesis	37
4.2 General aim	37
4.2.1 Particular aims	37

5. MATERIALS AND METHODS	38
5.1 Materials	38
5.1.1 Reagents	38
5.2 Methods	45
5.2.1 Isolation of T cells from human peripheral blood	45
5.2.2 Cell culture	45
5.2.3 Flow cytometry analysis of T cells	46
5.2.4 T cell activation	46
5.2.5 Lentivirus production	47
5.2.6 Lentiviral transduction of Jurkat cells	47
5.2.7 IS formation using CD3 stimulation by FACS	48
5.2.8 Analysis of phospho-ERK by flow cytometry	48
5.2.9 Chemotaxis assay	49
5.2.10 F-actin polymerization assay by flow cytometry	49
5.2.11 RNA isolation	50
5.2.12 cDNA synthesis	50
5.2.13 End point PCR	50
5.2.14 qRT-PCR	51
5.2.15 Spheroid colonization assay	52
5.2.16 Leukemic T cell xenografts	52
5.2.17 Mice	53
5.2.18 Isolation of T cells from murine SLOs	53
5.2.19 Analysis of IS formation by IF	53
5.2.20 Adhesion assays on ICAM-1 and VCAM-1	54
5.2.21 Statistics	54
6. RESULTS	55
6.1 Cortactin is expressed in T cells	55
6.2 Molecules important for synapse formation and migration are expressed in T cells	56
6.3 Cortactin is recruited to the IS in T cells	58
6.4 Cortactin expression is upregulated in T cells upon TCR engagement, with mouse T cells switching isoforms	61
6.5 Cortactin expression is similar in CD4 ⁺ and CD8 ⁺ T cells	63

6.6 Cortactin-depleted Jurkat cells present similar expression of adhesion molecules and similar rates of proliferation and apoptosis.....	64
6.7 Cortactin-depleted Jurkat cells show reduced IL-2 mRNA transcription upon TCR engagement and impaired migration towards CXCL12 due to poor actin dynamics	67
6.8 T cell subsets in the lymph nodes, peripheral blood, spleen and in the thymus of <i>Cttn</i> ^{-/-} and <i>Cttn</i> ^{+/+} mice are similar.....	71
6.9 Homing of <i>Cttn</i> ^{-/-} CD4 ⁺ and CD8 ⁺ T lymphocytes to SLOs is reduced due to defective CXCR4 responses	73
6.10 TCR-mediated proliferation and CXCR4-mediated TCR-costimulation are impaired in <i>Cttn</i> ^{-/-} T cells	76
6.11 <i>Cttn</i> ^{-/-} T cells fail to properly polarize F-actin to the IS	80
6.12 Cortactin controls BM organoid colonization and infiltration into the CNS in a xenograft model of T-ALL	83
7. DISCUSSION	85
8. CONCLUSION	93
9. PERSPECTIVES	93
10. REFERENCES	94

ABBREVIATIONS

°C	Centigrade grades
µg	Micrograms
µL	Microliters
µm	Micrometers
µM	Micromolar
3D	3-dimensional
ABP	Actin-binding protein
ADAP	Adhesion and degranulation-promoting adapter protein
ALL	Acute lymphoblastic leukemia
APC	Allophycocyanin
APCs	Antigen-presenting cells
Arp2/3	Actin related protein 2/3 complex
B-ALL	B-cell acute lymphoblastic leukemia
B-CLL	B-cell chronic lymphocytic leukemia
BM	Bone marrow
BSA	Bovine serum albumin
CCR#	C-C motif chemokine receptor #
CCL#	C-C motif chemokine ligand #
CD#	Cluster differentiation #
cDC	Conventional dendritic cell
cDNA	Complementary DNA
CFDA,SE	Carboxifluorescein diacetate succinimidyl ester
CLP	Common lymphoid progenitor
CMP	Common myeloid progenitor
CNS	Central nervous system
CRAC	Calcium-release-activated calcium channel
CTL	CD8 ⁺ cytolytic T cells
CTLA-4	Cytotoxic T lymphocyte antigen-4
CTTN	Cortactin

CXCR#	C-X-C motif chemokine receptor #
CXCL#	C-X-C motif chemokine ligand #
DAG	Diacylglycerol
DEPC	Diethyl pyrocarbonate
DMEM	Dulbecco modified Eagle's Medium
DMSO	Dimethyl sulfoxide
DN	Double negative
DNA	Deoxyribonucleic acid
dNTPs	Deoxynucleotide triphosphate
DP	Double positive
DTT	Dithiothreitol
EC	Endothelial cells
ECGF	Endothelial cell growth factor
EDTA	Ethylenediaminetetraacetic acid
ELP	Early lymphoid progenitor
ERK	Extracellular signal-regulated kinase
ETP	Early T-cell precursor
F-actin	Filamentous actin
FBS	Fetal bovine serum
FRCs	Fibroblastic reticular cells
G-CSF	Granulocyte colony stimulating factor
GAG	Glycosaminoglycans
GAPDH	Glyceraldehyde-P-dehydrogenase
GMP	Granulocyte-monocyte progenitor
GM-CSF	Granulocyte-monocyte colony stimulating factor
GPCR	G-protein coupled receptor
GRB2	Growth-factor-receptor-bound protein-2
GADS	GRB2-related adaptor protein-2 (also known as GRAP2)
HBSS	Hank's balanced saline solution
HEPES	N-(2-Hydroxyethyl)piperazine-N'-(2-ethanesulfonic acid)
HEV	High endothelial venules

HPK1	Hematopoietic progenitor kinase 1
HRP	Horse radish peroxidase
HS1	Hematopoietic cell-specific 1
HSC	Hematopoietic stem cells
ICAM-1	Intercellular adhesion molecule-1
ID2	Inhibitor of DNA binding 2
IFN γ	Interferon- γ
IL-#	Interleukin #
ILC	Innate lymphoid cells
ILP	Invadosome-like protrusions
IP ₃	Inositol triphosphate
IS	Immunological synapse
JAM	Junctional adhesion molecule
KDa	Kilodaltons
KSL	Kit ⁺ Sca1 ⁺ Lin ⁻ fraction
LAT	Linker for activation of T cells
LCK	Lymphocyte-specific protein kinase
LFA-1	Leucocyte function-associated antigen-1
LMPP	Lymphocyte-primed MPP
LN	Lymph node
LPS	Lipopolysaccharide
LSP	Lymphocyte L-selectin-expressing progenitor
Lt α	Lymphotoxin α
M	Molar
M-CSF	Monocyte colony stimulating factor
MadCAM-1	Mucosal addressin cell adhesion molecule-1
MEK	Mitogen-activated protein kinase kinase
MEP	Megakaryocytic-erythroid progenitor
MFI	Mean fluorescence intensity
mg	Milligrams
MHC	Major histocompatibility complex

min	Minutes
mL	Milliliters
mm	Millimeters
mM	Millimolar
MMP-9	Matrix metalloproteinase-9
MPP	Multipotent progenitor
Na ₃ VO ₄	Sodium orthovanadate
NaF	Sodium fluoride
NEAA	Non-essential amino acids
NF-κB	Nuclear factor-κB
NFAT	Nuclear factor for activation of T cells
ng	Nanograms
NIH	National Institute of Health
NK	Natural killer cell
nM	Nanomolar
NPF	Nucleation promoting factor
NSG	NOD- <i>scid</i> IL2Rgamma ^{null}
NTA	N-terminal acidic domain
PB	Peripheral blood
PBS	Phosphate buffered saline
PCR	Polymerase chain reaction
pDC	Plasmacytoid dendritic cell
PE	Phycoerythrin
PECAM-1	Platelet/Endothelial cell adhesion molecule-1
PerCP	Peridinin chlorophyl
PI3K	Phosphatidylinositol-3-kinase
PKCθ	Protein kinase C θ
PLCγ1	Phospholipase C-γ1
pMBMEC	Primary mouse brain microvascular endothelial cells
PNAd	Peripheral node addressins
PRR	Proline-rich region

PSGL-1	P-selectin glycoprotein ligand-1
Pyk-2	Proline-rich tyrosine kinase-2
RAG1	Recombinase activating gene 1
RNA	Ribonucleic acid
ROI	Region of interest
ROR γ t	Retinoid acid receptor-related orphan receptor gamma-T
rpm	Revolutions per minute
RPMI	Roswell Park Memorial Institute-1640 medium
RT	Room temperature
s	Seconds
Sca-1	Stem cell antigen-1
SCID	Severe combined immunodeficiency
SDF-1 α	Stromal-derived factor-1 α
SDS	Sodium dodecyl sulfate
SEE	Staphylococcal superantigen E
SH3	Src homology 3
SHP2	SRC homology 2-domain-containing protein tyrosine phosphatase
SLO	Secondary lymphoid organ
SLP76	SCR homology-2 (SH2)-domain containing leukocyte protein of 76 KDa
SMAC	Supramolecular activation complex
SV#	Splicing variant #
T-ALL	T-cell acute lymphoblastic leukemia
TBS	Tris buffer saline
TCR	T-cell receptor
TEM	Transendothelial migration
TEMED	N,N,N',N-Tetramethylethylenediamine
TGF- β	Tumor growth factor- β
TNF- α	Tumor necrosis factor- α
TSP	Thymus-seeding progenitors
U	Units
V	Volts

VCAM-1	Vascular cell adhesion molecule-1
VLA-4	Very late antigen -1
WAVE2	WASp-family verprolin homologous protein 2
WASp	Wiskott-Aldrich Syndrome protein
WIP	WASp-interacting protein
WT	Wild type
ZAP70	ζ -chain-associated protein kinase-70

LIST OF FIGURES

- Figure 1.** Main lineage precursors in hematopoiesis.
- Figure 2.** Identity of T cell progenitors seeding the thymus.
- Figure 3.** Stages and characteristic surface markers of T-cell development in the thymus.
- Figure 4.** Early T-cell development in the thymus.
- Figure 5.** General overview of common steps that lymphocytes perform to achieve extravasation.
- Figure 6.** The conformational states of integrins.
- Figure 7.** The mature T-cell immunological synapse (IS).
- Figure 8.** Signaling pathways downstream of TCR engagement.
- Figure 9.** Different subsets of CD4⁺ T cells and their cytokine expression profile.
- Figure 10.** Signaling complex regulating F-actin dynamics during T cell activation.
- Figure 11.** Schematic representation of the cortactin gene, mRNA and protein domains.
- Figure 12.** Cortactin splice variants and their functionality.
- Figure 13.** Post-translational modifications regulate different functions of cortactin.
- Figure 14.** Cortactin is recruited to the IS and colocalizes with WASP and F-actin in T cells.
- Figure 15.** Surface expression of CXCR4 in leukemic T-cells depends on cortactin and calcineurin.
- Figure 16.** Cortactin expression in different human and murine T cells.
- Figure 17.** Expression of adhesion molecules and chemokine receptors in human T-ALL cell lines.
- Figure 18.** Expression of adhesion molecules and CXCR4 in murine T-ALL cell line 6645/4.
- Figure 19.** Cortactin colocalizes with HS1 in resting cells and is recruited to the IS.
- Figure 20.** Cortactin localizes at the IS with Jurkat cells.
- Figure 21.** Cortactin colocalizes at the cell periphery in resting cells and is recruited to the IS.
- Figure 22.** Cortactin expression increases in human and murine T cells upon activation.
- Figure 23.** Cortactin expression increases in human T cells upon activation using PMA and ionomycin.

- Figure 24.** Cortactin expression is similar in resting and activated human CD4⁺ and CD8⁺ T cells.
- Figure 25.** Characterization of cortactin-depleted Jurkat cells.
- Figure 26.** Cortactin-depleted and control Jurkat cells have similar apoptosis and proliferation rates.
- Figure 27.** Expression of adhesion molecules and CXCR4 is similar in cortactin-depleted Jurkat cells.
- Figure 28.** Cortactin-depleted Jurkat cells form similar numbers of conjugates.
- Figure 29.** Expression of IL-2 mRNA is reduced in cortactin-depleted Jurkat cells upon TCR engagement.
- Figure 30.** Early phosphorylation of ERK is similar in cortactin-depleted and control Jurkat cells upon TCR stimulation.
- Figure 31.** Cortactin-depleted Jurkat cells migrate less towards a CXCL12 gradient.
- Figure 32.** Cortactin-depleted Jurkat cells show reduced F-actin content in basal conditions and impaired actin polymerization upon TCR and CXCR4 engagement.
- Figure 33.** Expression of cortactin mRNA in CD3⁺ cells isolated from spleen of *Cttn*^{+/+} and *Cttn*^{-/-} littermates.
- Figure 34.** Thymocyte subpopulations are similar in the *Cttn*^{-/-} mice.
- Figure 35.** Analysis of B cell, T cell and monocyte populations in the LNs, spleen and peripheral blood of the *Cttn*^{-/-} mice.
- Figure 36.** CD4⁺ cell population is reduced and CD8⁺ is increased in the LNs and spleen of *Cttn*^{-/-} mice.
- Figure 37.** Characterization of the surface expression of adhesion molecules in *Cttn*^{-/-} T cells.
- Figure 38.** *Cttn*^{-/-} T cells migrate less towards CXCL12.
- Figure 39.** *Cttn*^{-/-} T cells show impaired proliferation upon TCR stimulation.
- Figure 40.** *Cttn*^{-/-} T effector cells generated with the MLR assay display normal production of cytokines and Granzyme B.
- Figure 41.** *Cttn*^{-/-} T cells induce similar upregulation of IL-2, CD25 and CD69 upon TCR engagement.
- Figure 42.** *Cttn*^{-/-} T cells fail to induce CXCR4-costimulation.
- Figure 43.** *Cttn*^{-/-} T cells show reduced number of conjugates with A20 cells.

- Figure 44.** TCR-mediated LFA-1 activation is similar in *Cttn*^{-/-} T cells.
- Figure 45.** *Cttn*^{-/-} T cells show impaired F-actin polarization at the IS.
- Figure 46.** Jurkat cells infiltrate mostly the BM and the CNS.
- Figure 47.** Infiltration of the CNS and BM is reduced in cortactin-depleted Jurkat cells.

LIST OF TABLES

Table 1. List of chemicals and reagents used in this work.

Table 2. List of antibodies used in this work.

Table 3. List of kits used in this work.

Table 4. List of culture medium used in this work.

Table 5. List of plasmids used in this work.

Table 6. List of buffers and solutions used in this work.

Table 7. Sequences of sgRNA for the generation of stable cortactin knock-down cells.

Table 8. Primer sequences used for end-point and quantitative PCR of T cells.

Table 9. Characteristics of the different T-ALL cell lines

1. RESUMEN

La cortactina es una proteína de unión a actina que se encuentra expresada de manera ubicua, con la excepción de algunas células hematopoyéticas, donde su homóloga, HS1, se encuentra altamente expresada. El papel de HS1 en la activación de células T y sus funciones efectoras ha sido ampliamente estudiado. De manera interesante, la expresión de cortactina ha sido recientemente descrita en células T normales y leucémicas, donde cortactina es reclutada hacia la sinapsis inmunológica (SI). Sin embargo, su función específica en células T no ha sido descrita. Además, la sobreexpresión de cortactina ha sido asociada con una mayor infiltración en diferentes leucemias de tipo B. Sin embargo, el papel de cortactina en la leucemia linfoblástica aguda de células T (LLA-T) no ha sido experimentalmente comprobado aún. Por lo tanto, el objetivo de este proyecto fue la caracterización sistemática de la expresión, localización y función de cortactina en células T normales y leucémicas.

En el presente trabajo, demostramos que la isoforma de 70 KDa de cortactina se encuentra expresada en células T primarias de humano y ratón, así como en diferentes líneas celulares de LLA-T en condiciones basales. Además, la expresión de cortactina fue incrementada después de la estimulación del TCR en células T humanas, mientras que las células T de ratón cambiaron a la expresión de la isoforma WT de 80 KDa de cortactina. La expresión de cortactina en linfocitos CD4⁺ y CD8⁺ de humano fue similar. También corroboramos que cortactina se recluta a la SI utilizando diferentes métodos. De manera importante, la cortactina es necesaria en la SI para una adecuada dinámica de F-actina, ya que la ausencia de cortactina redujo de manera significativa la polarización de F-actina al sitio de contacto entre las células. Así mismo, también demostramos que células T deficientes de cortactina presentaban defectos en la polimerización de actina mediada por CXCR4 y el TCR, en la migración dependiente de CXCR4, la producción de IL-2 y la proliferación dependiente del TCR. Utilizando un modelo *in vivo* de xenotrasplante, encontramos que ratones NSG inyectados con células Jurkat deficientes de cortactina desarrollaron una enfermedad menos grave, caracterizada por una reducción en el número de blastos en sangre periférica y médula ósea, comparada con ratones inyectados con células Jurkat control. De manera importante, la deficiencia de cortactina eliminó la capacidad de las células Jurkat a infiltrar al SNC. Nuestros resultados revelan un nuevo papel funcional para cortactina en la activación y migración de los linfocitos T normales, así como en la patogénesis de la LLA-T, resaltando a la cortactina como un potencial blanco terapéutico para prevenir la activación aberrante de los linfocitos T y la infiltración de órganos por células T leucémicas para un mejor control de enfermedades autoinmunes y LLA-T, respectivamente.

1. ABSTRACT

Cortactin is an actin-binding protein ubiquitously expressed, except for some hematopoietic cells, where its homolog HS1 is highly expressed. In T cells, HS1 is well known for its essential roles in regulating activation and effector functions. Surprisingly, cortactin expression has been recently also described in normal and leukemic T cells, where it is to the immunological synapse (IS). However, its specific functions in T cells remain unknown. Moreover, cortactin overexpression has been correlated with increased infiltration in different B type leukemias. However, its role in T-cell acute lymphoblastic leukemia (T-ALL) has not been experimentally tested yet. Therefore, the focus of this project was to systematically characterize the expression, localization, and function of cortactin in normal and leukemic T cells.

In this work, we demonstrated that the cortactin SV1 isoform of 70 KDa is expressed in mouse and human primary T cells, as well as in different T-ALL cell lines under basal conditions. Moreover, expression of cortactin was upregulated upon TCR engagement in human T cells, whereas mouse T cells switched the expression to the 80 kDa WT isoform of cortactin. Expression of cortactin in CD4⁺ and CD8⁺ was similar in human T cells. Using different approaches, we corroborated that cortactin is recruited to the IS upon TCR engagement. Importantly, cortactin at the IS is required for proper F-actin dynamics as cortactin-depletion significantly reduced F-actin polarization to the site of cell-cell contact. Furthermore, we also demonstrated that cortactin-deficient T cells presented defects in CXCR4- and TCR-mediated actin polymerization, CXCR4-mediated migration, and TCR-mediated IL-2 production and proliferation. Using an *in vivo* model of leukemic cell xenotransplantation, we found that NSG mice injected with cortactin-depleted Jurkat cells developed a milder disease, characterized by reduced blast counts in the peripheral blood and the bone marrow compared to mice injected with control Jurkat cells. Importantly, cortactin depletion abolished the capacity of Jurkat cells to infiltrate the CNS. Taken together, our findings unveil a novel functional role of cortactin in the activation and migration of normal T cells, as well as in the pathogenesis of T-ALL. Our data highlight cortactin as a potential pharmacological target to prevent aberrant T cell activation and organ infiltration by leukemic cells to better control autoimmune diseases and T-ALL, respectively.

2. INTRODUCTION

2.1 T cell lymphocytes

The adaptive immunity involves a highly regulated interplay between antigen-presenting cells and T and B lymphocytes¹. T cells play pivotal roles in the development of pathogen-specific immunologic effector pathways, as well as the generation of immune memory and the regulation of host immune homeostasis¹. Mature T cells are generated in the thymus under a rigorous selection process that allows for the development of several antigen receptors needed to recognize a wide array of pathogens without producing self-reactive lymphocytes^{1,2}. Moreover, T cells divide into two major subsets characterized by the expression of CD4 or CD8 adaptor molecules¹⁻³. After activation, CD4⁺ T cells can further differentiate into distinct effector populations that regulate immune responses through the secretion of specific sets of cytokines, that then regulate different processes ranging from activation of different cells including cells of the innate immune system, B cells and CD8⁺ cytotoxic cells, to the suppression of immune reactions³. On the other hand, CD8⁺ cytolytic T cells act by eliminating cells harboring intracellular pathogens such as virus or bacteria, as well as cancer cells¹. The complexity of T cell generation as well as the activation and effector functions will be discussed in the following chapters.

2.2 T cell lymphopoiesis

The entirety of the immune system emerges from hematopoietic stem cells (HSC) that reside in the bone marrow (BM)⁴ (**Figure 1**). These cells give rise to several progenitor populations with increasingly restricted lineage potential the more differentiated they become, finally generating all lineages of mature hematopoietic cells⁵. In adults, hematopoiesis takes place in the marrow of bones such as the pelvis, sternum, ribs, vertebrae and the proximal ends of humeri and femora⁶. Most of the blood cells fully develop in the BM, however, T cell maturation takes place in a specialized organ called thymus, where early T cell precursors (ETP) derived from the BM become mature, self-tolerant and functional T cells⁵. The generation of all blood cells can be traced morphologically, phenotypically, and functionally. Expression of CD34 is typically found on BM precursors from lymphoid, macrophage/granulocytic, megakaryocytic and erythroid lineages, however, co-expression of CD34 and CD2 indicates a commitment to the T cell lineage⁷.

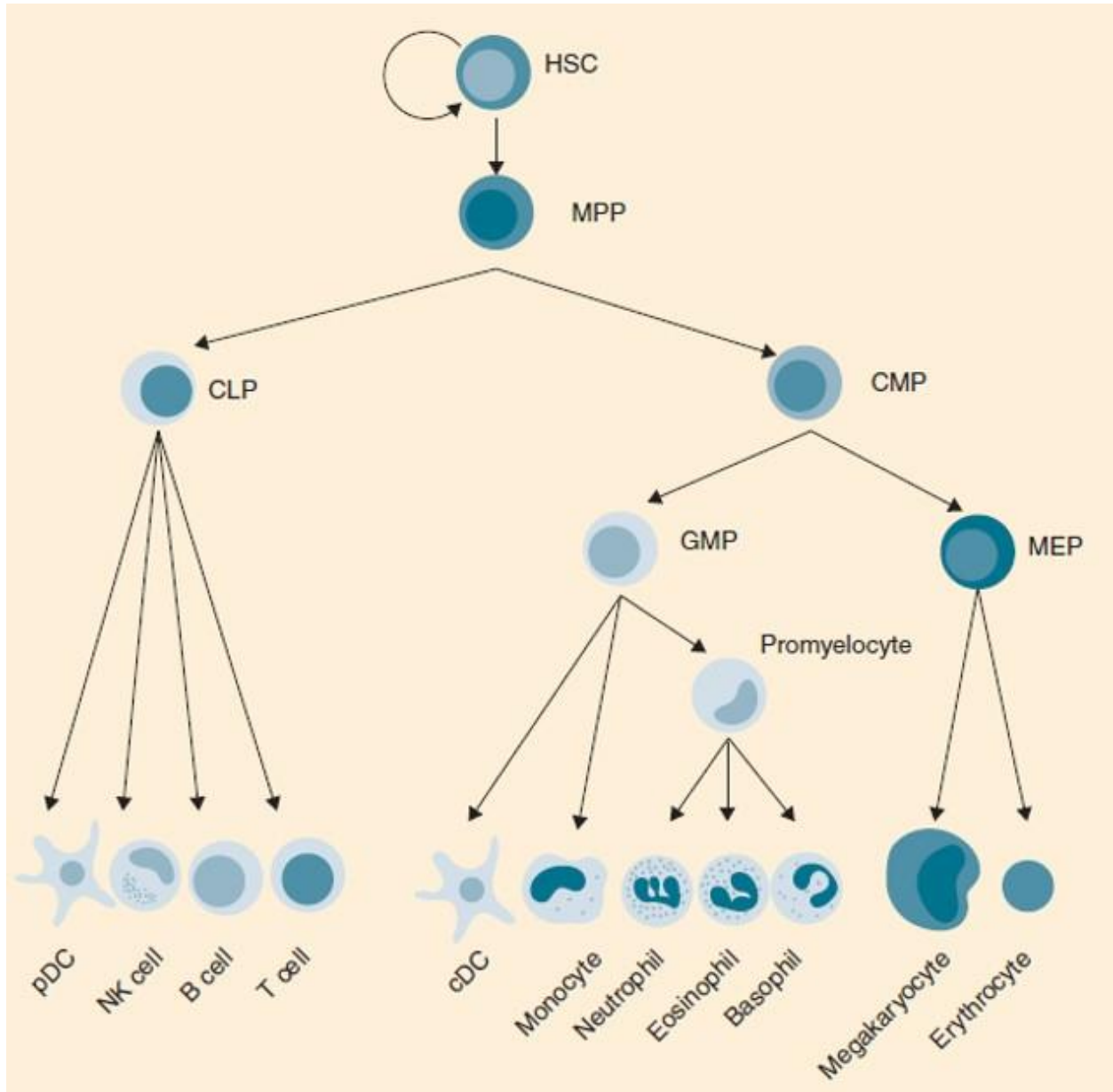


Figure 1. Main lineage precursors in hematopoiesis. On top of the hierarchy are the self-renewing HSCs, with potential to give rise to several MPP, from which all mature blood cells are derived through a series of steps known as lineage commitment⁸. cDC, conventional dendritic cell; CLP, common lymphoid progenitor; CMP, common myeloid progenitor; GMP, granulocyte-monocyte progenitor; HSC, hematopoietic stem cell; MEP, megakaryocytic-erythroid progenitor; MPP, multipotent progenitor; pDC, plasmacytoid dendritic cell.

2.2.1 T cell progenitors in the BM

Lymphopoiesis, from the latin words *lymp*ha (water) and *poiesis* (to create), is the process by which new lymphocytes, including B, T and natural killer (NK) cells are generated⁶. HSC are the apex of the hierarchy of all precursor cells; however, identification of a true HSC population remains challenging⁹. For example, mouse HSCs are identified by surface expression of CD117 (c-Kit), stem cell antigen-1 (Sca1) and the lack of expression of lineage markers (c-Kit⁺Sca1⁺Lin⁻, also known as KSL fraction), however, only 3% of this population possesses true HSC activity⁹⁻¹². Nowadays, human HSC are characterized as Lin⁻CD34⁺CD38⁻CD45RA⁻CD90⁺CD49f⁺ cells that can give rise to the multipotent progenitors (MPP) that are characterized by the loss of expression of CD90 and CD49f¹³. Subsequently, MPP further differentiate creating two branches: the multilymphoid progenitors (MLP) characterized as CD34⁺CD38⁻CD45RA⁺CD90⁻ from which NK, B and T cells emerge; and the common myeloid progenitors (CMP) identified as Lin⁻CD34⁺CD38⁻CD45RA⁻CD135⁺ that can further branch off to create the megakaryocytic-erythroid progenitors (MEP) and the granulocyte-monocyte progenitors (GMP)^{13,14}. Of note, some studies have pointed out the role of the superfamily of transmembrane receptors Notch in stem cell fate decision¹⁵. Notch proteins are a family of conserved transmembrane receptors that regulates cell fate choices in the development of several cell lineages¹⁶. Differential expression of Notch has been detected in multiple bifurcation points in hematopoiesis that can trigger activation of genes related to one specific lineage and suppress the genes associated to the other^{17,18}. In humans, the MLP retain some potential for myeloid development, in contrast to the common lymphoid progenitor (CLP) that are precursors strictly for lymphocytes and not for myeloid cells¹⁹⁻²¹. Moreover, recent studies have discovered a new lineage of lymphocytes derived from the CLP, the innate lymphoid cells (ILCs) that do not express the TCR, but do express the IL-2R γ chain and the transcriptional repressor inhibitor of DNA binding 2 (ID2) for their development^{22,23}. These cells are commonly divided into three different subsets (ILC1, ILC2 and ILC3) identified by the cytokine expression pattern and the transcription factors needed for its development²². Erythrocytes, granulocytes and myeloid cells are derived from the MEP and GMP⁸ and its production is stimulated by growth factors such as erythropoietin, granulocyte-CSF (G-CSF), granulocyte-macrophage-CSF (GM-CSF) and macrophage-CSF (M-CSF), respectively, whereas thrombopoietin induces the production of platelets and IL-5 the production of eosinophils²⁴. Once matured, newly formed cells in the BM exit through sinusoid capillaries into the bloodstream⁷.

2.2.2 Thymic seeding of early T cell progenitors and T cell maturation

Thymus-seeding progenitors (TSPs) from the BM migrate to the thymus where they finally commit to the T-cell lineage and develop into functional T cells. Because maturation in the thymus induces loss of self-renewal properties of T cell precursors, a continuous production and migration of BM precursors is needed to maintain T lymphopoiesis²⁵. These immigrant precursors access the thymus through veins at the cortical tissue near the corticomedullary junction and subsequently migrate into the thymic tissue²⁶. This process mainly depends on the chemokine receptors CCR7 and CCR9 and the adhesion molecule P-selectin glycoprotein ligand-1 (PSGL-1)^{27,28}. The identity of ETPs is unclear (**Figure 2**), but they may belong to the lymphocyte-primed MPP (LMPPs) category^{27,28}, defined as Lin⁻Sca1⁺c-Kit⁺Flt3⁺ cells that besides its T-cell potential, still can give rise to macrophages, DCs, NK cells and B cells in mice²⁹⁻³¹, whereas the human counterpart in addition retains erythroid potential³². After entering the thymus, T-cell precursors must go through different steps of differentiation that involve gradual stages of lineage commitment, defined as the loss of the capacity to produce a different kind of descendant than T-cells, and a specific transcriptional program⁸, as described in detail below.

2.2.3 T cell maturation in the thymus

The process of differentiation beginning with the thymic entry to the expression of functional TCR chains can be better described as two separate major parts depending on either Notch- or TCR-stimulation⁴ (**Figure 3**). Upon engagement with ligands of the Delta or Jagged family, the intracellular part of Notch is proteolytically cleaved and can act as a transcriptional activator⁴. The most primitive T cell precursors do not express a TCR, but proliferation and differentiation is induced via Notch signalling⁴. In the murine thymus, Delta1 is expressed at the cortex-medulla junction, thus, as soon as TSPs enter the thymus using this route, engagement of Notch1 by Delta1 expressed in thymic stromal cells can instruct the differentiation towards T- or NK-lineages, but not B-cell lineage³³⁻³⁵. These committed precursors are known as double negative (DN) thymocytes, and can be further subdivided based on the surface expression of the IL-2R α chain (CD25) of the IL-2 receptor, and the adhesion molecule CD44²⁷: DN1; CD44⁺CD25⁻; DN2:

CD44⁺CD25⁺; DN3: CD44⁻CD25⁺; and DN4: CD44⁻CD25⁻; as depicted in **Figure 3**. The most immature thymocyte precursors, the ETP, belong to the DN1 subset^{27,36}.

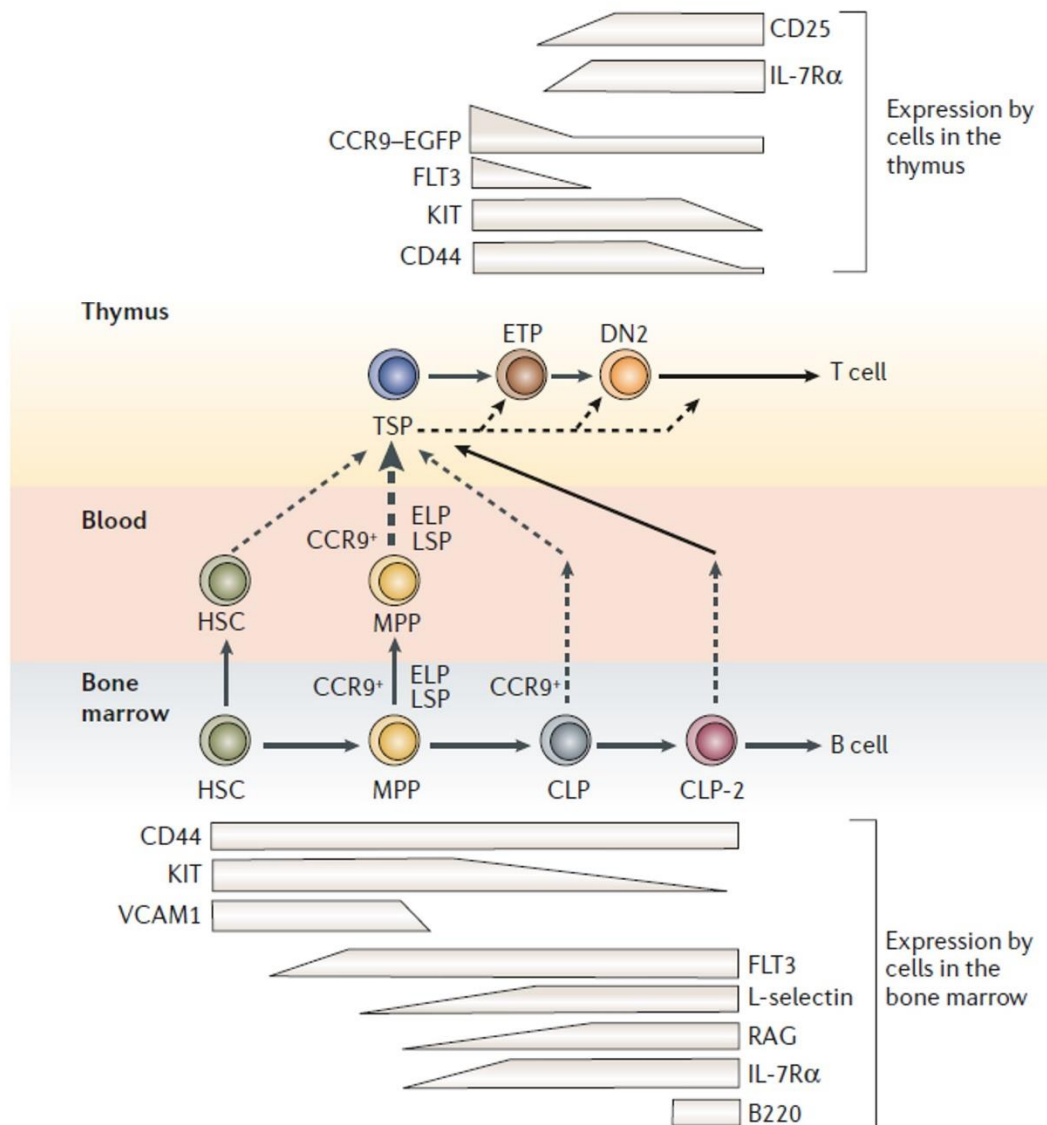


Figure 2. Identity of T cell progenitor seeding the thymus. HSC from the BM differentiate into MPPs. A small fraction of these cells are recognized as ELPs due to expression of RAG1, or LSPs due to its expression of L-selectin. Other progenitors include the CLPs. HSCs and MPPs are also found in circulation through the bloodstream. The dashed arrow that connects MPPs in PB to the thymus represents an already proven pathway, however it is unclear whether only one subset of MPP can settle in the thymus. Dotted arrows represent pathways for which there is less information, while solid arrows represent well-known trafficking and differentiation pathways. The precise identity of the TSP from which ETPs, DN2 and other cells arise remains elusive, but it is thought that they derive from MPP. Additionally, it is possible that TSP give rise to DN2 or DN3 stages without going through the ETP stage²⁷. CLP,

common lymphoid progenitor; DN, double-negative; ELP, early lymphoid progenitor; ETP, early T cell precursor; LSP, lymphocyte L-selectin-expressing progenitor; MPP, multipotent progenitor; RAG, recombination-activating gene; TSP, thymus-seeding progenitor.

These ETPs proliferate vigorously by stimuli from the thymus, although the nature of these stimuli remains elusive³⁷. Notch signaling induces the expression of the TF T-cell factor-1 (TCF1-)³⁸, which is essential for the transition from DN1 to DN2 by inducing activation and silencing of its target genes *GATA3* and *RUNX1*^{39,40}. During DN2a and DN2b transition, T-cell lineage commitment occurs, while the potential of alternative lineage development is lost^{41,42} and expression of CD25 and IL-7R (CD127) provides them T-cell identity⁴³.

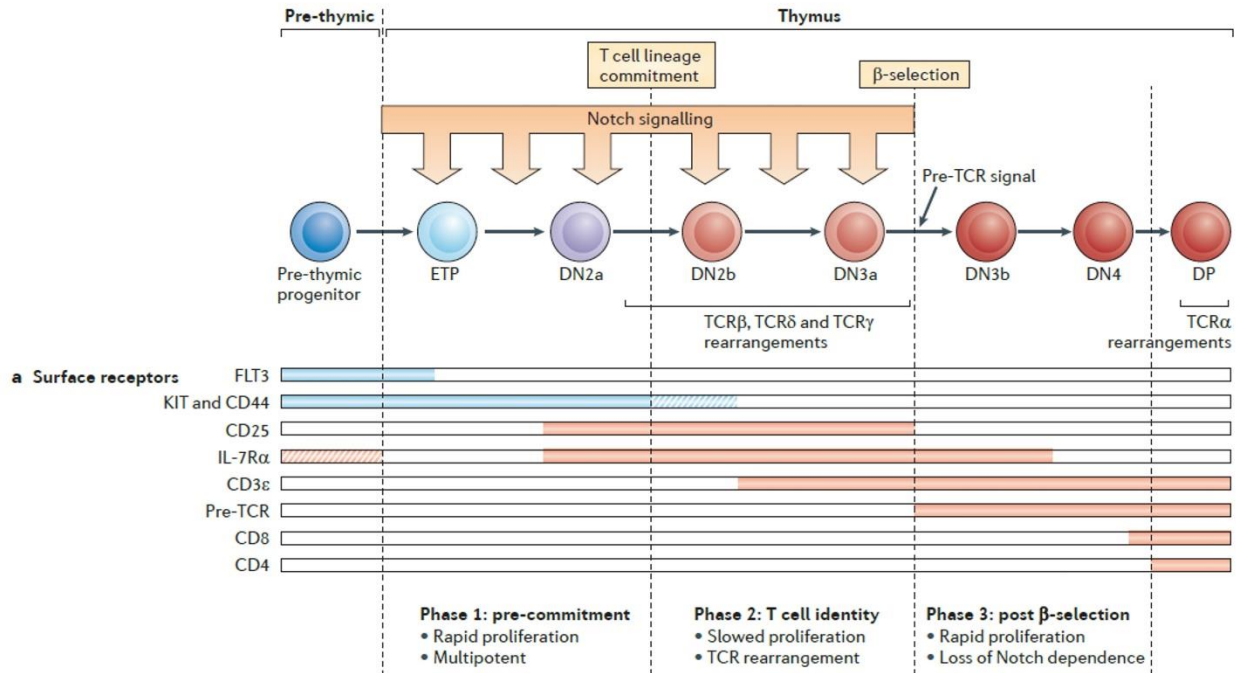


Figure 3. Stages and characteristic surface markers of T-cell development in the thymus. Pre-thymic progenitors in the thymus differentiation are divided in three major phases that are controlled by Notch- and TCR-stimulation. Notch induces the transit through the first two phases: during pre-commitment, cells transiting from ETP (DN1) to DN2a present vigorous proliferation. These progenitors express high KIT (also known as CD117), IL7-R α and CD44. As cells transit to the second phase of T cell identity, DN2b and DN3a stages slow down proliferation, whereas TCR- β , - δ and - γ chains rearrangement and expression take place during this transition. During DN3a to DN3b transition, T cell differentiation and survival becomes dependent on TCR signals, as CD3 ϵ chain and pre-TCR are expressed, and Notch expression is reduced. The last phase of post β -selection is characterized by high proliferation of DN3b and DN4 subsets induced by pre-TCR stimulation. During the DP stage, CD4 and CD8 are expressed, and cells stop

proliferation as they begin to rearrange the TCR α chain. Dashed lines divide the three phases of development in the thymus. Expression of surface markers is presented in the lower part during the different stages of differentiation⁴. DN, double negative; DP double positive; ETP, early T cell precursor; TCR, T-cell receptor.

Notch is expressed in ETPs, but it is progressively upregulated until reaching a peak in DN3 stage, after which it is gradually reduced⁴³. During DN3, expression of most T cell identity genes are induced, whereas concomitant downregulation of CD44 and CD117 occurs^{5,25}. These genes include critical regulators of TCR rearrangement such as the recombinase activated gene 1/2 (RAG1/2) recombinases, TCR complex assembly such as the pre-T α chain and CD3 ϵ , and mediators of TCR signaling such as LCK, ZAP-70 and LAT, which prepare the cells for TCR-dependent survival^{25,43-45}. Of note, the development from the ETP stage to the DN3 stage is independent of the TCR, but instead is regulated by migration through distinct thymic microenvironments (**Figure 4**)⁴⁶. RAG1/2 induces the rearrangement of the TCR β -chain (*Tcrb*) loci through V-D-J recombination, which is required for the assembly of the TCR⁴⁷⁻⁵⁰. At this point, only those cells that successfully rearranged their TCR β chains undergo further differentiation, whereas those who failed undergo apoptosis. Functional TCR β chains associate with the invariant pre-T α and CD3 signaling molecules to form the pre-TCR complex⁸. The pre-TCR complex mediates β -selection, a process where pre-TCR signaling rescues cells from apoptosis, and induces vigorous cell proliferation and the termination of the TCR β locus recombination (also known as allelic exclusion, that restricts the TCR expression to one kind of TCR β chain per cell)^{50,51}. Pre-TCR assembly during DN3b stage also leads to the downregulation of CD25 expression, upregulation of co-stimulatory molecule CD28, and subsequent transition to the DN4 or pre-double positive (DP) population³⁶. At this point, thymocytes start expressing the co-receptor proteins CD8 and CD4, to form the large population of DP cells that comprises around 90% of the thymocyte population³⁶. During this stage, the *Tcra* locus is also recombined to generate the TCR α -chain. Subsequently, expression of the surrogate pre-T α is lost, which then results in the surface expression of the mature TCR $\alpha\beta$ coupled to the CD3 complex³⁶.

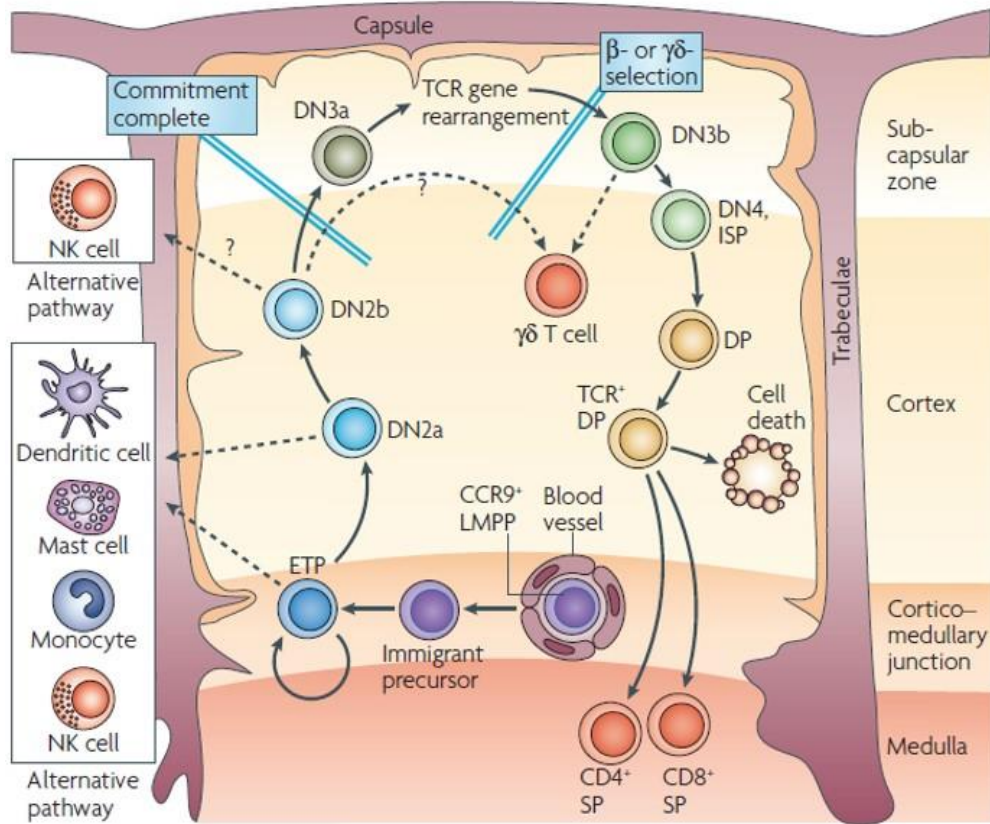


Figure 4. Early T-cell development in the thymus. Section of an adult thymus lobule showing the development and maturation of T cell progenitors. Immigrant precursors derived from the BM enter the thymus via capillaries near the cortico-medullary junction. ETPs then migrate and differentiate from DN to DP and SP states as they pass through distinct microenvironments in the thymus. Of note, ETP cells retain the potential to self-renew to a certain degree or proceed to DN2 and continue the migration into the thymus cortex. As they move to the subcapsular zone, DN2 cells proceed to the DN3 stage where the β -selection occurs. For the later stages of T cell development, DN3 cells migrate back towards the medulla where positive and negative selection takes place to generate functional T cells that do not react to self-antigens. Dashed arrows represent potential developmental pathways that are still possible before complete commitment to the T-cell lineage²⁵. BM, bone marrow; DN, double negative; DP double positive; ETP, early T cell precursor; SP, single positive.

The DP $\text{TCR}\alpha\beta^+$ cells that fail to recognize self-MHC molecules are eliminated by apoptosis in a process termed death-by-neglect⁵². On the other hand DP with intermediate affinity and/or avidity for self-MHC are then positively selected to differentiate into mature single-positive (SP) thymocytes (also known as positive selection)^{52,53}. Successful positive selection of DPs is concomitant with surface TCR upregulation, as well as CD5 and CD69 activation marker

upregulation, together with the survival factor Bcl-2². Moreover, DP or SP cells that possess TCR $\alpha\beta$ with high affinity for self-antigens presented in MHC molecules are also eliminated (negative selection)^{52,53}. This way, many non-functional and autoreactive T cells are eliminated by apoptosis as their TCR yield no signal or too strong TCR signal, respectively^{8,52,54}. Functional naïve CD4⁺ T-helper cells and CD8⁺ cytolytic T cells (CTLs) reside within the thymic medulla for 12 to 14 days before they emerge and migrate to the periphery^{2,8,54}. In the periphery, mature naïve T cells migrate to secondary lymphoid organs (SLOs) such as the spleen, LNs and mucosa-associated lymphoid tissue in search for their specific antigen^{51,55}. This trafficking is regulated by several adhesion molecules and chemokine gradients, as described in more detail below.

2.3 T cell migration

Among leukocytes, lymphocytes have remarkable migration potential as they continuously recirculate in and out of lymphoid and non-lymphoid tissues throughout their life^{56,57}. Moreover, distinct subsets of T-cells possess unique migration capabilities due to different surface receptor patterns, and activation state depending on the vascular bed and the available counterreceptors expressed on endothelial cells (EC)⁵⁸⁻⁶⁰. For example, after patrolling in peripheral tissue, memory T cells enter the draining lymph nodes (LN) preferentially through the afferent lymphatic vessels, whereas the majority of naïve T cells access the LN via specialized high endothelial venules (HEVs) directly into the T cell zone⁶¹. *In vitro* studies using human T-cells demonstrated that the behavior of T cells is different from other leukocytes regarding trans-endothelial migration (TEM)⁶⁰. For instance, T cells can adhere randomly to the endothelium and locomote on the EC surface allowing enough time to induce chemokine-chemokine receptor crosstalk necessary for T cell integrin activation and subsequent TEM⁶². Furthermore, this contact time enables the TCR to recognize potential antigens presented on the surface of EC, a newly explored pathway to achieve TEM⁶³. T cell extravasation involves a set of common and T cell-specific molecules that participate in the different steps of T cell recruitment⁶⁰ as described below (**Figure 5**).

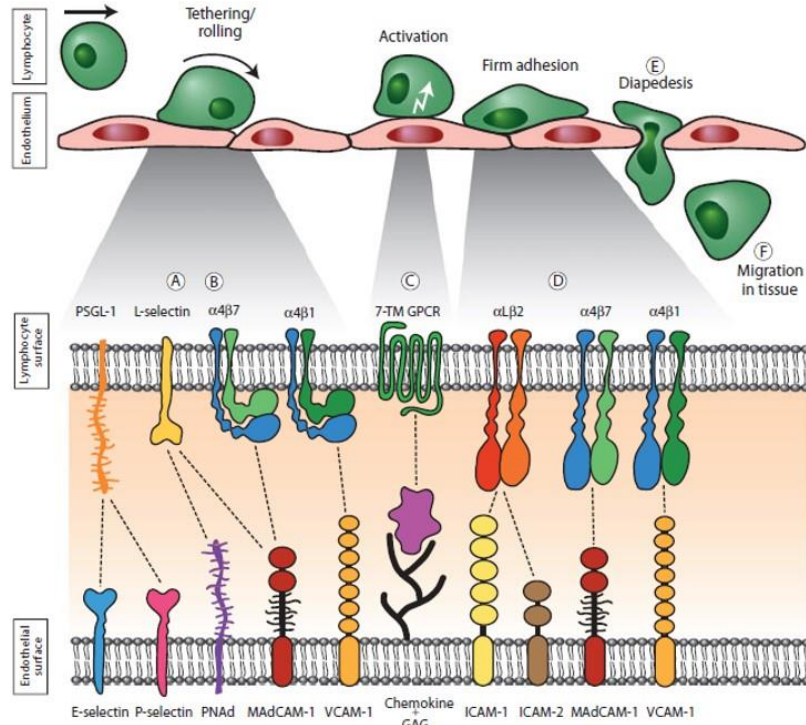


Figure 5. General overview of common steps that lymphocytes perform to achieve extravasation. Homing involves a stepwise adhesive process starting on the endothelium of post-capillary venules. Lymphocytes initiate tethering and rolling (upper panel) through transient interaction of selectins (A) and α_4 integrins (B) expressed on T cells and its respective ligands expressed on ECs (lower panel). Subsequently, firm adhesion is achieved by binding of T cell GPCRs (C) to chemokines presented on GAGs of endothelial cells allowing integrins on T cells (D) to acquire its high affinity state that support firm adhesion and arrest. Firmly adhered T cells polarize and transmigrate across the endothelium (E). Transmigrated T cells follow cytokine gradients and ECM to guide within the tissue (F)⁵⁹. EC: endothelial cells; ECM: extracellular matrix; GAG: glycosaminoglycans; 7-TM GPCR: seven transmembrane G-protein coupled receptor.

2.3.1 Tethering and rolling

In search of specific antigens, mature naïve lymphocytes continuously circulate through the body migrating from one lymphoid organ to another via the blood stream and the lymphatics⁶⁴. Lymphocytes exit the blood stream within the LN via HEV, which are specialized post-capillary venules. The first step of T cell TEM in HEV is the capture and tethering of circulating lymphocytes (**Figure 5**)⁶⁴. T cells in the bloodstream are surrounded by short microvilli that are enriched with low affinity adhesion molecules such as L-selectin (CD62L) and very late antigen-4 (VLA-4) at the tip, thus allowing initial tethering and rolling in the vessel walls^{65–67}. These

transient interactions between HEV EC and naïve lymphocytes are mediated by selectins expressed on the lymphocyte surface and sialomucins, also called peripheral node addressins (PNAd) that are constitutively expressed on the HEV surface such as GlyCAM-1, CD34, podocalyxin, endomucin, CD300g and mucosal addressin cell adhesion molecule-1 (MAdCAM-1)⁵⁷. Quick selectin-ligand association rates facilitate the initial capture on EC, whereas rapid dissociation rates allow leukocytes to roll forward^{68,69}. In mesenteric LN HEVs, however, MAdCAM-1, a sialomucin containing two immunoglobulin-like domains⁷⁰ functions as vascular addressin for T cells expressing integrin $\alpha_4\beta_7$, which mediates rolling and adhesion⁷¹. E- and P-selectin can also be induced on the EC surface in inflamed tissues to further enhance capturing of T cells from the blood stream via the T cell ligands L-selectin and PSGL-1, respectively⁷². It is important to mention that although all T cells express PSGL1, only certain subsets of T cells, such as Th1, express the correctly glycosylated form of PSGL-1 capable of binding to selectins⁷³. CD44 is another surface molecule capable of binding to the extracellular matrix glycosaminoglycan hyaluronan as well as E-selectin that is important for slowing down the rolling velocity of T cells⁷⁴. *De novo* expression of E-selectin on microvascular EC is induced in response to cytokines such as IL-1, TNF- α , and other stimuli like bacterial lipopolysaccharide (LPS). On the other hand, P-selectin is stored in Weibel-Palade bodies that are rapidly mobilized to the plasma membrane of EC in response to mediators of acute inflammation thus allowing for a quick and efficient initiation of immune cell recruitment to combat the cause of inflammation⁷⁵.

2.3.2 Adhesion

While selectins are constitutively active, integrins that mediate firm adhesion of T cells to EC need to be activated first⁵⁷. Integrins exist in three conformational states: a bent conformation that has a closed headpiece and thus low affinity for its ligands, and two extended conformations with either closed (intermediate affinity) or open headpiece (high affinity) (**Figure 6**)⁷⁶. Engagement of selectins in leukocytes stimulates inside-out signals that increase the affinity of integrins such as lymphocyte function-associated antigen-1 (LFA-1) and VLA-4⁷⁷ to mediate firm adhesion to EC adhesion molecules such as intercellular adhesion molecule-1 (ICAM-1), vascular adhesion molecule-1 (VCAM-1) and MAdCAM-1⁶⁴. In addition, CXCL12 binding to its receptor CXCR4 induces further polarization and chemotaxis of T cells on the EC surface⁶². Chemokines are usually

positively charged and are able to bind to negatively charged glycosaminoglycans (GAG) expressed constitutively on HEVs, which prevents chemokine washing off by the blood flow^{57,78}. On the other hand, CCR7 and CXCR4 chemokine receptors in naïve T lymphocytes, upon binding to their ligands CCL19, CCL21, and CXCL12, respectively, further increase integrin affinity by inside-out signals leading to T cell arrest^{60,77,79,80}.

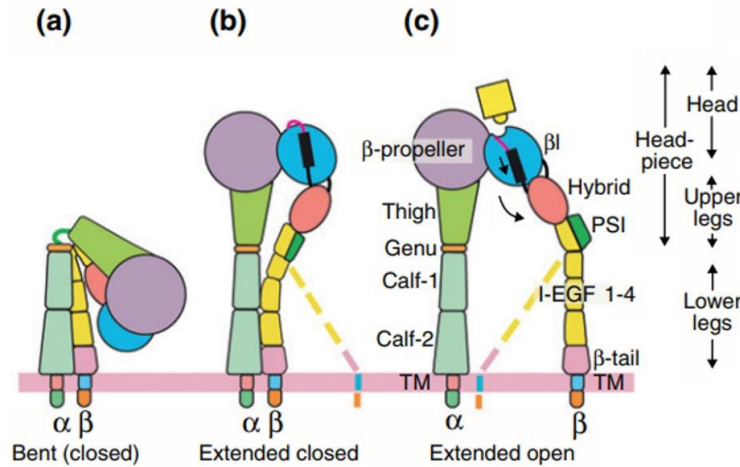


Figure 6. The conformational states of integrins. In basal conditions, integrins are dynamically equilibrated in the three states. The bent-closed conformation (a) has low affinity for its ligands; the extended-closed conformation (b) has intermediate affinity; and the extended-open conformation (c) has high affinity. Conformational changes into the high-affinity form is commonly triggered by chemokines during inflammation⁷⁶.

VLA-4 ($\alpha_4\beta_1$ -integrin, CD49d/CD29) belongs to the β_1 integrin subfamily comprised of at least 6 members (VLA-1–VLA-6) with different α -chains associated with the β_1 chain. They function as receptors for extracellular matrix proteins such as collagen, fibronectin, laminin and osteopontin, as well as for the EC adhesion molecules VCAM-1 and MadCAM^{81,82}. VLA-4 plays major roles in tissue-specific migration of T-cells during inflammation and metastasis⁸³. Also, VLA-4 activation (high-affinity conformation) in T cells is essential for VCAM-1 recognition on activated EC and subsequent TEM⁸⁴. On the other hand, LFA-1 ($\alpha_L\beta_2$ -integrin, CD11a/CD18) not only plays a role in T cell migration but also for T cell activation⁸⁵. Adhesion of active LFA-1 to ICAM-1 allows firm adhesion to ECs, prolong the contact with antigen-presenting cells (APCs), and binding to target cells for killing in the case of cytotoxic T cells^{85,86}. Basal expression of ICAM-1

in EC is low, but it is highly upregulated during inflammatory processes via the transcription factor nuclear factor- κ B (NF- κ B)³⁷. Unlike ICAM-1, VCAM-1 expression depends on the expression and activation of the Rho-GEF Trio and its target Rac-1, by directing the translocation of the transcription factor Ets2 to the nucleus³⁷.

After firm adhesion, naïve T lymphocytes start to crawl along the luminal surface of HEVs in a VLA-4-dependent manner⁸⁴, in search for a suitable spot for transmigration⁸⁷. Moreover, it has been pointed out that during spreading and lateral migration over ECs, lymphocytes extend cylindrical protrusions from its bottom to the surface of the ECs⁸⁸⁻⁹¹. These structures, known as invadosome-like protrusions (ILPs), are similar to invadopodia and podosomes observed in other cells⁹². ILPs are enriched in and functionally depend on LFA-1, the actin-binding proteins (ABP) Wiskott-Aldrich Syndrome protein (WASp) and the cortactin homolog hematopoietic-cell-specific lyn substrate-1 (HS1), and the kinase Scr⁸⁹. ILPs protrude from the T cells to probe or sense the biomechanical characteristics (such as stiffness) of the endothelial substrate as they move⁹³. This random sensing allows for the identification of spots with less resistance as the ILPs progressively extends until it breaches the endothelial barrier to initiate diapedesis^{89,94}.

2.3.3 Diapedesis

Arrested lymphocytes must cross the endothelial layer to get access to the tissue. Diapedesis can occur in two ways: paracellularly between the junction of two EC; or transcellularly through the body of a single EC⁸⁵. More than 90% of most migrating leukocytes use the paracellular route^{95,96}, whereas 72% of CD4⁺ T cells use the paracellular route across inflamed primary mouse brain microvascular endothelial cells (pMBMECs)⁹⁷. However, high levels of ICAM-1 expression in pMBMECs favor transcellular (52% of cells using this route) over paracellular diapedesis of CD4⁺ T cells⁹⁷. Interestingly, absence of platelet-endothelial adhesion molecule-1 (PECAM-1) has been shown to also favor transcellular over paracellular T-cell diapedesis on pMBMECs under flow conditions⁹⁸. Although the mechanism is not completely understood, the authors proposed that abnormal organization of junction molecules might reduce paracellular T-cell diapedesis in brain EC models⁹⁸. Thus, ICAM-1 density, monolayer organization and “hot spots” for diapedesis can direct leukocytes across the endothelium⁹⁵. During paracellular diapedesis, T effector cells (T_{eff}) use molecules such as PECAM-1, CD99 and LFA-1, which bind to PECAM-1 (homophilic), CD99

(homophilic) and ICAM-1/Junctional adhesion molecule-A (JAM-A) on ECs, respectively⁹⁹. On the other hand, transcellular diapedesis requires the formation of a pore through the body of the endothelial cell, a process that is dependent on SNARE-mediated membrane fusion, Ca⁺⁺ influx and caveolae enriched in ICAM-1- and F-actin on ECs, and the formation of ILPs on T cells^{88,100}.

The HEV basal lamina has several pores through which naïve T cells can pass to reach the abluminal face of HEVs without altering the basal lamina⁵⁷. Once across the endothelium, chemokines such as CCL19, CCL21, CXCL12 and CXCL13 presented in the extracellular matrix create a guidance structure for directed trafficking of lymphocytes from HEVs into the parenchyma of lymphoid tissue in the LN⁷⁸.

2.4 Activation in secondary lymphoid organs and differentiation

After full maturation in the thymus, T cells migrate to secondary lymphoid organs (SLOs), such as the lymph nodes and spleen, where antigens from the periphery are presented by APCs¹. Furthermore, lymphocyte recirculation between blood, and lymphoid and non-lymphoid tissues is an essential mechanism that regulates both humoral and cellular immune responses *in vivo*⁵⁷ as it allows for antigen recognition and the generation of properly acquired immune responses. Activation of T cells in response to antigen recognition is an extremely precise process that can be divided into multiple phases including T cell motility in the LN and interactions of T cells with APCs¹⁰¹. In the first phase, T cells migrate along fibroblastic reticular cells (FRCs) in LN as they scan for antigens. During a second phase, T cells slow down as they actively interact with APCs, which induces expression of cytokines, such as IL-2 and IFN γ , that allow for posterior T cell proliferation and polarization towards a specific subset, respectively. Finally, activated T cells gain high proliferation and migration capabilities and effector functions, before exiting the lymphoid tissue¹⁰¹. Newly arrived T cells in the LN or spleen usually undergo several rounds of homeostatic proliferation in response to self-peptides/MHC complexes or stimulation with IL-7 and IL-15¹⁰². This phenomenon helps to maintain the T cell pool in the peripheral blood and can be especially enhanced during states of lymphopenia, such as after chemotherapy or irradiation¹⁰³. To prevent premature or excessive activation, T cells require two independent signals to achieve proper activation: 1) the antigen-specific interaction of the TCR with the peptide-bound major

histocompatibility complex (MHC) on APC; and 2) binding of either chemokines or co-stimulatory proteins presented on the APC such as CD80 or CD86. Receiving signal 1 without co-stimulation results in anergy, a phenomenon also known as peripheral tolerance².

2.4.1 T cell activation and formation of the immunological synapse

Migration of T cells through FRCs allows for random interaction with antigen-bearing DCs. These brief transient interactions, termed kinapses, diminish T cell motility¹⁰⁴. Interaction with the APC is dictated by the affinity of the peptide-MHC (pMHC) complex and the TCR¹⁰⁵. CD8⁺ T cells can interact with peptides on all nucleated cells that express MHC class I in their membranes, which are peptides derived from endogenous or viral proteins produced in the cell, or from pathogens replicating intracellularly¹. CD4⁺ T cells, on the other hand, recognize peptides presented on MHC class II, the expression of which is restricted to professional APCs. These peptides can be microbes-derived, exogenous and self-proteins that are captured in different environments and processed by the APCs¹. Upon encounter with the specific antigen-bearing APC, T cells stop and induce large pseudopodia and lamellipodia towards the APC, resulting in the formation of a flattened, F-actin rich interface known as the immunological synapse (IS)^{101,104,106}. The IS is characterized by the recruitment and segregation of several essential molecules into a typical “bullseye” pattern divided into three sections referred to as supramolecular activation clusters or SMACs^{85,107} (**Figure 7**). In the center of the bullseye, the so-called cSMAC, the TCR/CD3 complex and the co-stimulatory molecules CD28 and PKC θ are enriched. Intriguingly, at least 10 agonist-pMHC need to cluster to induce the formation of the cSMAC¹⁰⁸. LFA-1 and its cytoskeletal linker talin-1 are enriched in the central ring of the bullseye known as peripheral-SMAC (pSMAC), suggesting that the pSMAC might be essential to maintain T cell-APC adhesion^{109,110}. The most external ring known as the distal-SMAC (dSMAC) is composed of large molecules such as CD43 and CD45 that do not participate directly in T cell activation signaling. However, CD45 is a key phosphatase for the activation of different kinases including LCK, whereas CD43 is an anti-adhesive molecule that regulates T:APC interactions¹⁰⁷. Upon formation, the IS supports sustained TCR signaling and adhesion, exo- and endocytic processes, receptor internalization and direct communication with APCs through secretion of cytokines and granules^{111–114}.

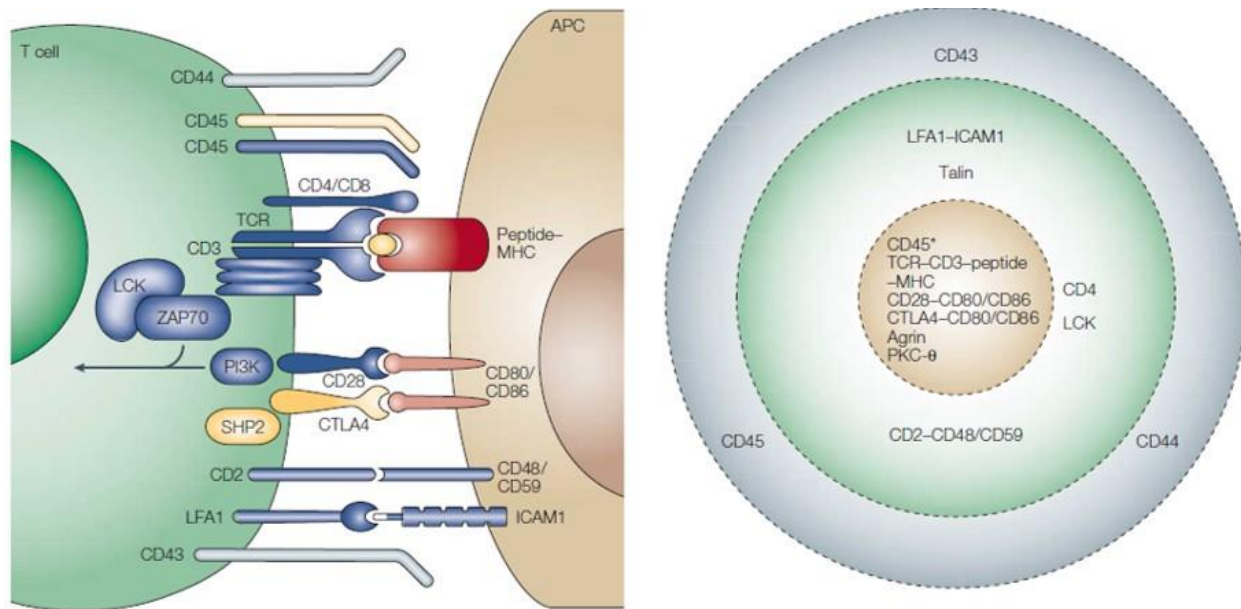


Figure 7. The mature T-cell immunological synapse (IS). Left: representation of an IS showing key ligand pairs and signaling molecules essential for T-cell recognition of antigens. The stimulatory peptide-MHC complex is shown in red, co-stimulatory proteins are blue, inhibitory proteins are yellow and in grey are depicted proteins not contributing to signaling. Arrows represent converging signaling for T cell activation. Right: characteristic “bullseye” zone pattern of the IS as well as ligand pairs enriched within each zone including: the cSMAC depicted in yellow contains the TCR complex, co-stimulatory molecules and the proximal signaling complex that allows for TCR signaling; the pSMAC, highlighted in green is known to contain adhesion molecules, such as ICAM-1 and CD2 that stabilizes and prolongs the binding of T:APC to allow for proper IS formation; and, the dSMAC, filled with grey, it is considered as a recycling pool for different molecules needed in the c- and pSMAC, on the other hand it also contains CD45 that do not contribute directly to TCR signaling, however it is a key phosphatase for the activation of different kinases, e.g., Lck¹⁰⁷. CTLA4, cytotoxic T lymphocyte antigen 4; ICAM-1, intercellular adhesion molecule-1; LFA-1, leukocyte function-associated antigen-1; PI3K, phosphatidylinositol 3-kinase; SHP2, SCR homology 2-domain-containing protein tyrosine phosphatase; TCR, T cell receptor; ZAP70, ζ -chain associated protein 70.

2.4.2 The proximal signaling complex

In the cSMAC on the T cell side, CD3 (γ , δ , ϵ and ζ chains) and $\alpha\beta$ -TCR bind to the pMHC, which is stabilized by the interaction of CD4/CD8 co-receptors to non-polymorphic regions of the MHC class II or class I complex, respectively¹ (**Figure 7**). This cluster brings the cytosolic domains of the receptors in close proximity, and as a result, LCK that is bound to the cell membrane is able to phosphorylate cytoplasmic immunoreceptor tyrosine-based activation motifs (ITAMs) within the

cytoplasmic tail of CD3¹. This induces rapid recruitment and engagement of several signaling molecules such as ζ -chain-associated protein kinase of 70 KDa (ZAP70), linker for the activation of T cells (LAT), growth-factor-receptor-bound protein-2 (GRB2), GRB2-related adaptor protein-2 (GRAP2; also known as GADS) and SCR homology-2 (SH2)-domain containing leukocyte protein of 76 KDa (SLP76)^{1,115}. Of note, the pan-leukocyte marker CD45, which contains 2 tyrosine phosphatase domains, plays essential roles in TCR activation by dephosphorylating the inhibitory residues of Src family kinases such as Lck. Mutations in the *PTPRC* gene, which encodes for CD45, provokes a severe combined immunodeficiency (SCID)¹. Of all the targets of ZAP70, LAT and SLP76 form the scaffold of the signaling complex that organizes the rest of the effector molecules to allow proper spatiotemporal activation of multiple signaling pathways^{116–118}. LAT contains nine sites for phosphorylation, which then allow for interaction with PLC γ 1, the p85 subunit of phosphoinositide 3-kinase (PI3K), GRB2 and GADS, leading to recruitment of SLP76 via GADS interaction^{118,119}. SLP76 is composed of three modular domains: a N-terminal acidic domain (NTA) with three tyrosines prone to phosphorylation that allows interaction with SH2 domains of Vav1, Nck and Itk; a proline-rich region (PRR) that binds constitutively to GADS and PLC γ 1; and a SH2 domain in the C-terminus that is able to bind to adhesion and degranulation-promoting adapter protein (ADAP) and hematopoietic progenitor kinase 1 (HPK1)¹¹⁶. Itk is then necessary for the recruitment of Vav1, and in turn, Vav1 phosphorylates SLP76 required for recruitment to LAT and Itk activation^{120–122}. Itk then phosphorylates and activates PLC γ 1, that in turn hydrolyzes the membranal lipid PI(4,5)P₂, producing the second messengers diacylglycerol (DAG) and inositol triphosphate (IP₃), key factors for T cell activation¹²³. The previously described signaling events link TCR engagement to the activation of transcription of multiple target genes required for proliferation and effector functions of T cells, such as IL-2, IL-6, TNF and CXCL8¹²⁴ to name a few.

2.4.3 Downstream transcription factors

One of the most important upregulated genes upon activation is the T cell growth factor interleukin-2 (IL-2), whose expression is regulated by multiple transcription factors (TF) such as AP1, nuclear factor of activated T cells (NFAT) and nuclear factor- κ B (NF- κ B), all of which are activated upon TCR engagement² (**Figure 8**).

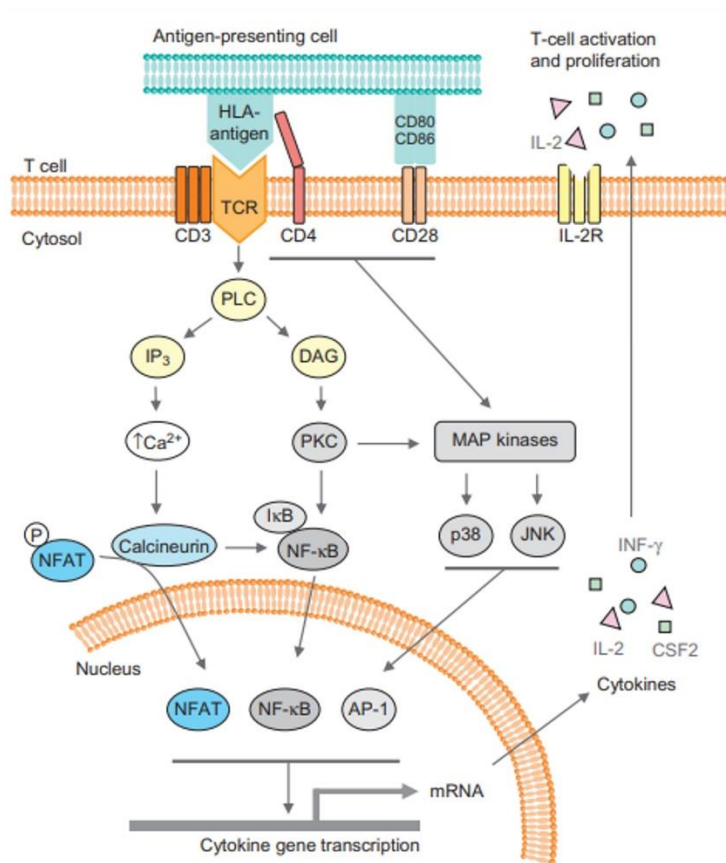


Figure 8. Signaling pathways downstream of TCR engagement. Antigen presentation activates several pathways needed for proper T cell activation, proliferation, and differentiation. The TCR proximal complex activates PLC γ 1, which generates the second messengers DAG and IP $_3$ that activate NF- κ B and calcineurin, respectively. On the other hand, co-stimulatory molecules activate MAP kinases leading to the activation of the AP-1 transcription factor that together with NFAT and NF- κ B induce the transcription of IL-2, IFN γ and CSF2, among other genes¹²⁵. CSF2, colony stimulating factor 2 (also known as GM-CSF); DAG, diacylglycerol; IFN γ , interferon- γ ; IL-2, interleukin-2; IP $_3$, inositol triphosphate; MAP, mitogen-activated protein kinase; NFAT, nuclear factor for activation of T cells; NF- κ B, nuclear factor- κ B.

In addition to PLC γ 1, TCR downstream signaling leads to the activation of Ras. Ras initiates a signaling cascade that includes the activation of the kinases Raf-1, mitogen-activated protein kinase kinase (MEK) and extracellular signal-regulated kinase (ERK), leading to the expression of the TF Fos. In addition, co-stimulation by CD28 induces the activation of the c-Jun N-terminal kinase (JNK) and the phosphorylation of the TF c-Jun, which associates to Fos to form AP1². On the other hand, DAG produced by the activation of PLC γ 1 activates protein kinase C θ (PKC θ) together with CARD-recruited membrane associated protein (CARMA) triggers the NF- κ B pathway¹²⁶. Finally, IP $_3$ also produced in response to PLC γ 1 activation induces an increase in intracellular calcium levels, thus activating the calcium/calmodulin-dependent phosphatase calcineurin that induces NFAT dephosphorylation and translocation to the nucleus, where it forms together with AP-1 a heterotrimeric TF for the *Il2* gene^{2,127}. IL-2 acts as a potent T cell growth factor that induces both proliferation and survival of T cells, and on the other hand, contributes to

the generation of effector and memory T cells¹²⁸. Moreover, IL-2 can influence Th1 and Th2 fate decision during activation of CD4⁺ T cells by controlling the expression of cytokine receptors, transcription factors, chromatin regulators and effector cytokines¹²⁹. On the other hand, IL-2 influences the effector activities of CD8⁺ T cells by regulating the expression of IFN γ , TNF α , and lymphotoxin α (Lt α), as well as the expression of the cytotoxic effector molecules granzyme B and perforin, and lastly by enhancing target cell killing^{130–133}.

2.4.3 T cell differentiation

Conventional T cells can be divided into two major subsets depending on the recognition of peptides presented by either MHC class I or II molecules and the respective expression of CD8 or CD4 co-receptors, respectively². CD4⁺ T cells are known as helper T cells since they provide via direct contact or cytokine release signals to enhance both B- and CD8⁺ T-cell responses, *i.e.* antibody production and cytotoxic activities, respectively, as well as inducing the activation of macrophages¹. On the other hand, CD8⁺ T cells act as cytolytic T cells (also known as CTLs) by eliminating pathogen-infected and cancer cells¹. Upon antigen presentation, CD4⁺ T cells can further differentiate into several subsets of effector cells characterized by their cytokine expression pattern and their transcriptional program including T helper 1 (Th1), Th2, Th17, follicular helper T cells (Tfh) and Tregs^{1,2,134,135} (**Figure 9**).

Th1 differentiation and functions. One of the main characteristics of Th1 cells is the production of IFN γ , Lt α and IL-2, as well as the activation of macrophages via IFN γ that results in enhanced phagocytic activities.^{134,136,137} Th1 cells are also crucial for host defense against intracellular pathogens such as virus, protozoa and bacteria, and the regulation of antigen presentation and cellular immunity¹³⁸. On the other hand, they are also responsible for the development of some forms of autoimmunity such as multiple sclerosis and type 1 diabetes^{135,138–140}. Th1 cells differentiate from Th0 precursors under the influence of IL-12 and IFN γ ¹. The T-box transcription factor (T-bet) is the master regulator of Th1 differentiation, not only by promoting the expression of genes that induce Th1 differentiation, but also by suppressing the development of other Th subsets such as Th2 and Th17^{141–143}.

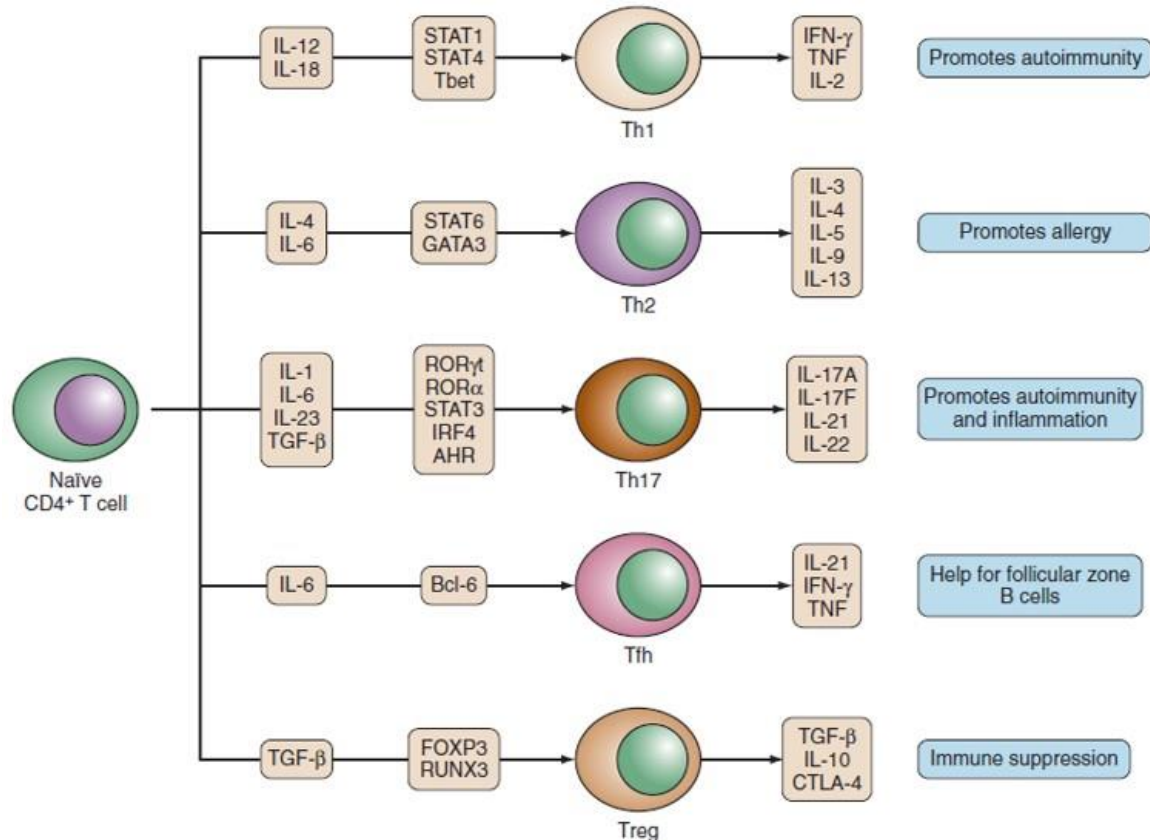


Figure 9. Different subsets of CD4⁺ T cells and their cytokine expression profile. Naïve CD4⁺ cells can be polarized to different Th subsets upon TCR engagement by the presence of a specific combination of cytokines. This stimulus triggers the expression of different transcription factors that act as master regulator of the effector functions of each specific subset. These polarized subsets possess a specific profile of cytokine production and surface molecules that allow them to regulate different aspects of the immune response. However, they are also associated with specific immune pathologies².

Th2 differentiation and functions. Th2 cells regulate the immune responses against extracellular parasites, including helminths; however, they can also play pathologic roles in allergies^{144,145}. Key effector Th2 cytokines include IL-4, IL-5, IL-9, IL-13, IL-10 and IL-25^{3,134}. IL-4 induces IgE switching and secretion in B cells, and the production of proinflammatory mediators such as IL-6, GM-CSF and VCAM-1^{146,147}. IL-5 induces the production and recruitment of eosinophils^{147,148}. IL-10 acts as an anti-inflammatory cytokine that helps achieving homeostasis after pathogen clearance¹⁴⁹. IL-13 boosts anti-helminth responses and elimination of intracellular pathogens such as *Leishmania*¹⁵⁰. IL-25 promotes Th2 responses as it induces the production of mucus,

eosinophilia, and IgE switching by increasing expression of IL-4, IL-5 and IL-13¹⁵¹. The regulation of Th2 differentiation depends on IL4 stimulation, which upregulates the TF STAT6, which in turn promotes the expression of GATA3, the master regulator of Th2 differentiation¹⁵²⁻¹⁵⁴.

Th9 differentiation and functions. Th9 cells were initially considered as a distinct IL-9-producing subset of Th2; however, later it was found that TGF- β in combination with IL-4 directly induced the differentiation to Th9. Th9 are characterized by the expression of large amounts of IL-9¹⁵⁵. Recent studies have associated Th9 cells with many inflammatory diseases such as allergic rhinitis, asthma, atopic dermatitis, contact dermatitis and food allergy¹⁵⁶.

Th17 differentiation and functions. Th17 cells are responsible for regulating the immune responses against extracellular bacteria and fungi; however, Th17 cells mediate many autoimmune diseases such as psoriasis, multiple sclerosis, rheumatoid arthritis and inflammatory bowel disease^{157,158}. The cytokine profile of Th17 cells includes IL-17A, IL-17F, IL-21 and IL-22^{3,134}. IL-17A and IL-17F are able to recruit and activate neutrophils as well as to stimulate epithelial, endothelial and immune cells within several tissues such as skin, lung, intestine and joints to produce inflammatory cytokines such as IL-6, IL1 and TNF α ^{134,159,160}. IL6, IL21, IL23 and TGF- β are main regulators of Th17 polarization, and the TF retinoid acid receptor-related orphan receptor gamma-T (ROR γ T) acts as the master regulator of Th17 differentiation³.

Regulatory CD4⁺ T cell differentiation and functions. There are two distinct types of Tregs, natural thymus-derived characterized by the expression of the TF Foxp3 (nTreg) and peripherally induced Tregs (iTreg) that differentiate from CD4⁺CD25⁻ cells after antigen encounter in an environment enriched with TGF- β ¹⁶¹. Both types of Tregs control immune tolerance, differentiation and effector functions of other T cells, as well as the termination of immune responses after the clearance of pathogens, thus preventing chronic inflammation^{158,162-164}. TGF- β is the main cytokine responsible for iTreg commitment by inducing the expression of the master regulator of the Treg program, Foxp3^{161,165-167}.

Follicular helper T cell differentiation and functions. Tfh are CXCR5⁺ cells located at follicular areas of lymphoid tissues, where they contribute to the development of antibody-producing B cells^{168,169}. Tfh have been classified according to their cytokine expression: Tfh1 cells secrete IFN γ , which promotes IgG2a production; Tfh2 cells produce IL-4, which induces production of IgG1 and IgE; and Tfh10 cells promote IgA production through secretion of IL-10¹⁷⁰. Cytokines such as IL-6 and IL-21 induce expression of the TF Bcl6, that is selectively expressed in Tfh cells,

and its differentiation while inhibiting differentiation to other subsets^{171,172}. On the other hand, Tfh differentiation is also dependent on the engagement of the costimulatory molecule inducible T cell costimulatory (ICOS) by its ligand ICOS-ligand (ICOSL)¹⁷³.

2.5 The actin cytoskeleton in T cell activation and migration

Several aspects of T cell biology are regulated by the actin cytoskeleton including T cell development, differentiation and signaling, migration and effector functions. In the past years, many studies have focused on individual actin-regulatory proteins, which together, have widened our understanding of the actin cytoskeleton in the regulation of T cell structure and functions, which suffer dramatic changes depending on whether cells are migrating through tissues or interacting with APCs¹⁰⁶.

The actin cytoskeleton undergoes dynamic polymerization and depolymerization during T cell activation regulated by the activity of several actin regulatory proteins¹⁷⁴. F-actin redistribution is essential for T cell function as it enables the reorganization of cellular receptors and the assembly of the signaling complex that results in the formation of the IS^{175,176}. For example, disruption of F-actin by pharmacological treatments or by depletion of actin-regulatory molecules impair IS formation and T cell activation¹⁷⁵⁻¹⁷⁷. Moreover, recognition of pMHC by the TCR leads to the rapid induction of actin cytoskeleton polarization towards the site of cell-cell contact in T cells^{175,177,178} in the form of a lamellipodium structure that enhances the surface of T-cell-APC contact that forms the basis of the IS^{175,178}. On the other hand, this pMHC-TCR interaction also induces the formation of an actin rich structure at the opposite pole, also known as the distal-pole complex¹⁷⁹. This TCR engagement activates multiple actin-regulatory proteins that together control the maturation of the IS including the actin-related protein 2/3 (Arp2/3) complex and the nucleation-promoting factors (NPFs) WASp/WIP, WAVE2 and HS1^{106,174,180} (**Figure 10**), among others.

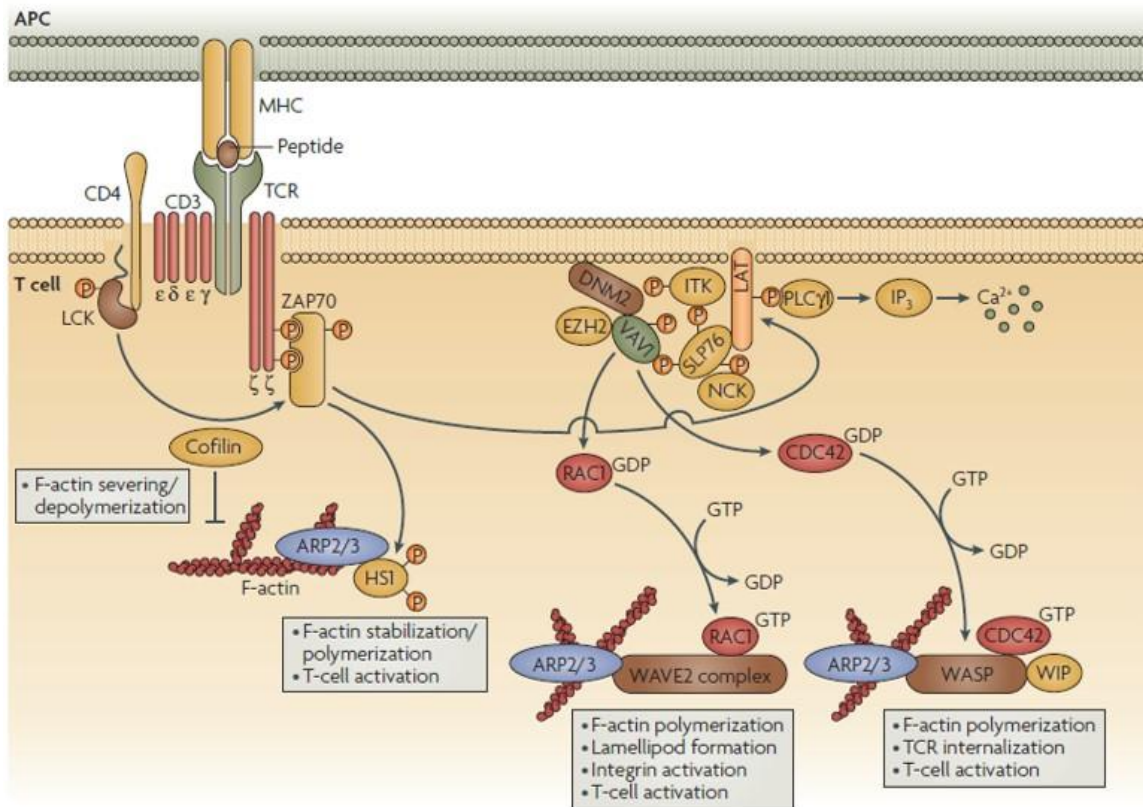


Figure 10. The signaling complex regulating F-actin dynamics during T cell activation. Upon TCR engagement, Lck and ZAP70 are activated, this leads to phosphorylation of LAT by ZAP70 and SLP76 is recruited to LAT. LAT and SLP76 act as scaffold for actin-regulatory proteins, such as PLC γ 1, Nck, Itk, and Vav1. Additionally, PLC γ 1 leads to calcium mobilization, which is essential for F-actin rearrangement. Vav1 then activates the small GTPases Cdc42 and Rac1 by exchanging GDP for GTP. Cdc42 in turn activates WASP/WIP that induce F-actin polymerization via the Arp2/3 complex. Rac1 induces activation of the Arp2/3 complex via WAVE2 activation. HS1 is phosphorylated by TCR proximal kinases and stabilizes newly generated F-actin branches. Cofilin induces F-actin severing and depolymerization during T-cell activation¹⁷⁴. Arp2/3, actin-related protein complex 2/3; Cdc42, cell division control protein 42 homolog; Itk, interleukin-2-inducible T cell kinase; Nck, non-catalytic region of tyrosine kinase; WASP2, Wiskott-Aldrich syndrome protein; WIP: WASP-interactin protein; WAVE2, WASP-family verprolin-homologous protein 2.

These molecules function downstream of the guanine nucleotide exchange factors (GEF) Vav1, as well as other GEFs that activate the Rho GTPases Rac1 and Cdc42¹⁰⁶, as described in more detail below. As previously stated, Vav1 is recruited to the IS through its association with SLP76 and Itk^{122–124}. Vav1 then induces the exchange of GDP for GTP in Cdc42 and Rac1, that in turn recruit

and activate WASp/WIP and WAVE2, respectively, that bind to the Arp2/3 complex and induce the nucleation of F-actin¹⁸¹⁻¹⁸³. WASp constitutively interacts with WIP, and disruption of this interaction results in WASp degradation^{184,185}. The importance of the WASp/WIP complex was discovered as loss-of-function mutations in WASp were responsible for severe immunodeficiencies in patients carrying this mutation¹⁸⁶. Moreover, WIP-deficient T cells showed strong defects in actin rearrangements and IL-2 production upon TCR-engagement¹⁸⁷, however, these defects were more intense in WIP-deficient than in WASP-deficient T cells, suggesting that WIP has other unknown roles besides stabilization of WASP¹⁸². On the other hand, WAVE2-deficient T cells display impaired F-actin accumulation at the IS and fail to generate lamellipodial protrusions upon TCR stimulation, in addition to reduced TCR-mediated proliferation^{188,189}. Additionally, the ABP HS1 is recruited to the IS via Vav1 upon phosphorylation by TCR proximal kinase ZAP70, which allows the stabilization of newly produced actin branches¹⁹⁰. Moreover, HS1 deficiency impedes the formation of F-actin-rich structures at the IS upon TCR stimulation¹⁹⁰, because direct interaction of HS1 with F-actin is needed to stabilize actin filaments¹⁸². Disruption of actin dynamics leads to impaired activation of the three TF that control the expression of the IL-2 gene¹⁰⁶. Similarly, disturbing calcium influx affects the signaling pathways leading to NFAT^{177,191,192}, a phenomenon that has been observed in T cells deficient for Vav1, WASp, WAVE2 and HS1, as described above.

TCR signaling not only induces the nucleation of F-actin, but also the activation of mechanisms that negatively regulate F-actin assembly, as both are necessary for dynamic cytoskeleton rearrangement¹⁷⁴. Coronin-1 is a protein that inhibits Arp2/3-mediated F-actin polymerization by direct interaction with the Arp2/3 complex. Moreover, Coronin-1-deficient T cells showed defects in chemokine-mediated migration and homing, in addition to an increased rate of apoptosis upon TCR-stimulation that was associated with a diminished pool of monomeric actin¹⁹³. On the other hand, the actin-severing protein cofilin is also required for proper IS formation¹⁹⁴, but the exact mechanism controlling cofilin functions in T cells is not well understood.

On the other hand, the T cell actin cytoskeleton controls cell shape and plasticity, while also providing mechanical forces required for T cell motility¹⁸⁰. These forces are controlled by the Rho family of GTPases, particularly Rac1 and Cdc42, as they are associated with the extension of the leading edge into the direction of migration¹⁹⁵. Expression of mutant forms of these GTPases

impair polarization and migration towards the chemokine CXCL12^{196,197}. As mentioned above, downstream effectors of these GTPases include WASp and WAVE2 that induce actin polymerization through the Arp2/3 complex. WASp has proven to be required for chemotaxis, however, several studies indicate that WAVE2 is more important for leukocyte migration^{189,198–200}. Another important GTPase for T cell migration is RhoA, that activates the protein kinase ROCK leading to phosphorylation of the myosin light chains and increased actomyosin contractility^{201,202}. RhoA is considered as a downstream effector of chemokine G protein-coupled receptors (GPCRs) and it is also involved in the activation of the high affinity state of integrins^{201,202}. Thus, Rho proteins upon GPCR engagement activate myosin, which enables the sliding of membrane patches towards the cell rear, therefore generating forward thrust in the rest of the cell¹⁹⁵. Movement of T cells is ameboid, meaning it is driven by protrusion of actin-rich pseudopodia at the leading edge, whereas contractile forces are found at the rear uropod²⁰³. While Rac1 induces the extension of the leading edge, RhoA controls the uropod tail retraction, and Cdc42 the overall cell polarity^{196,204–206}.

While many other proteins are known to regulate the functionality of the actin cytoskeleton in T cells, here, we will focus on the HS1-homolog cortactin, which was only recently found to be expressed in T cells, where only little is known about its functions.

2.5.1 The actin-binding protein cortactin

Cortactin was originally characterized as a 80/85 KDa substrate of Src kinase and later recognized as an ABP targeting actin filaments (F-actin) at the cell periphery^{207,208}. Cortactin is found to be localized at sites of dynamic actin assembly such as the leading edge of lamellipodia and podosome/invadopodia in migrating cells; and promotes the secretion of matrix metalloproteases^{208–211}. Moreover, cortactin has a hematopoietic-specific homolog known as hematopoietic cell-specific lyn substrate-1 (HS1)²¹². Both of these proteins are considered type II nucleation-promoting factors (NPF) that interact with F-actin and the Arp2/3 complex, thus regulating actin polymerization, branching, and cell motility^{212,213}. In humans, cortactin is encoded by the *CTTN* gene (formerly known as *EMS*) localized at the chromosomal region 11q13²¹⁴ (**Figure 11**).

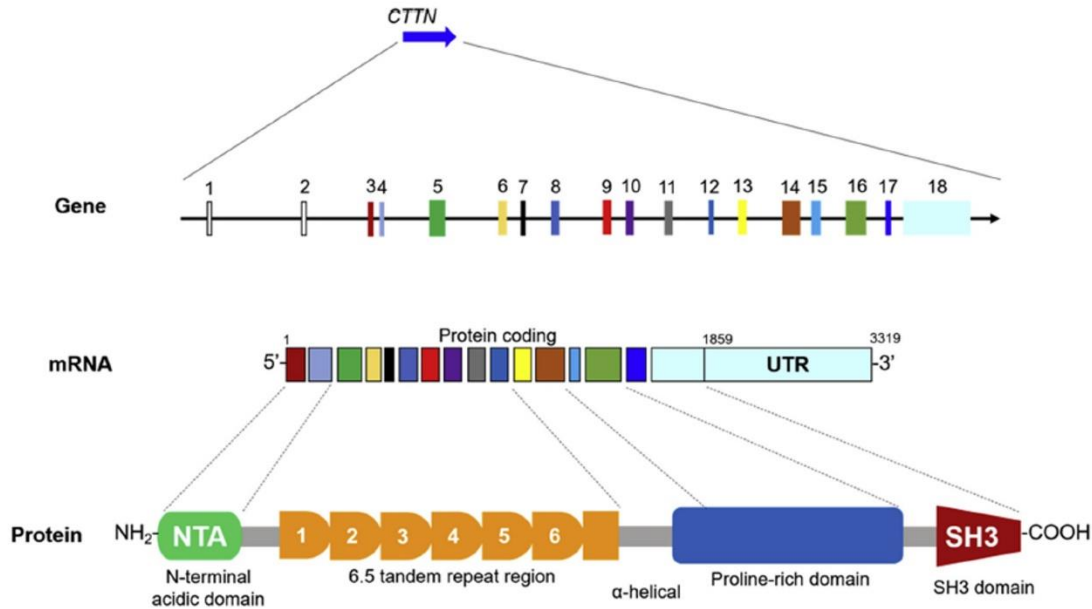


Figure 11. Schematic representation of the cortactin gene, mRNA and protein domains. The human cortactin protein is encoded by the *CTTN* gene that is located at the chromosomal region 11q13. It is composed of 18 exons, with only 16 being coding. The mature mRNA consists of 3310 bp that encodes a 80-kDa polypeptide composed of 550 amino acids resulting in the shown multi-domain protein structure²¹⁵.

The *CTTN* gene generates the almost ubiquitously expressed wild-type form of 80 kDa, and two splice variants (SV): the SV1 that lacks the exon 11 (encoding the sixth actin-binding repeat region), generating a 70 kDa protein; and the SV2 that lacks both exon 10 and 11 (encoding the fifth and sixth repeat, respectively) generating a 60 kDa protein²¹⁶ (**Figure 12**). Cortactin has a multidomain structure (**Figure 11**) comprising: 1) the N-terminal acidic (NTA) domain harboring a tryptophan at position 22 essential for Arp2/3 complex interaction; 2) the 6.5 tandem repeat region (shorter in SV1 and SV2) that mediates F-actin binding; 3) an α -helical domain with yet unknown function; 4) a proline-rich region (PRR) harboring several tyrosine, threonine and serine residues prone to phosphorylation in response to diverse stimuli; and 5) a Src homology (SH) 3 domain at the C-terminus that mediates the interaction of cortactin with several other actin-regulatory proteins^{208,215,217}.

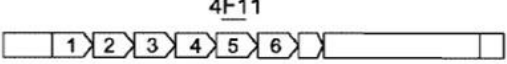


		F-actin binding	Arp2/3 activation	F-actin cross-linking	migration assays (%)	cortical localization	tyrosine phosphorylation	antibody 4F11 binding
wt		++	++	+++	160	yes	yes	yes
SV1		++	++	+/-	120	yes	yes	yes
SV2		+	+	-	90	yes	yes	no

Figure 12. Cortactin splice variants and their functionality. The SV2 variant of cortactin has the lowest affinity for F-actin binding as it lacks the actin-binding repeats 5 and 6, and it has lower Arp2/3 activation and migration-inducing capability compared to the SV1 and WT variants. However, no differences were observed in cortactin localization or phosphorylation among the variants. The 4F11 antibody against cortactin was generated targeting the 5th repeat and is thus not able to recognize the SV2 variant²¹⁶.

Moreover, cortactin functions can be modulated by post-translational modifications in response to different signaling pathways downstream of integrin engagement, chemokines and growth factor receptors²⁰⁸ (**Figure 13**). Kinases such as the Src family (including Fer, Fyn, Syk and Src), tyrosine kinases (Abl and Arg) and serine/threonine kinases (ERK1/2, p21 activated kinase and protein kinase D) are able to phosphorylate and modulate cortactin activity. For example, phosphorylation of cortactin in the PRR by Src kinases induce cell migration^{218–220}. Moreover, cells expressing the cortactin mutant Y421A fail to phosphorylate ERK in a Src-dependent manner in response to CXCR4 engagement, which resulted in impaired chemotaxis²²¹. Additionally, cortactin functions are also regulated by acetylation and deacetylation of the tandem-repeat region by histone-acetyltransferases p300 and histone deacetylase-6, respectively. Acetylation occurs in lysine residues within the tandem repeat region, that neutralizes positively charged lysine residues thus diminishing cortactin affinity for negatively charged F-actin leading to decreased cell migration^{222,223}.

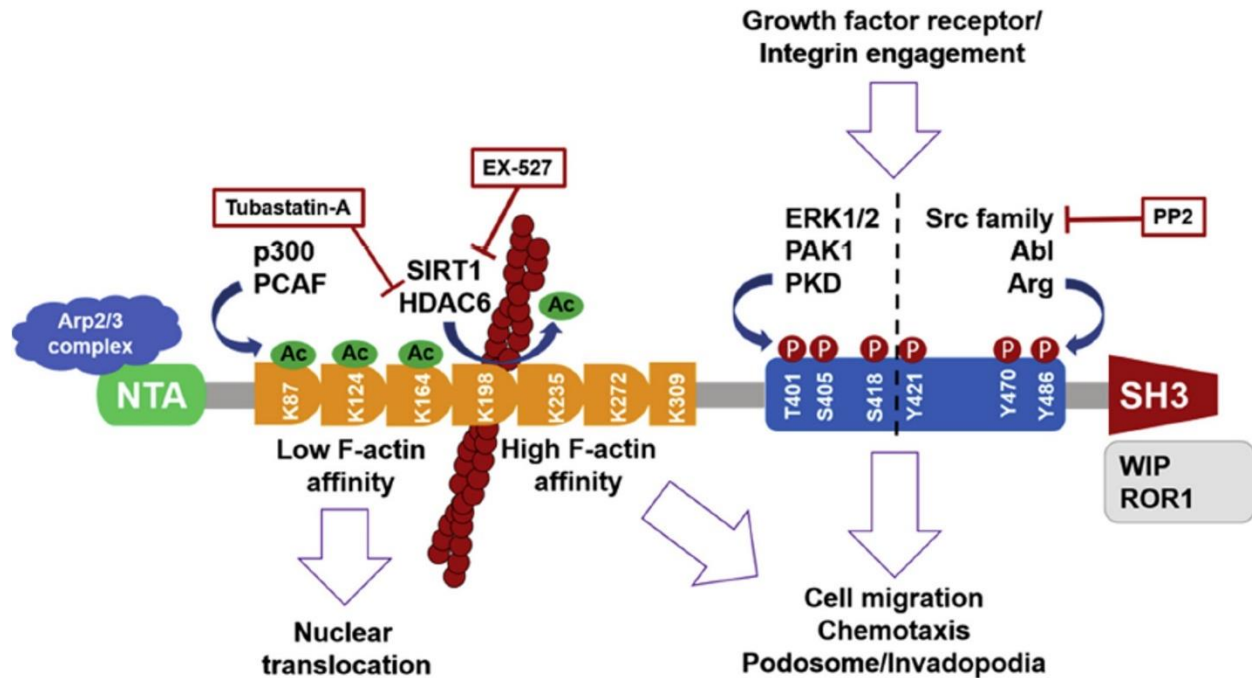


Figure 13. Post-translational modifications regulate different functions of cortactin. The cortactin protein contains many residues that are targets for post-translational modifications, such as acetylation and phosphorylation. Acetylation/deacetylation in the tandem-repeat region regulates the affinity of cortactin for F-actin, being the deacetylated form with the highest affinity. Pharmacological inhibitors of histone deacetylases can induce hyperacetylation of cortactin and its importation to the nucleus, however there is not a function associated to cortactin in the nucleus. On the other hand, phosphorylation of cortactin can regulate the activity of the protein, most likely by altering its three-dimensional structure, induce further phosphorylations or induce degradation via proteasome. Pharmacological inhibition of Src family or ERK have proven to block phosphorylation of cortactin and migration in different types of cells²¹⁵.

2.5.2 Cortactin expression in hematopoietic cells

In addition to humans, cortactin has been found expressed and fairly conserved among different organisms including sponges, worms, shrimps, insects, urochordates, fishes, amphibians, birds and other mammals^{224,225}.

Cortactin is almost ubiquitously expressed in human tissues, except for some hematopoietic cells. In accordance, the mammalian cortactin gene promoter contains putative SP-1 transcription factor binding sites similar to the ones found on TATA-less promoters or “wide-expressed housekeeping genes” promoters²²⁵. While long being considered absent in hematological cells, recent studies revealed the functional expression of cortactin messenger and protein in several types of

hematopoietic cells, as well as in hematologic malignancies, as extensively reviewed by our team²¹⁵. For example, cortactin plays important roles in platelet formation and aggregation^{226,227}; and in invadopodia formation, matrix degradation, phagocytosis and migration of dendritic cells and macrophages^{228–230}. B, NK and T cells from healthy donors only express low amounts of cortactin²³¹, and its functional relevance in these cells remains elusive. However, strong expression of cortactin has been detected in a mouse model of leukemic T cells and its expression is dependent on the presence of the serine/threonine phosphatase calcineurin²³². On the other hand, overexpression of cortactin is related to a worse outcome in B-cell chronic lymphocytic leukemia (B-CLL); and to drug resistance, organ infiltration and relapse in B-cell acute lymphoblastic leukemia (B-ALL) patients^{231,233,234}, as further discussed below.

2.5.3 HS1 and cortactin in T cell activation and migration

The functional relevance of HS1 was discovered by observing defective T cell activation and proliferation upon TCR engagement in HS1-deficient T cells²³⁵. HS1 was found to stabilize the actin filaments that support and stabilize the formation of the IS, depending on the phosphorylation at residues Y378 and Y397 by Lck and ZAP70 kinases¹⁹⁰ (**Figure 10**). These phosphorylations allowed the interaction with Vav1, Itk, the subunit p85 of PI3K and PLC γ 1, which are necessary for correct localization of HS1 at the IS^{190,236}. Moreover, depleting HS1 from T cells also resulted in reduced IL-2 production due to impaired formation of the PLC γ 1 signaling complex and therefore reduced Ca⁺⁺ influx^{190,236}.

Kv1.3 is a voltage-dependent potassium channel that plays essential roles in T cell activation as it is necessary to sustain calcium-release-activated calcium (CRAC) channel-mediated calcium mobilization^{237–239}; and HS1 colocalized with Kv1.3 at the IS upon TCR engagement, but not in resting cells²⁴⁰. Furthermore, Kv1.3 can be recruited to the IS independently of HS1, however, it is suggested that the interaction of these two through their SH3 domains is necessary for sustained localization of Kv1.3 at the IS^{212,240}. In addition, HS1 is phosphorylated at Y378 by Nck upon CXCL12 stimulation to induce actin polymerization and T cell migration²⁴¹.

On the other hand, evidence for cortactin relevance in T cell biology is scarce. For example, analysis of IS formation using staphylococcal superantigen E (SEE)-loaded Nalm-6 and Jurkat

cells showed that cortactin is recruited to the IS, colocalizing with WASP and filamentous actin²⁴² (**Figure 14**). However, the functional relevance of cortactin at the IS was not analyzed. Moreover, cortactin has been found to mediate CXCR4-dependent cell migration in T-ALL, as described in more detail below²³². Otherwise, cortactin functions in T cells are hitherto unknown.

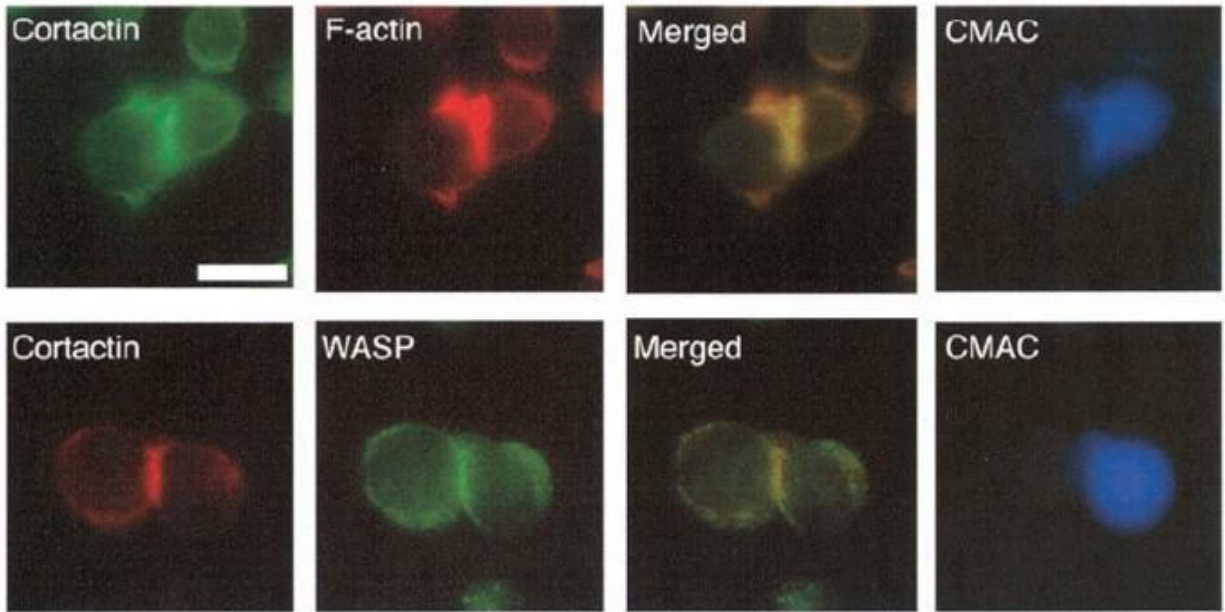


Figure 14. Cortactin is recruited to the IS and colocalizes with WASP and F-actin in T cells. Immunofluorescence staining of Jurkat cells and Nalm-6 cells (blue) stimulated with staphylococcal superantigen E. Cells were stained for cortactin (green, top; red, bottom), filamentous actin (red; top) and WASP (green; bottom). Colocalization is observed as yellow. CMAC, 7-amino-4-chloromethylcoumarin²⁴².

2.6 Pathophysiological relevance of T cell activation in T-ALL

T-ALL is an aggressive leukemia derived from the malignant transformation of T-cell precursors that accounts for 25% of all ALL cases in adults²⁴³ and 15% in children²⁴⁴. T-ALL patients have usually a worse prognosis than other ALL patients²⁴⁵. Of note, T-ALL remains an important cause of fatalities in both children and adults; however, the etiology of this disease remains elusive and is the object of intensive research²⁴⁶. An important factor that contributes to T-ALL development is the accumulation of mutations in certain genes. For, example, it has been shown that 70% of chromosomal translocations in childhood T-ALL involve genes belonging to oncogenic TFs with important roles during hematopoiesis²⁴⁷. Gain-of-function mutations in the oncogenes *SCL*, *LMO1*

and *NOTCH1*, in addition to an active pre-TCR were sufficient to induce malignant transformation of T-cell progenitors²⁴⁷. Moreover, constitutive expression of active Notch1 protein by retroviral delivery in HSCs induced T-ALL development²⁴⁸. Of note, *NOTCH1* and *CDKN2A/2B* genes are mutated in more than 50% of adult and childhood T-ALL cases²⁴⁹; and patients with *NOTCH1* mutations have shown that additional mutations or deletions in the tumor suppressor *PTEN* gene, which causes aberrant phosphatidylinositol 3-kinase (PI3K)-AKT signaling, have a worse prognosis than patients with only *NOTCH1* mutations^{250,251}.

Based on stage-specific differentiation markers, T-ALL can be sub-classified into early T-cell precursor-ALL (ETP-ALL), cortical, and mature T-ALL. ETP-ALL is characterized by the absence of CD4, CD8, and CD1a and expression of one or more myeloid-lineage markers²⁵². ETP-ALL presents a block at the earliest stages of T cell differentiation (CD4⁻CD8⁻) and a transcriptional program that resembles that of the early T-lineage progenitor cells, HSCs and myeloid progenitors. On the other hand, cortical T-ALLs characterized by a CD1a⁺CD4⁺CD8⁺ immunophenotype usually presents with a favorable prognosis. Finally, the more mature late cortical thymocyte T-ALL presents a CD4⁺CD8⁺CD3⁺ immunophenotype and is characterized by gain-of-functions mutations in the *SCL* oncogene²⁵². Standard chemotherapy regimens result in remission in approximately 80% of pediatric and 45% of adult T-ALL patients, but not in ETP-ALL that has a higher rate of relapse, with a 10-year overall survival of only 19% compared to 84% for all other T-ALLs²⁵³.

Infiltration of the CNS is an important aspect of T-ALL pathophysiology²⁵⁴. However, the mechanisms that govern invasion of the CNS by T-ALL cells are not fully understood. In addition, leukemic T cells also infiltrate frequently other organs such as skin, lungs, and the gastrointestinal tract when compared with leukemic leukocytes of other hematopoietic malignancies²⁵⁵. T-ALL cells achieve this migratory potential by exploiting many of the TCR downstream effector pathways, and chemokine and adhesion molecules expressed on activated T cells, as described below.

Adhesion assays on IL-1 β -treated HUVEC using blocking antibodies revealed that blockage of E-selectin, but not VCAM-1 or LFA-1, completely inhibited T-ALL cell adhesion, hence suggesting that binding of E-selectin with its counterreceptors PSGL-1, L-selectin, CD44 or CD43 might initiate the firsts steps of TEM of leukemic T-cells²⁵⁶. T-ALL cells overexpress chemokine

receptors such as CXCR4^{232,257,258}, CXCR7²⁵⁹ and CCR7^{258,260}. Pharmacological inhibition of CXCR4 in xenotransplantation experiments of T-ALL cells into NSG mice significantly reduced leukemic engraftment to BM and CNS involvement²⁵⁴. On the other hand, CXCR7 was shown to improve CXCL12-induced migration of T-ALL in *in vitro* models²⁵⁹. In addition, specific knock-down of CCR7 in leukemic T cells or depletion of its ligand CCL19 in animal models specifically inhibited T-ALL cell infiltration to CNS²⁶⁰. High levels of ZAP-70, a Syk-family tyrosine kinase constitutively expressed in T cells mediated downstream signaling of pre-TCR and fully mature TCR²⁶¹, that enhanced migration towards the chemokines CXCL12, CCL21 and CCL19 *in vitro*²⁵⁸. This phenomenon was mediated by ZAP70-dependent phosphorylation of ERK that, in turn, induced up-regulation of CXCR4 and CCR7 on the cell surface. Moreover, high ZAP70 levels in CNS-infiltrated T-ALL patient samples positively correlated with high expression of CCR7 and CXCR4²⁵⁸, thus likely enhancing T-ALL infiltration due to overexpression of these receptors. Stimulation of CXCR4 by CXCL12 in the BM is important for the maintenance of HSCs, as well as leukemic T cell homing and stemness maintenance by positioning T-ALL cells in supportive niches within the BM²³². Using *in vivo* imaging, T-ALL cells were found to be intimately in contact with CXCL12-producing vascular endothelial cells within the BM²⁵⁷. Furthermore, conditional deletion of the *Cxcr4* gene in murine T-ALL cells greatly reduced the overall number of T-ALL cells and suppressed the infiltration to BM, spleen, thymus and other organs²⁵⁷. Moreover, *Cxcr4* gene deletion in T-ALL after leukemia establishment prolonged the survival of mice²⁵⁷. Several studies have found that calcineurin is hyperactive in human and mouse models of lymphomas and ALL^{262–265}. Critical effectors of calcineurin include the NFAT transcription family, which are essential for T cell development, as well as for T cell differentiation, activation and anergy^{266,267}. Moreover, calcineurin was found to be crucial for T-ALL maintenance and infiltration^{262,268}. The authors have demonstrated that T-ALL cells lacking calcineurin presented impaired chemotaxis and migration due to defective CXCR4 trafficking²³². Moreover, they showed that calcineurin inactivation in these cells inhibited the expression of cortactin²³², a protein that binds to F-actin and other proteins involved in F-actin polymerization^{208,269}. Given the requirement of actin polymerization for CXCR4 trafficking, they proposed that cortactin deficiency may disturb CXCR4 dynamics²³² (**Figure 15**). However, other roles of cortactin in the pathophysiology of leukemic T cells remain unexplored.

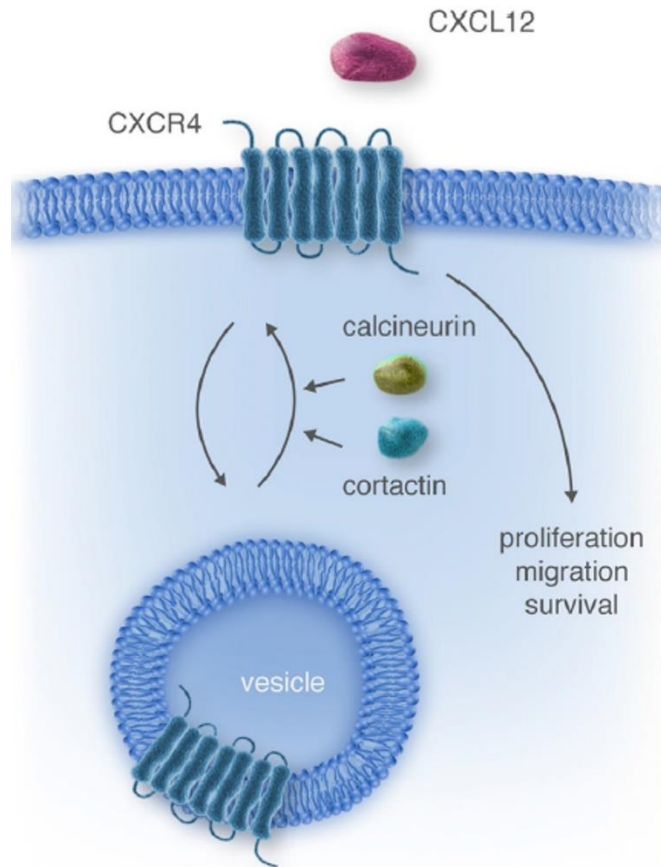


Figure 15. Surface expression of CXCR4 in leukemic T-cells depends on cortactin and calcineurin. T-ALL cells display hyperactive calcineurin activity. Calcineurin controls the expression of cortactin in leukemic T cells, which is essential for CXCR4 trafficking to the cell membrane. Moreover, high CXCR4 expression in T-ALL induces leukemic T cell proliferation, migration and T-ALL disease progression²⁷⁰. T-ALL, T-cell acute lymphoblastic leukemia.

3. JUSTIFICATION

Cortactin is an actin-binding protein important for several cellular processes in different types of cells. In T cells, most studies have focused on the cortactin homolog HS1, since cortactin expression has long been considered absent. However, recent evidence demonstrated the expression of cortactin in T cells, and that it is recruited to the IS. However, the functional relevance of cortactin expression in T cells is still unknown. Moreover, cortactin is overexpressed in different leukemic cells and has been associated with a worse outcome for patients with B-CLL and B-ALL, but the importance of cortactin in T-ALL has never been investigated. Thus, it is tempting to speculate that cortactin is also related with the poor prognosis and the aggressive phenotype observed in T-ALL leukemia.

4. HYPOTHESIS AND AIMS

4.1 Hypothesis

Cortactin is necessary for T cell activation, migration and effector functions; and is associated with the aggressive infiltrative phenotype of T-cell acute lymphoblastic leukemia.

4.2 General aim

To elucidate the role of cortactin in the activation of normal T cells and in the pathophysiology of T-cell acute lymphoblastic leukemia.

4.2.1 Particular aims

- I. To characterize the expression and localization of cortactin in T cells upon activation.
- II. To analyze the functional relevance of cortactin during T cell activation and migration.
- III. To explore cortactin-associated signaling pathways and actin dynamics downstream of TCR engagement.
- IV. To determine the role of cortactin in T-ALL pathophysiology.

5. MATERIALS AND METHODS

5.1 Materials

5.1.1 Reagents

Table 1. List of chemicals and reagents used in this work.

Chemicals	Company and catalogue number
2-propanol	Sigma # I9516
30% Acrylamide/bis solution	BioRad #161-0153
Accutase®	Sigma #A6964-100ML
Acetic acid glacial	J.T Baker #9508-05
Agarose	Cleaver Scientific Ltd #CSL-AG500
Ammonium persulfate	BioRad #161-0700
Alexa Fluor 488™ phalloidin	Invitrogen™ #A12379
ANESKET® (Ketamine)	PiSA #Q-7833-028
Antibiotic Antimycotic 100X	Corning #30-004-CI
BD Pharm Lyse™	BD Biosciences #555899
Bovine serum albumin	Sigma #A2153-100G
Brefeldin A Solution (1,000X)	Biolegend #420601
CaCl ₂	J.T. Baker #1313-01
Chloroform	Sigma #C2432
Complete protease inhibitor cocktail	Roche #11697498001
D-glucose	Macron #4912-12
Ethylenediaminetetraacetic acid (EDTA)	Sigma #E9884-500G
Ethylene glycol-bis(2-aminoethylether)-N,N,N',N'-tetraacetic acid (EGTA)	Sigma #E3889
Ethyl alcohol	Sigma #E703-1L
Fetal bovine serum	Biowest #S1810
Glycerol	Sigma #G6279-500ML
Glycine	J.T. Baker #4059-06
HCl	J.T Baker #9535-05
HEPES	Biowest #P5455-100GR
Hoechst33342	Sigma #B2261

Imidazole	Sigma #I2399
Ionomycin calcium salt from <i>Streptomyces conglobatus</i>	Sigma #I0634
KCl	J.T. Baker #3040-01
KH ₂ PO ₄ •3H ₂ O	Macron #7088-04
L-glutamine 100X	Gibco #A2916801
Lymphoprep™	Alere technologies #04-03-9391/02
MEM NEAA 100X	Gibco #11140-050
Methyl alcohol	J.T. Baker #9070-03
MgSO ₄ •7H ₂ O	Merck #A999986
Mitomycin-C	Sigma#M5353
Murine SDF-1 α (CXCL12)	PreproTech #250-20A-10UG
Na ₂ HPO ₄ •7H ₂ O	J.T. Baker #3824-01
Na ₃ VO ₄	Sigma #S6508
NaCl	J.T. Baker #3624-05
NaF	Sigma #S7902
NaHCO ₃	Sigma #S5761-1KG
Na-pyruvate 100X	Gibco #11360-070
Nodinet™ P-40	Sigma #21-3277 SAJ
Paraformaldehyde	Sigma #158127-500G
Phorbol 12-myristate 13-acetate	Sigma #P1585
PhosSTOP phosphatase inhibitor	Roche #04-906-845-001
Polybrene® (Hexadimetrine bromide)	Sigma #107689
Ponceau S	Merck-Millipore #159270025
PROCIN® (Xylazine)	PiSA #Q-7833-099
Protein G Sepharose®, Fast Flow	Sigma #P3296
Recombinant Human ICAM-1-Fc (carrier-free)	Biologend #552906
Recombinant Human VCAM-1-Fc (carrier-free)	Biologend #553706
Rhodamine phalloidin	Invitrogen™ #R415
Saponin	Sigma #84510-100
Skim milk	Svelty
Sodium dodecyl sulfate (SDS)	BioRad #1610302
Sodium hydroxide	Macron #7708-10

Sodium pyruvate solution	Sigma #S8636
TEMED	BioRad #161-0801
TRI Reagent®	Sigma #93289
Tris•base	J.T. Baker #4109-06
Triton™ X-100	Sigma #T9284-500
TrypLE™ Express	Gibco #12604-013
Trypsin-EDTA 0.25%	Sigma #T4049-500ML
Tween® 20	Sigma #P1379-500ML
β-Mercaptoethanol	Sigma #M3148-25ML

Table 2. List of antibodies used in this work.

Antibodies	Company and catalogue number
Alexa Fluor® 488 anti-human CD3 Antibody	Biologend #300415
Alexa Fluor® 488 anti-mouse CD3 Antibody	Biologend #100210
Alexa Fluor™ 488 goat anti-mouse IgG (H+L)	Invitrogen #A11001
Alexa Fluor™ 647 goat anti-mouse IgG (H+L)	Invitrogen #A21236
Anti-cortactin Alexa Fluor® 488/647 conjugated, clone 289H10	Kindly provided by Dr. Rottner, TU Braunschweig, Germany
Anti-CXCR4 antibody produced in rabbit	Sigma #SAB3500383
Anti-GAPDH Antibody (0411)	Santa Cruz #sc-47724
Anti-γ Tubulin Monoclonal Antibody (4D11)	ThermoFisher Scientific #MA1-850
APC anti-human CD184 (CXCR4)	Biologend #306510
APC anti-human CD29	Biologend #303007
APC anti-human CD62L Antibody	Biologend #304810
APC anti-human CD7	Biologend #343108
APC anti-human/mouse Granzyme B Recombinant Antibody	Biologend #372203
APC anti-mouse CD11a/CD18 (LFA-1) Antibody	Biologend #141009
APC anti-mouse CD184 (CXCR4)	Biologend #146507
APC Rat Anti-Mouse CD62L	BD Pharmigen™ #553152
APC/Cy7 anti-mouse CD69 Antibody	Biologend #104526
Biotin Goat anti-hamster (Armenian) IgG Antibody	Biologend #405501

Brilliant Violet 421™ anti-ERK1/2 Phospho (Thr202/Tyr204) Antibody	Biolegend #369510
Brilliant Violet™ 421 anti-human CD184 (CXCR4) Antibody	Biolegend #306518
Brilliant Violet™ 421 anti-mouse CD19 Antibody	Biolegend #115537
Brilliant Violet™ 510 anti-human CD49d	Biolegend #304317
Brilliant Violet™ 510 anti-mouse TCRβ	Biolegend #109234
FITC anti-mouse CD4	Biolegend #100406
FITC anti-mouse CD8a	Biolegend #100803
Goat anti-Mouse IgG (H+L), Superclonal™ Recombinant Secondary Antibody, Alexa Fluor™ 488	Invitrogen #A28175
Goat anti-Mouse IgG-HRP (H+L) horse radish peroxidase conjugate	Invitrogen #G21040
HS1 (D5A9) XP® Rabbit mAb (Rodent Specific)	Cell Signaling #3892S
HS1 (D83A8) XP® Rabbit mAb (Human Specific)	Cell Signaling #3890
Human TruStain FcX™ (Fc Receptor Blocking Solution)	Biolegend #422301
Mouse Anti-rabbit IgG-HRP	Santa Cruz Biotechnology #sc-2357
p44/42 MAPK (Erk1/2) (137F5) Rabbit mAb	Cell Signaling #4695S
Pacific Blue™ anti-human CD69	Biolegend #310920
Pacific Blue™ anti-mouse CD25	Biolegend #154202
Pacific Blue™ anti-mouse CD3	Biolegend #100213
PARP (46D11) Rabbit mAb	Cell Signaling #9532
PE anti-human CD10	Biolegend #312204
PE anti-human CD11a	Biolegend #350606
PE anti-human CD162	Biolegend #328806
PE anti-human CD18	Biolegend #302107
PE anti-human CD194 (CCR7)	Biolegend #353204
PE anti-mouse CD29	Biolegend #102208
PE anti-mouse CD3	Biolegend #100206
PE anti-mouse CD4	Biolegend #100408
PE anti-mouse CD8	Biolegend #100708
PE anti-mouse IFN-γ	Biolegend #505807
PE/Cy5 anti-mouse CD8	Biolegend #100709

PE/Cy7 anti-human CD11a	Biolegend #350610
PE/Cy7 anti-human CD49d	Biolegend #304313
PE/Cy7 anti-human/mouse CD44	Biolegend #103029
PE/Cy7 anti-mouse IL-2	Biolegend #503832
PE/Cy7 anti-mouse TNF- α	Biolegend #506324
PerCP/Cy5.5 anti-human CD29	Biolegend #303024
PerCP/Cy5.5 anti-mouse CD14	Biolegend #123313
Phospho-p44/42 MAPK (Erk1/2) (Thr202/Tyr204) (D13.14.4E) XP® Rabbit mAb	Cell Signaling #4370S
Purified anti-Cortactin Antibody (clone 4F11)	Biolegend #868102
Purified anti-mouse CD28 Antibody (clone 37.51)	Biolegend #102102
Purified anti-mouse CD3 ϵ Antibody (clone 145-2C11)	Biolegend #100302
Purified Goat anti-mouse IgG (minimal x-reactivity) Antibody	Biolegend #405301
Purified NA/LE Mouse Anti-Human CD28	BD Pharmigen™ #567117
Purified NA/LE Mouse Anti-Human CD3 (clone HIT3a)	BD Pharmigen™ #555366
Purified NA/LE Mouse Anti-Human CD3 (clone UCHT1)	BD Pharmigen™ #567108
TruStain FcX™ PLUS (anti-mouse CD16/32) Antibody	Biolegend #156604
Ultra-LEAF™ Purified anti-human CD28 Antibody (clone CD28.2)	Biolegend #302934
Ultra-LEAF™ Purified anti-human CD3 Antibody (clone UCHT1)	Biolegend #300438

Table 3. List of kits used in this work.

Kits	Company and catalogue number
CellTrace™ Violet (CTV, DMSO)	Invitrogen #C34557
DNase I, RNase-free	Thermoscientific #EN0521
DC™ Protein assay	BioRad #5000112
Dynabeads™ Human T-activator CD3/CD28 kit	Gibco #11161D
First Strand cDNA Synthesis Kit	Thermoscientific #K1612
MojoSort™ Human CD3 T Cell Isolation	Biolegend #480131
MojoSort™ Human CD4 T Cell Isolation	Biolegend #480130

MojoSort™ Mouse CD3 T Cell Isolation	Biolegend #480024
SuperSignal® WestFemto	ThermoFischer Scientific #34095
SYBR™ Green PCR Master Mix	ThermoFischer Scientific #4309155
Vybrant™ CFDA SE Cell Tracer Kit	Invitrogen #V12883
Zombie Aqua™ Fixable Viability Kit	Biolegend #423101
Zombie NIR™ Fixable Viability Kit	Biolegend #423106

Table 4. List of culture medium used in this work.

Culture mediums	Company and catalogue number
Dulbecco Modified Eagle's Medium (DMEM) - high glucose	Sigma #D5648-10X1L
RPMI-1640 Medium	Sigma #R4130-10X1L
RPMI Medium 1640	Gibco #31800-022 10X1L

Table 5. List of plasmids used in this work.

Plasmids	Reference
psPAX2	Addgene #12260
pMD2.G	Addgene #12259
pLentiCRISPRv2 puro	Addgene #98290

Table 6. List of buffers and solutions used in this work.

Buffers	Composition
PBS 1X	138 mM NaCl
	3 mM KCl
	8.1 mM Na ₂ HPO ₄
	1.5 mM KH ₂ PO ₄
	pH 7.4
PBS-EDTA	PBS 1X
	5 mM EDTA
	0.04% Na ₃ N

TBS 1X	150 mM NaCl 10 mM Tris•base pH 8.0
TBS-T	TBS 1X 0.1% Tween® 20
HBSS 1X	8000 mg/L NaCl 400 mg/L KCl 40 mg/L Na ₂ HPO ₄ 60 mg/L KH ₂ PO ₄ 350 mg/L NaHCO ₃ 1000 mg/L D-glucose pH 7.4
HBSS 2X	16000 mg/L NaCl 800 mg/L KCl 80 mg/L Na ₂ HPO ₄ 120 mg/L KH ₂ PO ₄ 700 mg/L NaHCO ₃ 2000 mg/L D-glucose 50 mM HEPES pH 7.4
HBSS Ca⁺ Mg²⁺	HBSS 1X 140 mg/L CaCl ₂ 120 mg/L MgSO ₄
SDS-lysis buffer	25 mM HEPES pH 7.5 2 mM EDTA 25 mM NaF 1 % SDS 1X Complete protease inhibitor cocktail
5X Laemmli buffer	0.1875 M Tris-HCl pH 6.8 45% glycerol 2.5% SDS 1.78 M β-mercaptoethanol 0.00125% bromophenol blue
SDS-PAGE buffer	25 mM Tris 192 mM glycine 0.1% SDS pH 8.3
Transfer buffer	20% methanol 25 mM Tris 192 mM glycine 0.1% SDS

Blocking buffer	TBS-T 5% BSA or skim milk
MojoSort™ Buffer 1X	PBS 1X 0.5% BSA 2 mM EDTA pH 7.2

5.2 Methods

5.2.1 Isolation of T cells from human peripheral blood

Buffy coats from healthy donors were obtained from the blood bank of Hospital Juarez (Mexico City, Mexico). The blood collection procedure was performed according to international and institutional guidelines. The buffy coats were used to isolate mononuclear cells (MNCs) by gradient centrifugation using Lymphoprep™. Briefly, buffy coats were mixed with sterile 1X PBS at a 3:1 ratio, then 35 mL of cell suspension was added on top of 15 mL of Lymphoprep™ in a 50 mL falcon tube. Cells were centrifuged at 700xg for 30 min at RT. Subsequently, MNC layer was recovered from the interphase, washed thoroughly with 1X sterile PBS and either frozen or resuspended in ice-cold 1X Mojo Sort isolation buffer to purify human T cells. Human CD3⁺ or CD4⁺ T cells were purified using the Mojo Sort™ Human CD3 or CD4 T cell negative isolation kit (Biolegend) according to the manufacturer's instructions, respectively. All procedures were approved by the Ethics, Research, and Biosafety Committees at Hospital Juarez (HJM-DIE-002-MA). All the samples were collected after written informed consent from the donors.

5.2.2 Cell culture

The human cell lines Jurkat clone E6-1 (ATCC TIB-152™), CEM-CCRF (ATCC CRM-CCL-119™), Molt-3 (ATCC CRL-1552™) and Raji (ATCC CCL-86™) were maintained in RPMI medium supplemented with 10% fetal bovine serum (FBS) and 1% antibiotic/antimycotic (AA). These cells were maintained by the addition or complete replacement with fresh medium every two-three days. To propagate cultures, 5x10⁵ cells were transferred to a new flask containing 5 mL of fresh medium. Primary T cells from healthy donors were cultured in the same media. HEK293T cells were cultured in DMEM supplemented with 10% FBS, 1% L-glutamine, 1% non-essential amino acids (NEAA), 1% sodium pyruvate and 1% AA. Cells were maintained by subculturing

before reaching 100% confluency. Cells were detached using trypsin and seeded on a new plate at 1×10^5 cells/mL in fresh medium. The human BM stromal cell line HS5 (ATCC CRL-1882™) was cultured in DMEM supplemented with 10% FBS and 1% AA. Cells were maintained by subculturing when cells were around 80-90% confluency. Cells were detached using trypsin and seeding on a new plate 1×10^5 cells in 4 mL of fresh medium. Spheroids from these cells were maintained in the same medium. The human B cell lymphoma cell line A20 (ATCC TIB-208™) and primary murine T cells were cultured in RPMI media supplemented with 10% FBS, 1% AA and 25 mM HEPES. A20 cells were maintained by the addition or replacement of fresh medium every two-three days. To propagate A20 cultures, 1×10^6 cells were transferred to a new flask containing 5 mL of fresh medium.

5.2.3 Flow cytometry analysis of T cells

T cells were stained extracellularly with fluorochrome-coupled antibodies at a 1:200 dilution, unless otherwise stated, for 30 min. Then cells were washed with FACS buffer and fixed for 20 min with 4% PFA at RT. Intracellular staining was performed upon permeabilization with FACS containing 0.1% saponin (PermWash) and using antibodies at 1:100 dilution for 45 min at RT. Acquisition was performed using a FACS Canto II cytometer, and data was analyzed using FlowJo X software.

5.2.4 T cell activation

Plates for human T cell activation were coated using 2 $\mu\text{g/mL}$ anti-CD3 (clone UCHT1) and 5 $\mu\text{g/mL}$ anti-CD28 (clone CD28.2) in PBS for 2 h at 37°C or alternatively overnight at 4°C, then washed twice with PBS. Purified human T cells were seeded on anti-CD3/28-coated plates in RPMI-1640 supplemented with 10% FBS, 1% Pen/Strep. Alternatively, cells were activated using the Dynabeads™ Human T-activator CD3/CD28 kit (Gibco) according to the manufacturer's instructions. Cells were cultured up to 7 days with medium replacement every three days. Plates for murine T cell activation were coated using 10 $\mu\text{g/mL}$ anti-CD3 (clone 145-2C11) and 2 $\mu\text{g/mL}$ anti-CD28 (clone 37.51) in PBS for 2 h at 37°C or alternatively overnight at 4°C, then washed twice with PBS. For activation of murine T cells, cells were seeded on anti-mouse CD3/28-coated U-bottom wells (96-well plates) in RPMI-1640 supplemented with 10% FBS, 1% AA and 25 mM

HEPES for 3 days. Cells were harvested by gently pipetting up and down and transferred to a 15 mL tube at the indicated time points for analysis by FACS, WB, RNA extraction or functional assays.

5.2.5 Lentivirus production

5.5×10^6 HEK 293T cells were seeded in a 100 mm petri dish containing 14 mL of complete media. Cells were then incubated at 37°C, 5% CO₂ until they reached approximately 90% confluency (usually after 24 hours). Then, a mixture containing 10 µg of the plasmid pMD2.g, 40 µg of psPAX2 and 50 µg of transfer plasmid pLentiCRISPRv2 empty or containing the sgRNA sequences (**Table 7**) for CTTN were mixed in a final volume of 945 µL with sterile water. Subsequently, 105 µL of 2M CaCl₂ were added to the mix. Finally, 1050 µL of 2X HBSS were added dropwise while vortexing to induce DNA precipitation and to avoid large clumps. Afterwards, the transfection mix was incubated at RT for 3 min and then carefully added dropwise to the HEK293T cell culture. The culture plates were gently shaken to evenly distribute the transfection mix, and then incubated at 37°C, 5% CO₂ for no more than 16 h. After this time, the medium containing the transfection mix was exchanged with 14 mL of reduced serum medium, containing 5% FBS and all the above supplements. Cells were incubated for an additional 48 h. After this time, the medium containing the viral particles was carefully recovered in 50 mL conical tubes, centrifuged to remove cell debris and filtered using 0.45 µm PES syringe filters. Supernatants were then centrifuged at 13,000 rpm for 2 h at 4°C to precipitate viral particles. The supernatant was carefully removed, and viral pellets were resuspended in 1 mL of RPMI medium supplemented with 10% FBS and 1% AA.

Table 7. Sequences of sgRNA for the generation of stable cortactin knock-down cells

CTTN#2	ATCGGCCCCCGCGTCATCCT
CTTN#4	GTCCATCGCCCAGGATGACG

5.2.6 Lentiviral transduction of Jurkat cells

After resuspending the viral pellet, 1 mL of the viral suspension was mixed with 5×10^5 Jurkat cells in 1 mL of RPMI supplemented with 10% FBS and 1% AA, and Polybrene® (hexadimethrine

bromide) was added to a final concentration of 2 $\mu\text{g}/\text{mL}$ to increase transduction efficiency. The cell-virus mixture was then centrifuged at 1800xg for 2 hours at 32°C. Subsequently, the supernatant was discarded, and the cell pellet recovered, and cultured in 3 mL RPMI supplemented with 10% FBS and 1% AA at 37°C, 5% CO₂. Additionally, cells without the viral suspension were plated to use as a negative control for transduction. After 48 hours, the medium was replaced with selection medium (RPMI supplemented with 10% FBS, 1% AA and 2 $\mu\text{g}/\text{mL}$ puromycin) to eliminate non-transduced cells. Cells were maintained in selection medium until all negative control cells died. Then cells were cultured in RPMI supplemented with 10% FBS, 1% AA and used for further applications.

5.2.7 IS formation using CD3 stimulation by FACS

Jurkat cells were labeled with APC-CD7 (1:200) and Raji cells were labeled using PE-CD10 (1:200) for 15 min at RT. Then, cells were washed with PBS and mixed in a 1:1 ratio in 100 μL final volume. Subsequently, 1 $\mu\text{g}/\text{mL}$ anti-CD3 (clone HIT3 α) antibody was added to stimulate conjugate formation. Cells were briefly pelleted at 100xg for 1 min and incubated for 1 hour at 37°C to facilitate conjugation. Then, cells were fixed by adding 100 μL of warm 4% PFA and mixed gently by pipetting up and down ten times. Cells were then washed with FACS buffer and conjugates were analyzed by flow cytometry using a BD FACS Canto II. Conjugates were detected as CD7⁺CD10⁺ events using FlowJo software. Percentage of conjugates was calculated by dividing the CD7⁺CD10⁺ events between total CD7⁺ events.

5.2.8 Analysis of phospho-ERK by flow cytometry

Prior to stimulation, cells were either serum starved overnight in serum-free RPMI-1640 media (Jurkat) or were rested in 0.1% FBS supplemented media for 1 hour (primary T cells). Then, 500,000 cells in 100 μL were left unstimulated or incubated on ice with 5 $\mu\text{g}/\text{mL}$ of anti-CD3 and 2 $\mu\text{g}/\text{mL}$ anti-CD28 for 15 min, then washed with ice-cold PBS. Subsequently, surface bound antibodies were crosslinked with 100 μL of 5 $\mu\text{g}/\text{mL}$ goat anti-mouse IgG for 15 min on ice and non-bound antibodies were washed off with ice-cold PBS. Cells were resuspended in 100 μL complete medium and activation was started by placing the cells in a water bath at 37°C. After 2,

5 and 15 min of stimulation, cells were immediately placed on ice and 100 μ L of ice-cold 4% PFA were added. Cells were fixed for 20 min and washed twice with ice-cold 1X PermWash. Next, cells were incubated with primary anti-phospho ERK (Cell Signaling) antibody at a 1:1000 dilution for 30 min. The primary antibody was washed off and cells were stained with Alexa Flour™ 647 goat anti-rabbit (Invitrogen) 1:500 for 20 min. Acquisition was performed using a FACS Canto II cytometer, and data was analyzed using FlowJo X software.

5.2.9 Chemotaxis assay

Unstimulated (resting) or activated T cells (72-h culturing on plate-bound anti-CD3/28 as described before) were counted and adjusted to 2000 cells/ μ L in complete medium. Then, 100 μ L were added in the top chamber of a Transwell plate (5 μ m pore size) and 600 μ L of complete medium containing 100 ng/mL of CXCL12 as chemoattractant agent were added to the well and transwell filters were placed into the wells. Cells were incubated for 6 h at 37°C to allow for chemotaxis. Subsequently, migrated cells were recovered from the bottom wells, counted in a Neubauer chamber using trypan blue and percentage of chemotaxis was calculated using 200,000 cells as 100%. All samples were analyzed in duplicates.

5.2.10 F-actin polymerization assay by flow cytometry

250,000 Jurkat cells were resuspended in 100 μ L and kept on ice. The cold cell suspensions were supplemented with 5 μ g/mL anti-CD3 (clone HIT3a; Biolegend) and 2 μ g/mL anti-CD28 (clone 28.2; Biolegend) and incubated on ice for 15 min. Cells were washed with ice-cold PBS and subsequently incubated on ice for 15 min with 5 μ g/mL goat anti-mouse IgG to induce crosslinking. Stimulation was started by placing cells at 37°C in a water bath for 15, 30, 60 and 180 seconds. Alternatively, cells were incubated with 100 ng/mL CXCL12 and stimulated as described above. Cells were directly transferred to 100 μ L 4% PFA and incubated for 20 min at RT. Cells were then washed twice with PermWash and 1:400 Alexa Fluor™ 488-Phalloidin was used to stain F-actin for 30 min at RT. Acquisition was performed using a FACS Canto II cytometer, and data was analyzed using FlowJo X software.

5.2.11 RNA isolation

Total RNA was isolated from T cells. Briefly, T cells were lysed in TriReagent (Sigma, USA) by vortexing for 1 min. Then, 1 part of chloroform was added to 5 parts of TriReagent and the suspension was mixed gently by inversion, followed by a 3 min incubation at RT. Next, the mix was centrifuged for 30 min at 13,000 rpm at 4°C. Subsequently, the aqueous phase was carefully recovered in a new 1.5 mL Eppendorf tube and 2 parts of 2-propanol for each 5 parts of TriReagent were added, the solution was mixed and incubated for at least 10 min at 4°C. Subsequently, the mix was centrifuged for 30 minutes at 13,000 rpm at 4°C. The supernatant was discarded, and the pellet was washed twice with 500 µL of 70% ethanol (in 0.1% diethyl pyrocarbonate [DEPC] water, as RNase inhibitor). Then, the supernatant was discarded, and the pellet dried at RT for no more than 10 min. Finally, the pellet was resuspended in 0.1% DEPC water, and RNA concentration was quantified using a Nanodrop 2000 (Thermo Scientific, Waltham MA, USA).

5.2.12 cDNA synthesis

0.1-5 µg of total RNA was used for cDNA synthesis. RNA was mixed with 1 µL of oligo (dT)₁₈ primer brought to a final volume of 11 µL with nuclease-free water, mixed gently, centrifuged and incubated at 65°C for 5 minutes in order to dissipate secondary structures of RNA. Then, the sample was incubated on ice, followed by a brief spin to collect sample at the bottom of the tube, and incubated again on ice for 2 min. Next, 4 µL of First strand 5X reaction buffer, 1 µL of RiboLock RNase Inhibitor (20 U/ µL), 2 µL of 10 mM dNTP mix and 2 µL of M-MuLV Reverse Transcriptase (all from ThermoScientific) were added to each sample in a final volume of 20 µL. The solution was gently mixed and centrifuged. Then, cDNA synthesis was performed for 60 min at 37°C in a 96-well thermal cycler (Applied Biosystems).

5.2.13 End point PCR

Expression of the cortactin mRNA was analyzed using the *Cttn* primers described in Table 8. β -actin expression was analyzed as loading control. The PCR reaction mix was prepared as follows: 1X PCR buffer, 2.5 mM MgCl₂, 0.2 mM dNTPs, 0.2 µM forward primer, 0.2 µM reverse primer, 50 ng cDNA and 0.05 µL Taq polymerase enzyme in a final volume of 20 µL with molecular

biology grade water. Amplifications were performed in a thermocycler using the following conditions: denaturation for 3 min at 95°C, followed by 30 cycles of 30 s at 94°C, 30 s at 60°C and 30 s at 72°C followed by 5 min at 72°C for a final extension for amplification of both genes. PCR amplicons were analyzed in a 2% agarose gel for 30 min at 100 V.

5.2.14 qRT-PCR

Expression of human and mouse IL-2 was analyzed using the primers described in Table 8. 7SL or β -actin were used as housekeeping genes for human and mouse samples, respectively. The PCR reaction mix was prepared as follows: 5 μ L of 2X SYBR™ green PCR master mix, 0.1 μ L of forward primer, 0.1 μ L of reverse primer and 50 ng of cDNA in a final volume of 10 μ L with molecular biology grade water. All samples were prepared in duplicates. The cycle conditions were as follows: initial denaturation for 3 min at 95°C, followed by 35 cycles of 30 s at 95°C for denaturation, 30 s at 60°C for annealing and 30 s at 72°C of extension, followed by 5 min at 72°C for a final extension. C_T values were obtained using a StepOne Real-Time PCR system. C_T values are referred to the cycle number at which the fluorescence generated by the PCR reaction crosses the threshold line. Differences in mRNA expression were calculated by the $\Delta\Delta C_T$ method. Briefly, C_T value of the target gene was subtracted to the C_T value of the housekeeping gene to obtain the ΔC_T . Then, ΔC_T from the treated sample were subtracted to the unstimulated sample used to obtain the $\Delta\Delta C_T$. Then, to obtain the fold-change between samples the following formula was used:

$$\text{Fold-change} = 2^{-\Delta\Delta C_T}$$

Table 8. Primer sequences used for end-point and qRT-PCR of T cells.

Target		Primer sequences	
Human	<i>IL2</i>	Forward	5'-TCCCAAACCTCACCAGGATGC-3'
		Reverse	5'-TCCTCCAGAGGTTTGAGTTCTTC-3'
	<i>7SL</i>	Forward	5'-ATC GGG TGT CCG CAC TAA GTT-3'
		Reverse	5'-CAG CAC GGG AGT TTT GAC CT-3'
Mouse	<i>CTTN</i>	Forward	5'-TGGATAAAAGTGCTGTGGGC-3'
		Reverse	5'-AAGGGCACACTTGTCTCTGTC-3'

<i>IL2</i>	Forward	5'-ACAGGAACCTGAAACTCCCCAG-3'
	Reverse	5'-GAGGTCCAAGTTCATCTTCTAGGC-3'
<i>β-Actin</i>	Forward	5'-TATCCACCTTCCAGCAGATGT-3'
	Reverse	5'-AGCTCAGTAACAGTCCGCCTA-3'

5.2.15 Spheroid colonization assay

25,000 HS5 cells were plated onto agarose-coated U-bottom 96-well plates and incubated at 37°C and 5% CO₂ atmosphere to induce the formation of the 3D spheroid, which usually takes 24-48 h to form²⁷¹. The day of the experiment, control and cortactin-depleted Jurkat cells were stained with CTV and CFDA, respectively. Cells were mixed in a 1:1 ratio and 50,000 cells in 100 μL of Jurkat medium were added to the HS5 spheroids. After 24 h incubation, co-cultured spheroids with leukemic T cells were washed using 1X PBS containing 50 mM EDTA and 0.04% sodium azide to remove cells adhered to the surface. Then co-cultured spheroids were fixed for 1 h using 4% PFA. Subsequently, spheroids were washed again with PBS, and then with bidistilled water to remove the salts. Spheroids were then transferred to slides, allowed to dry, and subsequently mounted using DABCO mounting medium without DAPI for microscopy analysis. Spheroids cultured alone were used as control. Images were taken using Leica SP8. The number of cells in the spheroids was quantified using Imaris software.

5.2.16 Leukemic T cell xenografts

Cortactin-depleted and control Jurkat cells were expanded in complete medium. Cells were then harvested and washed with 1X sterile PBS. Finally, cells were resuspended in 0.9% saline solution at a concentration of 30,000 cells/μL. Under sterile conditions, NSG mice were injected via the tail vein with 3 million cells. Mice were kept in the animal facility and allowed to develop leukemia for around 5 weeks, during which, mice were constantly monitored for signs of disease such as impaired motility of posterior limbs. Mice were euthanized when paralysis of posterior limbs was observed, and then BM, brain and blood were harvested. BM was flushed from the femurs and tibias by cutting the bone caps and passing PBS with the help of a syringe. BM cell suspension was passed through a strainer to remove bone fragments. The brain was mechanically disaggregated by cutting into small pieces with surgical scissors and then passed through a cell

strainer with the help of a syringe plunger. Peripheral blood erythrocytes were lysed using 1X BD Pharm lyse™ buffer according to manufacturer's instructions. Single cell suspensions were analyzed for the presence of human CD45⁺ leukemic T cells by flow cytometry. Acquisition was performed in a FACS Canto II cytometer, and data was analyzed using FlowJo X software.

5.2.17 Mice

The Institutional Animal Care and Use Committee (IACUC) of CINVESTAV approved all animal studies. Mice were kept in the animal facility of CINVESTAV. Mice were euthanized by cervical dislocation. All mice used during this work were 6-8 week old C57BL/6 wild-type or *Cttn*^{-/-272}, and NOD.Cg-*Prkdc*^{scid} *Il2rg*^{tm1Wjl}/SzJ (NSG, Jackson Laboratory).

5.2.18 Isolation of T cells from murine SLOs

Cttn^{+/+} and *Cttn*^{-/-} mice were euthanized and the thymus, spleen and LNs (inguinal, braquial, axial and submaxillary) were harvested and kept in ice-cold RPMI containing 10% FBS and 1% AA. Cells were then extracted by mechanical disaggregation using a 40 µm cell strainer and a syringe plunger. Erythrocytes were lysed in spleen suspensions using 1X BD Pharm lyse buffer according to the manufacturer's instructions. Subsequently, cells were resuspended in RPMI and passed through a 40 µm cell strainer to remove cell clumps. Finally, LNs and spleen cell suspensions were resuspended in ice-cold 1X Mojo Sort isolation buffer and purified using the Mojo Sort™ Mouse CD3 T cell negative isolation kit (Biolegend) according to the manufacturer's instructions.

5.2.19 Analysis of IS formation by IF

A20 cells were stained with 1:1000 CellTrace® Violet (CTV) dye for 10 min at 37°C. Subsequently, mouse CD3⁺ cells were mixed with A20 cells in a 3:1 ratio and incubated for 1 hour at 37°C in 100 µL of complete medium to induce synapse formation. Afterwards, cells were fixed with 4% PFA for 20 min at RT. Cells were stained extracellularly using Alexa Fluor 488®-labelled anti-CD3, then washed and permeabilized with 0.5% Triton-X in PBS+3% BSA for 10 min. Then, cells were blocked in PBS+3%BSA for 1 hour. Next, cells were incubated overnight with 1:100 primary anti-CTTN antibody. Cells were washed and incubated for 2 h at RT with secondary anti-

mouse Alexa Fluor® 647 (1:500) to stain cortactin and 1:600 Rhodamine-Phalloidin to stain F-actin. Cells were washed thrice with PBS, then washed with bidistilled water to remove salts. Cells were mounted with DABCO mounting medium without DAPI. Images were taken using a Leica SP-8. Analysis of cell polarization and signal intensity was performed using Image J and Imaris softwares.

5.2.20 Adhesion assays on ICAM-1 and VCAM-1

96-well plates were coated with 50 μL of a 2.5 $\mu\text{g}/\text{mL}$ ICAM-1-Fc or 500 ng/mL VCAM-1-Fc solution in adhesion medium (HBSS⁺⁺ containing 0.1% BSA) for 2 hours at 37°C or alternatively overnight at 4°C. Next, the wells were washed two times with 100 μL of adhesion medium. A suspension of 2000 cells/ μL were stained with CFDA (5 μM CFDA for 5 min in a water bath with constant shaking) and 50 μL (100,000 cells) were added to each well. Then, 50 μL of the different treatments in adhesion medium were added to achieve the final concentrations (50 ng/mL PMA, 5 $\mu\text{g}/\text{mL}$ anti-CD3 or 100 ng/mL CXCL12). Cells were incubated for 15 min at 37°C. Subsequently, using a multichannel pipet, non-adherent cells were carefully washed away with 150 μL pre-warmed HBSS⁺⁺ three times with gentle shaking of the plate. Finally, wells were left with 100 μL of HBSS⁺⁺. Unwashed wells were used as 100% fluorescence control. All samples were analyzed as duplicates. The fluorescence of adhered cells at the bottom of the well was read at 488 nm in a TECAN infiniteF200PRO spectrometer and percentage of adhered cells was calculated by dividing the fluorescence of adhered cells between unwashed cells.

5.2.21 Statistics

Graph Pad Prism 5 software was used to perform statistical data analysis. Differences between two groups were analyzed by Student's T-test, considering statistically significant values of $p < 0.05$. Differences between more than two groups were analyzed by One-way ANOVA, whereas differences between more than two groups with different conditions was determined by Two-way ANOVA considering statistically significant values of $p < 0.05$.

6. RESULTS

6.1 Cortactin is expressed in T cells

Given the contradicting reports on cortactin expression in hematopoietic cells in general and T cells in particular^{190,231,242}, we first analyzed cortactin expression in different human and mouse primary cells and cell lines by western blot. For this, we used normal CD4⁺ T cells isolated from healthy donors, and the T-ALL cell lines, Jurkat, CEM and Molt-3, which are described in detail in **Table 9**. We detected a low expression of the 70 kDa SV1 isoform of cortactin in normal CD4⁺ T cells. Moreover, Jurkat and Molt-3 cells displayed a very prominent expression of the same SV1 isoform as in normal T cells, whereas expression of cortactin in CEM was low to undetectable (**Figure 16A**). On the other hand, normal murine T cells also expressed very low levels of the SV1 isoform of cortactin, whereas the leukemic T cell line 6645/4 expressed much higher levels (**Figure 16B**). As a control, murine B cells showed the expression of the 60 kDa SV2 isoform, as reported previously²³³. The cortactin hematopoietic homolog HS1, which we analyzed as positive control, showed high expression in normal human T cells, while it was reduced in leukemic T cells suggesting a potential compensatory role for cortactin in leukemic T cells.

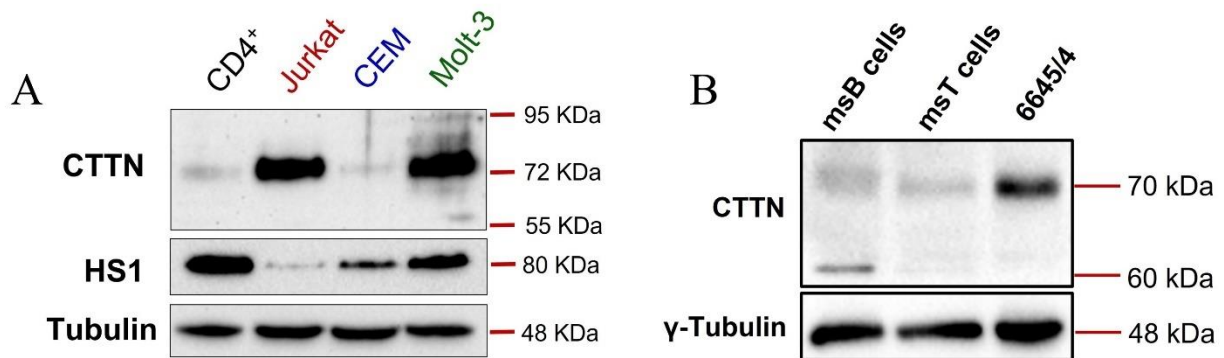


Figure 16. Cortactin expression in different human and murine T cells. Representative blots of cortactin (CTTN) and the cortactin homologue HS1 in different human (A) and mouse (B) primary T cells and T cell lines. Unstimulated cells were lysed in SDS-lysis buffer and proteins were separated in 8% SDS-PAGE. Blots were incubated with anti-CTTN antibody (clone 289H10) and specific human or rodent HS1. γ -tubulin was used as loading control. n=4 (human) and 3 (mouse).

Table 9. Characteristics of the different T-ALL cell lines

Cell line	Jurkat Clone E6	CCRF-CEM	MOLT-3
Cell type	T cell lymphoblast	T cell lymphoblast	T cell lymphoblast
Source	Peripheral blood	Peripheral blood	Peripheral blood
Debut or relapse	Relapse	Relapse	Relapse
Gender	Male	Female	Male
Age	14	4	19
Immunophenotype	CD3+	CD3+/-	CD2+
	CD4+	CD4+	CD4+
	CD5+	CD5+	CD6+
	CD6+	CD6+	CD8+
	CD7+	CD7+	CD7+
	TCR α/β +	TCR α/β +	CD5+
	CD8-	CD8-	CD3-
	CD13-	CD2-	TCR α/β -
	CD19-	CD34-	CD34-
		CD13-	CD13-
	CD19-	CD19-	

6.2 Molecules important for synapse formation and migration are expressed in T cells

We further characterized T-ALL cell lines for the expression of different adhesion molecules and chemokine receptors that mediate important T cell functions such as IS formation and migration. We analyzed the expression of CD62L (L-selectin), CD162 (PSGL-1), CD11b, CD11a/CD18 (LFA-1), CD49d/CD29 (VLA-4), CXCR4 and CCR7 (**Figure 17**). We detected that CEM, but not Jurkat and Molt-3, express significantly more CD11a than normal T cells. However, CD18 expression was significantly higher in all three cell lines. By contrast, expression of CD11b was not detected in T cells, suggesting that the integrin Mac-1 is not expressed in these T cells. We also found that all three leukemic cell lines displayed significantly higher levels of the integrin VLA-4 (CD49d and CD29) that is important for T cell migration²⁷³, and the homing and

dissemination of leukemic T cells into the BM and peripheral organs^{274,275}, as well as for inducing chemoresistance of T-ALL and B-ALL upon binding to its ligand VCAM-1^{276,277}, that is highly expressed in BM stromal cells.

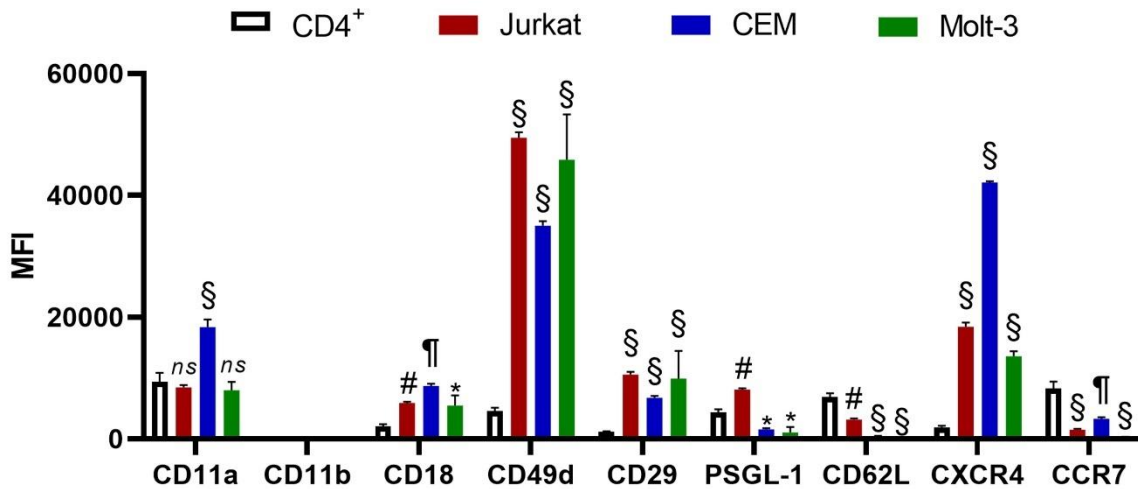


Figure 17. Expression of adhesion molecules and chemokine receptors in human T-ALL cell lines. Normal CD4⁺ and leukemic T cells were stained for the indicated surface molecules. Samples were acquired using a FACS Canto II cytometer. Data were analyzed by FlowJo X software and are presented as mean fluorescence intensity \pm SD n=3. Statistical analysis was performed by two-way ANOVA using Graph Pad. Significance was calculated by comparing expression in T-ALLs against expression in CD4⁺. *p \leq 0.05, #p \leq 0.01, ¶p \leq 0.001, § \leq 0.0001. ns, not significant.

Additionally, Jurkat cells express significantly more PSGL-1 than normal T cells, whereas PSGL-1 expression in CEM and Molt-3 was reduced compared to normal T cells. In addition, L-selectin expression was significantly lower in all three cell lines compared to normal T cells, with an especially low expression in CEM and Molt-3. Of note, expression of CXCR4 was significantly higher in all leukemic cell lines, with CEM displaying the highest expression suggesting that this cell line is able to migrate more efficiently towards a CXCL12 gradient. Moreover, CCR7 expression was diminished in Jurkat and CEM compared to normal T cells, and low to absent in Molt-3, thus, these cell lines seem to rely mostly on CXCR4 for migration.

On the other hand, analysis of murine cells revealed that expression of CD62L was also reduced in the mouse T-ALL cell line 6645/4 compared to normal T cells. We observed that expression of CD49d was similar in normal and leukemic T cells, whereas CD29 was increased in leukemic T

cells. Furthermore, we detected that LFA-1 expression was absent in murine leukemic T cells, whereas CXCR4 expression was also increased in murine leukemic T cells compared to normal murine T cells (**Figure 18**). Thus, this cell line possesses the molecular machinery for migration and IS formation. Given the absence of LFA-1 in the 6645/4 cell line, we suspect that this cell line might be dependent on VLA-4 for motility, however we do not discard that migration of this cell line rather relies on Mac-1, which we were not able to analyze here.

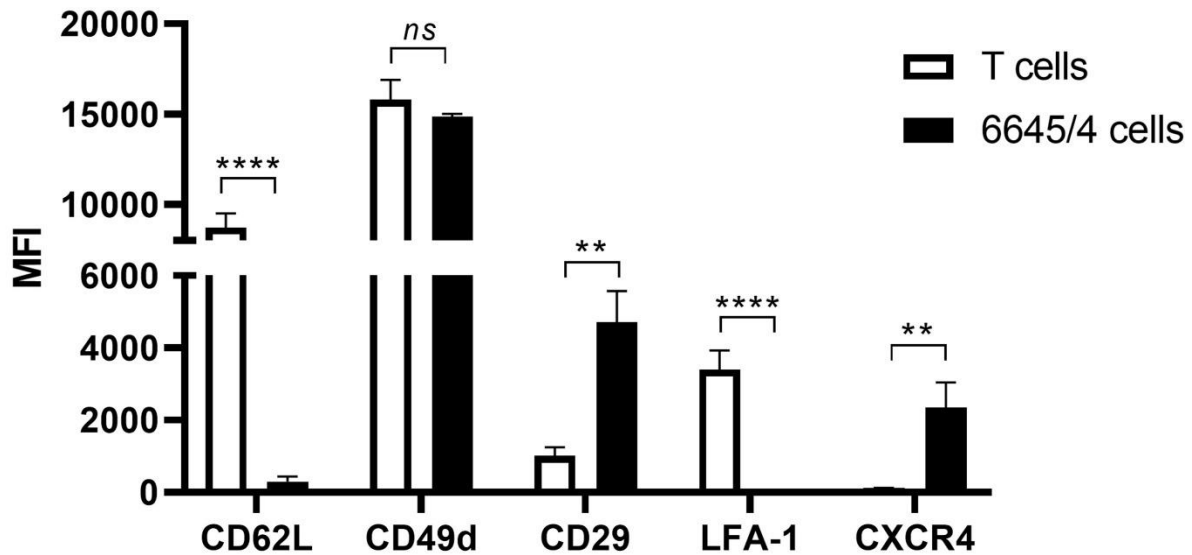


Figure 18. Expression of adhesion molecules and CXCR4 in murine T-ALL cell line 6645/4. Normal mouse CD3⁺ and leukemic T cell 6645/4 were stained for the indicated surface molecules. Samples were acquired using a FACS Canto II cytometer. Data were analyzed by FlowJo X software and are presented as mean fluorescence intensity \pm SD n=3. Statistical analysis was performed by two-way ANOVA using Graph Pad. Significance was calculated by comparing expression in 6645/4 cells against expression in T cells. *p \leq 0.05, **p \leq 0.011, ***p \leq 0.001, ****p \leq 0.0001. ns, not significant.

6.3 Cortactin is recruited to the IS in T cells

In order to identify the cellular localization of cortactin and its homologue HS1, we performed immunofluorescence stainings in primary human T cells. Using confocal microscopy, we observed that both cortactin and HS1 colocalized in the cell periphery (**Figure 19A**), similar to the cortical localization reported in the literature. Given that cortactin was detected at the IS in Jurkat cells²⁴²,

we wanted to corroborate this cortactin localization at the IS in T cells. To this end, we analyzed the formation of the IS either using APCs or anti-CD3/28 coated beads. We observed that cortactin was polarized to the site of cell-cell contact together with CD3 and F-actin when cells were conjugated with monocytes as APCs (**Figure 19B**). On the other hand, using anti-CD3/28 beads, we observed a pronounced polarization and recruitment of F-actin and cortactin around the site of cell-bead contact (**Figure 19C**).

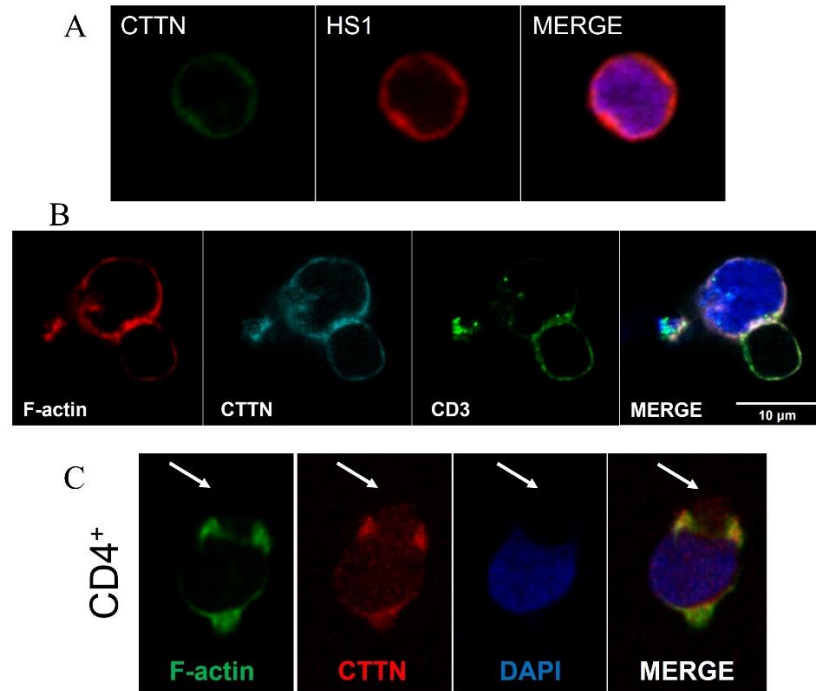


Figure 19. Cortactin colocalizes with HS1 in resting cells and is recruited to the IS. Representative images of resting and conjugated T cells. A) cortactin and HS1 staining in resting human CD4⁺ cells. B) human T cells were coincubated with monocytes (blue) and stimulated with anti-CD3 antibody (clone HIT3 α). Then, CD3, CTTN and F-actin were stained. CD3 (clone UCHT1) staining was used as control for polarization. C) Human CD3⁺ cells were conjugated with anti-CD3/28-coated beads and stained as before. The white arrow highlights the presence of the anti-CD3/28 bead. Representative images of 3 independent experiments are shown.

Next, we conjugated Jurkat cells, as example of a leukemic cell line with increased cortactin expression, with Raji B cells or anti-CD3/28-conjugated beads. Conjugation of Jurkat with Raji B cells resulted in a very pronounced polarization of F-actin, cortactin and CD3 to the site of cell-

cell contact where all 3 proteins colocalized (**Figure 20**). Therefore, our results suggest a potential important role of cortactin in T cell biology.

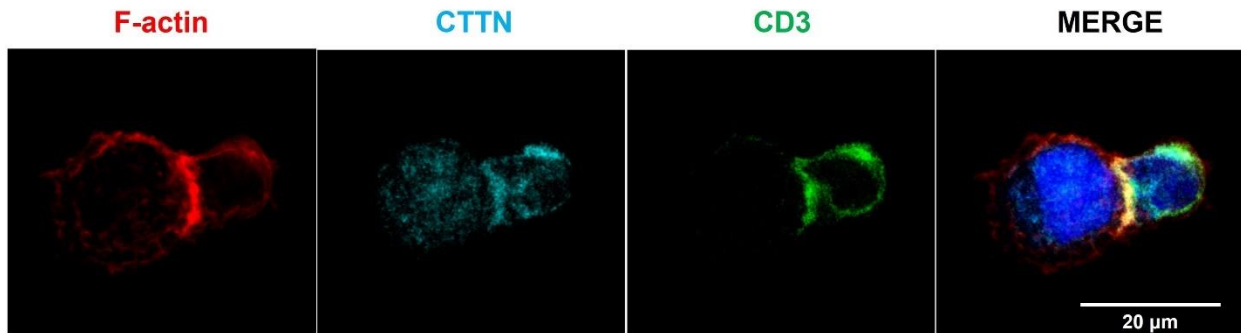


Figure 20. Cortactin localizes at the IS with Jurkat cells. Representative images of Jurkat cells conjugated with Raji B cells or anti-CD3/28 beads. Jurkat cells were stimulated with anti-CD3 antibodies to induce conjugation with Raji cells (blue). F-actin (red), cortactin (CTTN; cyan) and CD3 (green) were stained. Representative images of 3 independent experiments are shown.

Similar to human T cells, we also detected that cortactin is localized at the cell periphery together with CD3 and F-actin in resting mouse CD3⁺ cells (**Figure 21A**). Moreover, conjugation of mouse CD3⁺ cells with B-cell lymphoma cell line A20 revealed that CD3, F-actin, as well as cortactin were enriched at the site of cell-cell contact (**Figure 21B**), thus demonstrating that cortactin is also recruited to the IS in murine T cells and might have similar roles like in human T cells.

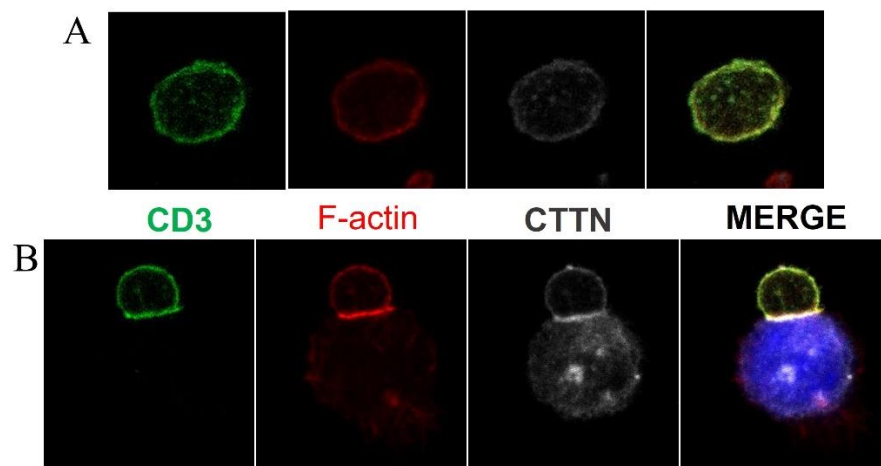


Figure 21. Cortactin colocalizes at the cell periphery in resting cells and is recruited to the IS. Representative images of resting and conjugated mouse T cells. A) CD3 (green), cortactin (gray) and F-actin (red) staining in resting mouse CD3⁺ cells. B) Mouse CD3⁺ cells were coincubated with B-cell lymphoma cell line A20 (blue) to induce the formation of the IS. Then, cells were stained as before. CD3 staining was used as control for polarization. Representative images of 3 independent experiments are shown.

6.4 Cortactin expression is upregulated in T cells upon TCR engagement, with mouse T cells switching isoforms

Given that cortactin is indeed recruited to the IS, it is also likely to be participating in T cell activation. Therefore, we next aimed to analyze cortactin dynamics upon T cell activation. To this end, we stimulated human and murine T cells with plate-bound anti-CD3/28 antibodies and then analyzed cortactin and HS1 expression by WB. We found that human T cells significantly increased the expression of cortactin over time upon activation. Of note, we observed significant downregulation of HS1 while cortactin increased (**Figure 22A&B**). In addition, resting murine T cells expressed the SV1 variant of cortactin of 70 KDa; and we observed a switch to the expression of the full-length 80 KDa form of cortactin upon activation (**Figure 22 C&D**). However, the overall amount of cortactin expression here remained unchanged. The mechanism driving this switch and the functional relevance remain elusive. Moreover, HS1 expression in murine T cells was unaffected by activation.

Stimulating different leukemic T cell lines including Jurkat, CEM, Molt-3 and normal human primary T cells with a combination of phorbol 12-myristate 13-acetate (PMA) and ionomycin (**Figure 23**), we observed a strong up-regulation of cortactin expression over time. Moreover, downregulation of HS1 was observed only in normal T cells after 3 days, whereas Jurkat cells significantly increased HS1 expression with these stimuli. HS1 expression in CEM and Molt-3 remained unchanged. Taken together, these results suggest that cortactin, by being upregulated, fulfills important functions in activated T cells.

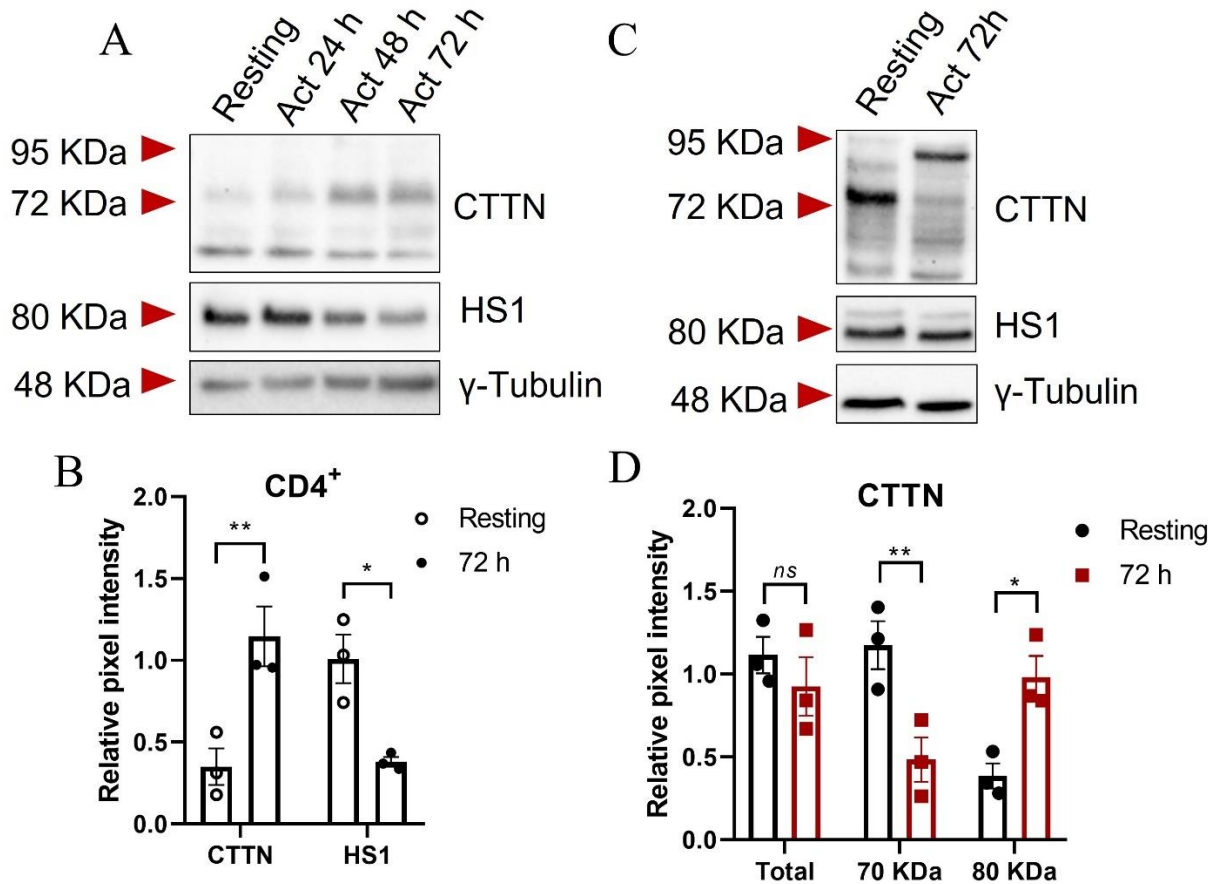


Figure 22. Cortactin expression increases in human and murine T cells upon activation. Cortactin and HS1 expression was determined by western blot using lysates from resting or activated human (A&B) or mouse (C&D) primary T cells. Cells were activated by incubation on plate-bound anti-CD3/28 for 72 h. γ -Tubulin was used as loading control. Densitometric analysis of the relative pixel intensity was performed using Image J software. Statistical analysis was determined by two-way ANOVA using Graph Pad software. Data are represented as mean \pm SD; n=3. * p <0.05, ** p <0.01. ns, not significant.

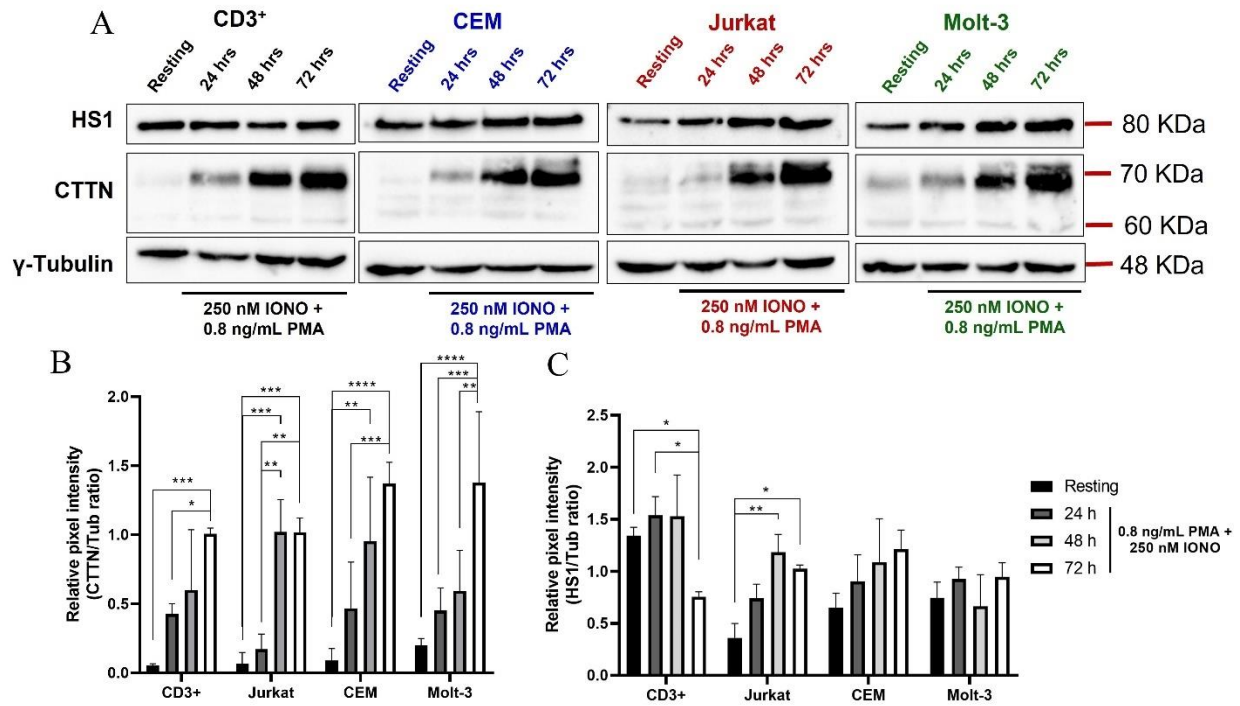


Figure 23. Cortactin expression increases in human T cells upon activation using PMA and ionomycin. Cortactin and HS1 expression was determined by western blot using lysates from resting or activated human T cells. Cells were activated using PMA and ionomycin for the indicated times. γ -Tubulin was used as loading control. A) Representative blots from four independent experiments are shown. B&C) Relative pixel intensity of cortactin and HS1 from the blots shown in A. Densitometric analysis of the relative pixel intensity was performed using Image J software. Statistical analysis was determined by two-way ANOVA using Graph Pad software. Data are represented as mean \pm SEM; n=3. * $p \leq 0.05$, ** $p \leq 0.01$, *** $p \leq 0.001$, **** $p \leq 0.0001$.

6.5 Cortactin expression is similar in CD4⁺ and CD8⁺ T cells

T cells differentiate into different subsets that control different aspects of immune responses. The most prominent subsets are characterized by the expression of CD4 or CD8. Therefore, we wanted to analyze whether cortactin is differentially expressed in these subsets. Using flow cytometry, we identified that expression of cortactin in both CD4⁺ and CD8⁺ T cells was similarly low under basal conditions (resting cells), whereas upon activation, both T cell subtypes upregulated the expression of cortactin in a similar fashion over four days (**Figure 24**), before again reducing cortactin expression probably due to the lack of continuous stimulation. Thus, our data suggest

that cortactin might play essential roles in activated human T cells regardless of their differentiation stage as T helper or cytotoxic T cells.

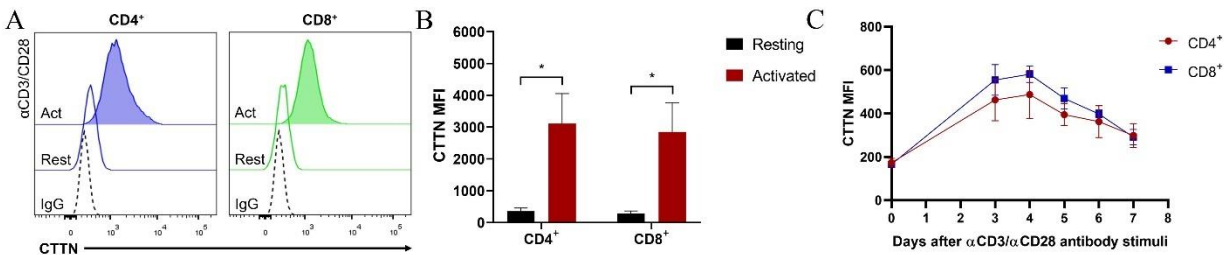


Figure 24. Cortactin expression is similar in resting and activated human CD4⁺ and CD8⁺ T cells. Cortactin expression was analyzed in resting and activated CD4⁺ and CD8⁺ T cell subsets. A) Representative flow cytometric histograms of cortactin expression in CD4⁺ and CD8⁺ T cell subsets. B) Quantification of the mean fluorescence intensity (MFI) of cortactin from the histograms shown in panel A. C) Analysis of cortactin expression in T cells after activation with anti-CD3/28 antibodies at the indicated times. Samples were acquired using a BD FACS Canto II. Data were analyzed by FlowJo X software. Data are represented as MFI \pm SD; n=3. Statistical analysis was performed by two-way ANOVA using Graph Pad. *p \leq 0.05.

6.6 Cortactin-depleted Jurkat cells present similar expression of adhesion molecules and similar rates of proliferation and apoptosis

To analyze the role of cortactin in T cells, we generated stable cortactin-depleted Jurkat cells. We confirmed significant cortactin-depletion of around 75% by flow cytometry and western blot (**Figure 25**). Moreover, we observed that the cortactin homolog, HS1, remained unchanged indicating that HS1 does not compensate for the depletion of cortactin. Further characterization of cortactin-depleted Jurkat cells showed that cortactin absence does not impact on apoptosis measured as proportion of cleaved vs total PARP (**Figure 26A&B**). On the other hand, we measured proliferation by CFDA dilution. Briefly, cells were rested overnight in RPMI medium without serum, then cells were stained with the vital colorant CFDA. Cells were then incubated again with medium containing serum. Each time cells divide the intensity of fluorescence reduces by 50%. By measuring the intensity of CFDA fluorescence by flow cytometry, we observed a similar reduction of the signal intensity over time, thus, the proliferation of cortactin-depleted Jurkat cells was similar to control cells (**Figure 26C**).

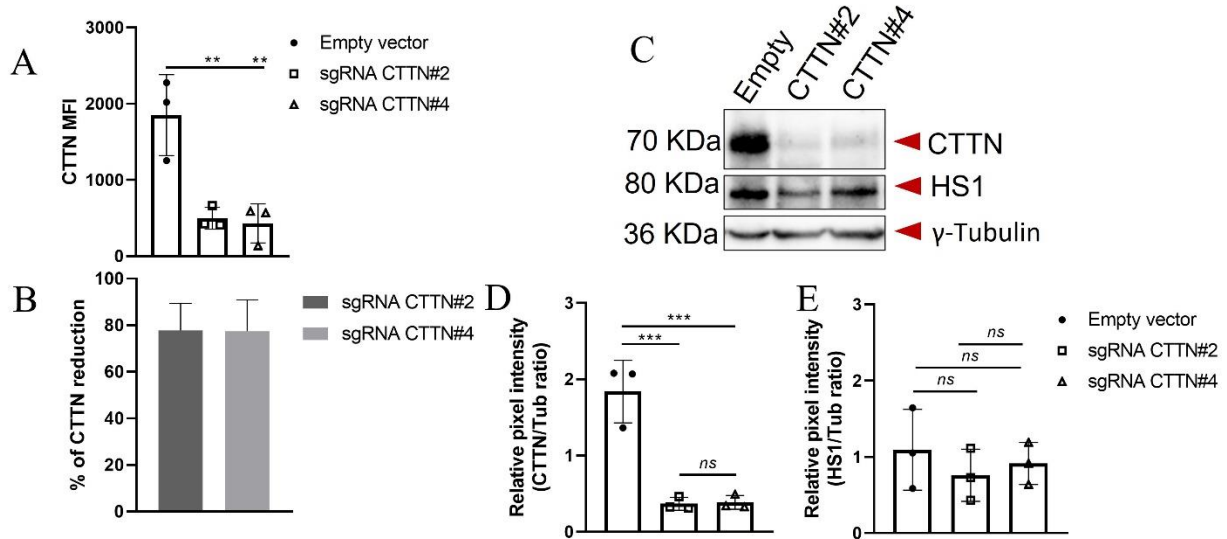


Figure 25. Characterization of cortactin-depleted Jurkat cells. Cortactin-depletion in Jurkat cells was corroborated by flow cytometry and western blot. A) Cells were stained intracellularly for cortactin, and data were acquired using a FACS Canto II cytometer. Data were analyzed by FlowJo X software. Data are presented as mean fluorescence intensity \pm SD $n=3$. B) Percentage of cortactin reduction calculated using data in panel A. C) Representative blot of four independent experiments is shown. GAPDH was used as loading control. D&E) Densitometric analysis of cortactin and HS1 band pixel intensities shown in panel C. Data are presented as mean relative pixel intensity normalized to GAPDH \pm SD. $n=4$. Data analysis was performed by one-way ANOVA using Graph Pad Prism 5 software. * $p \leq 0.05$, ** $p \leq 0.01$, ns: not significant.

Moreover, cortactin depletion did not affect the expression of different important surface molecules, such as CD3 and the adhesion molecules CD62L, PSGL-1, LFA-1 and VLA-4 that are essential for T cell migration (**Figure 27**). Although it has been reported that cortactin controls surface expression of CXCR4 in a murine model of T cell leukemia²³², we did not observe differences in CXCR4 surface expression in cortactin-depleted Jurkat cells (**Figure 27**), suggesting that cortactin in Jurkat cells does not control CXCR4 surface expression.

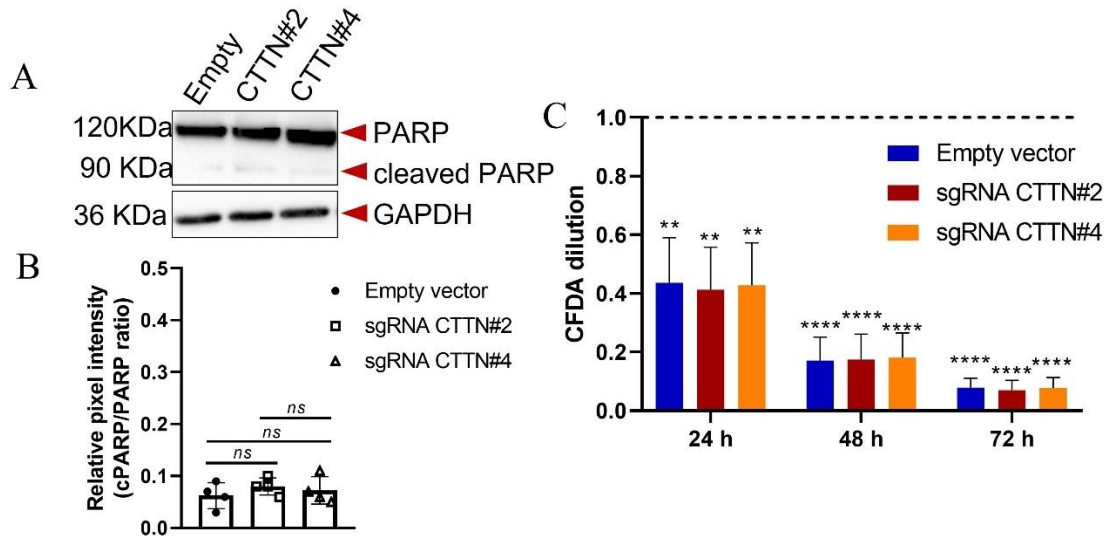


Figure 26. Cortactin-depleted and control Jurkat cells have similar apoptosis and proliferation rates. A) Representative blot for PARP of four independent experiments. GAPDH was used as loading control. B) Densitometric analysis of cleaved PARP in relation to total PARP using Image J. Data analysis was performed using Graph Pad Prism 5 software. Data are presented as mean relative pixel intensity \pm SD. $n=4$. C) Flow cytometric analysis of CFDA dilution in Jurkat cells. Samples were acquired using a FACS Canto II cytometer. Data were analyzed by FlowJo X software. Data are presented as normalized intensity \pm SD; $n=3$. Statistical analysis was performed by two-way ANOVA using Graph Pad. * $p \leq 0.05$, ** $p \leq 0.01$, **** $p \leq 0.001$, ns: not significant. CFDA, carboxyfluorescein diacetate.

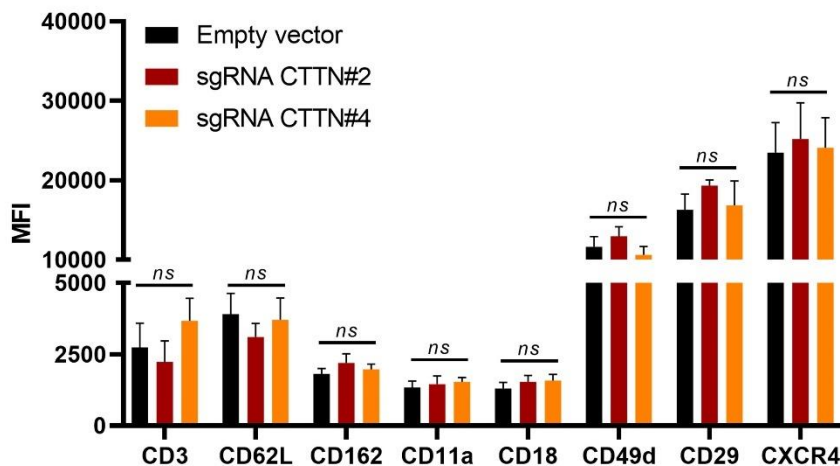


Figure 27. Expression of adhesion molecules and CXCR4 is similar in cortactin-depleted Jurkat cells. Cortactin-depleted and control Jurkat cells were stained for the indicated surface molecules. Data were acquired using a FACS Canto II cytometer and are presented as mean fluorescence intensity \pm SD $n=3-6$. Data were analyzed by FlowJo X software. Statistical analysis was performed by two-way ANOVA using Graph Pad. ns, not significant.

6.7 Cortactin-depleted Jurkat cells show reduced IL-2 mRNA transcription upon TCR engagement and impaired migration towards CXCL12 due to poor actin dynamics

We next wanted to analyze whether the absence of cortactin causes impaired TCR signaling. To address this, we first evaluated the formation of conjugates by flow cytometry using Raji B cells as APCs. We observed that cortactin-depleted Jurkat cells formed conjugates similar to control cells (**Figure 28**).

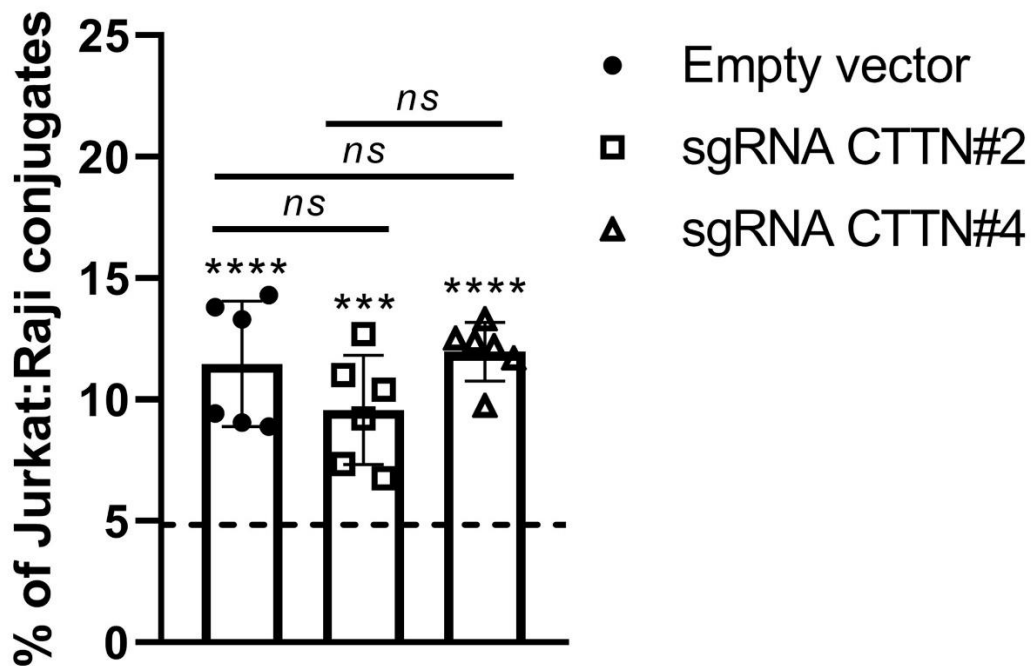


Figure 28. Cortactin-depleted Jurkat cells form similar numbers of conjugates. Cortactin-depleted and control Jurkat were co-incubated with Raji cells at a 1:1 ratio in the presence of anti-CD3 antibody to induce formation of IS (conjugates). Cells were fixed and stained for specific markers against Jurkat (CD7) and Raji (CD10). Samples were analyzed using a FACS Canto II cytometer. Data were analyzed by FlowJo X software. Data are presented as percentage of Jurkat cells forming conjugates \pm SD; n=6. Dashed line represents the percentage of conjugates formed in basal conditions. Significance of each bar was calculated by comparing percentage of conjugate formation upon anti-CD3 antibody stimulation vs basal conjugate formation. Statistical analysis was performed by ANOVA using Graph Pad. *** $p \leq 0.001$, **** $p < 0.0001$. ns, not significant.

Given that upregulation of IL-2 is one of the main consequences of IS formation and T cell activation, we next analyzed the expression of IL-2 mRNA, which is dependent on the proper activation of different signaling pathways downstream of the TCR complex including MAP kinases, NF- κ B and NFAT. We observed that in cortactin-depleted Jurkat cells expression of IL-2 mRNA was significantly reduced upon TCR engagement after 24 h compared to control cells (Figure 29).

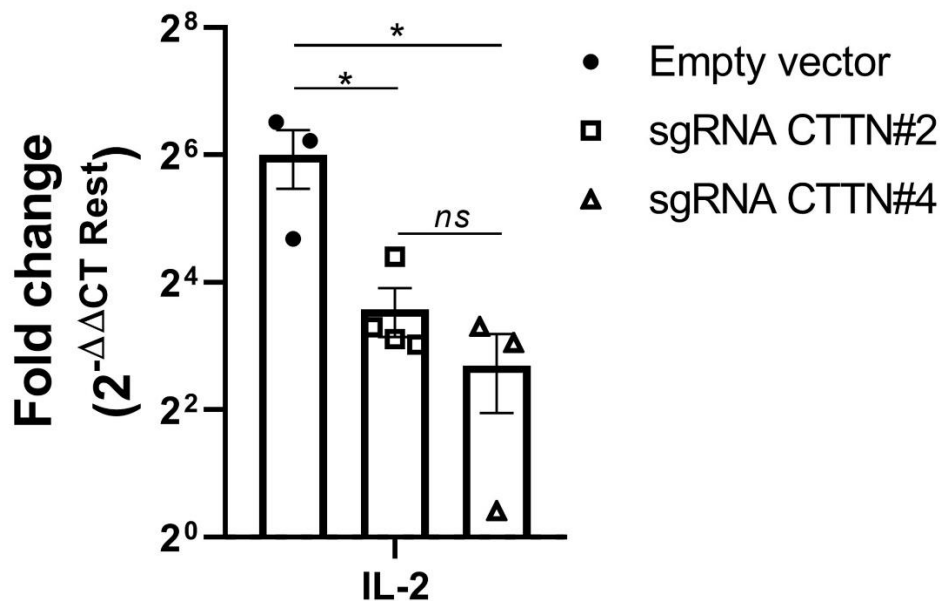


Figure 29. Expression of IL-2 mRNA is reduced in cortactin-depleted Jurkat cells upon TCR engagement. Jurkat cells were incubated for 24 h on plate-bound anti-CD3/28 antibodies. cDNA was obtained from total RNA of resting or stimulated cells and IL-2 mRNA was analyzed by quantitative RT-PCR. 7SL was used as housekeeping gene. Normalized data are presented as fold-change compared to unstimulated Jurkat cells \pm SD $n=3-4$. Significance was analyzed by one-way ANOVA using Graph Pad. $*p \leq 0.05$. ns, not significant

Since synapse formation was not impaired but IL-2 production was diminished in cortactin-depleted Jurkat cells, we next aimed to analyze early events in T cell signaling upon IS formation to detect whether cortactin-depletion affects the proximal signaling complex. To this end, we analyzed the phosphorylation of ERK upon TCR engagement, that regulates the activation of the AP-1 TF. Using flow cytometry, we found that ERK phosphorylation dynamics in cortactin-

depleted Jurkat cells were very similar to control cells, where phosphorylation of ERK was detected starting after 2 minutes of stimulation followed by a gradual decline over the next 13 minutes (**Figure 30**).

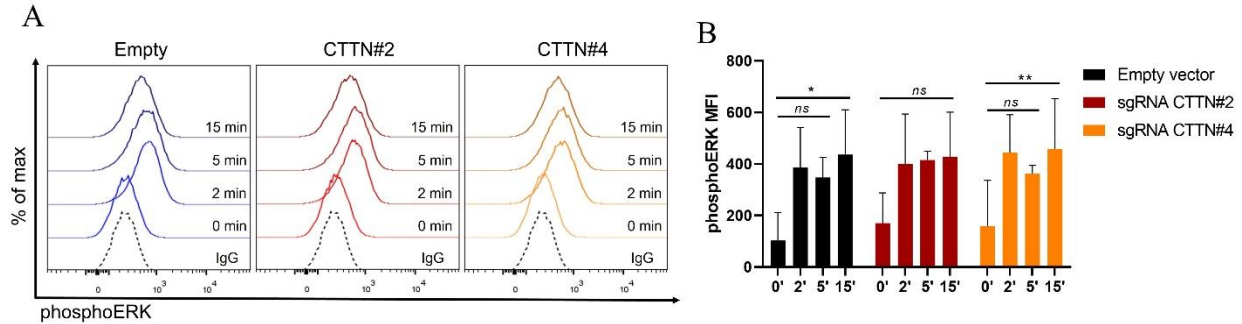


Figure 30. Early phosphorylation of ERK is similar in cortactin-depleted and control Jurkat cells upon TCR stimulation. Cortactin-depleted and control Jurkat cells were stimulated for the indicated time points with anti-CD3/28 antibodies and subsequently crosslinked with a goat-anti mouse antibody. Cells were then stained intracellularly with anti-phospho ERK antibody. Samples were acquired using a FACS Canto II cytometer. A) Representative histograms of three independent experiments and B) the corresponding quantification are shown. Samples were acquired using a BD FACS Canto II instrument. Data were analyzed by FlowJo X software. Data are presented as mean fluorescence intensity \pm SD; $n=3$. Statistical analysis was performed by ANOVA using Graph Pad. * $p \leq 0.05$, ** $p \leq 0.01$. ns, not significant.

Given the known participation of cortactin in the migration of several types of cells, we next wanted to determine whether cortactin-deficiency would affect cell migration. As shown above, both wild-type and cortactin-depleted Jurkat cells express high levels of the CXCR4 receptor, which is essential for the migration of T cells. However, using transwell filters and CXCL12 as chemoattractant, we found that loss of cortactin in Jurkat cells severely impaired migration towards a CXCL12 chemokine gradient, but did not affect random migration without the chemokine (**Figure 31**).

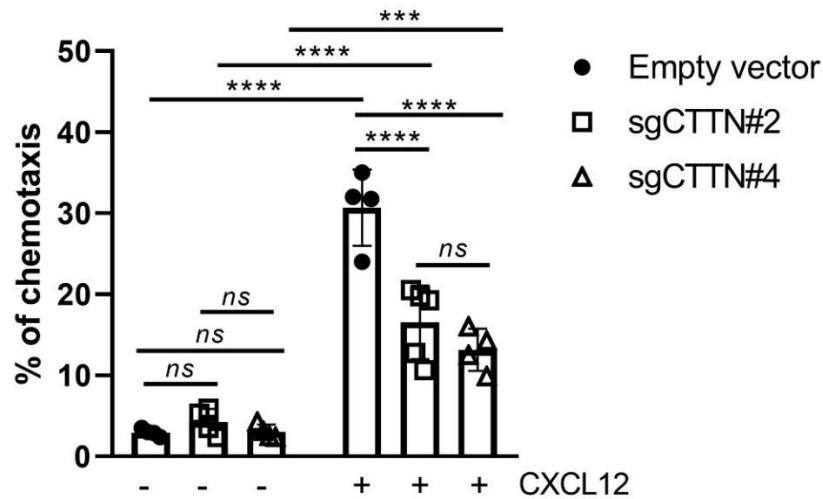


Figure 31. Cortactin-depleted Jurkat cells migrate less towards a CXCL12 gradient. Cortactin-depleted and control Jurkat cells were placed in the top chamber of a transwell filter. Filters were placed in wells containing media supplemented with 100 ng/mL CXCL12 and incubated for 3 h. Cells that migrated to the bottom chamber were stained with trypan blue and counted using a Neubauer chamber. The percentage of chemotaxis was calculated by dividing the number of cells in the bottom chamber between the total number of cells added on the transwell filter. Data are presented as mean percentage of chemotaxis \pm SD; n=4. Significance was analyzed by two-way ANOVA using Graph Pad. ****p<0.0001. ns, not significant

Given that actin remodeling contributes to the signaling events downstream of both TCR and CXCR4 leading to the transcription of IL-2 mRNA^{106,278}, together with the fact that cortactin modulates different cellular functions through the actin cytoskeleton, we wanted to know whether cortactin-depletion in Jurkat cells would affect actin remodeling upon TCR engagement. To this end, we stimulated cortactin-depleted Jurkat cells with anti-CD3/28 antibodies and then analyzed actin polymerization at different time points after TCR engagement. We found that in basal conditions, cortactin-depleted Jurkat cells had a reduced amount of F-actin. Moreover, upon TCR engagement, control Jurkat cells responded by significantly increasing F-actin polymerization, whereas cortactin-depleted cells responded with significantly less actin polymerization (**Figure 32A**). Furthermore, upon stimulation with CXCL12, cortactin-depleted Jurkat cells also failed to significantly induce actin polymerization over time (**Figure 32B**). Hence, reduced IL-2 expression in cortactin-depleted Jurkat cells might result from defective actin dynamics and actin-dependent signaling upon TCR stimulation. This idea is supported by the fact that disruption of the actin

cytoskeleton by depolymerizing agents such as cytochalasin D or latrunculin A, or depletion of Vav1, WASp, WAVE2 or HS1 have been demonstrated to affect both actin dynamics and IL-2 production¹⁰⁶. Together, these results highlight an active role of cortactin in T cell actin dynamics upon TCR engagement and in the migration of T cells.

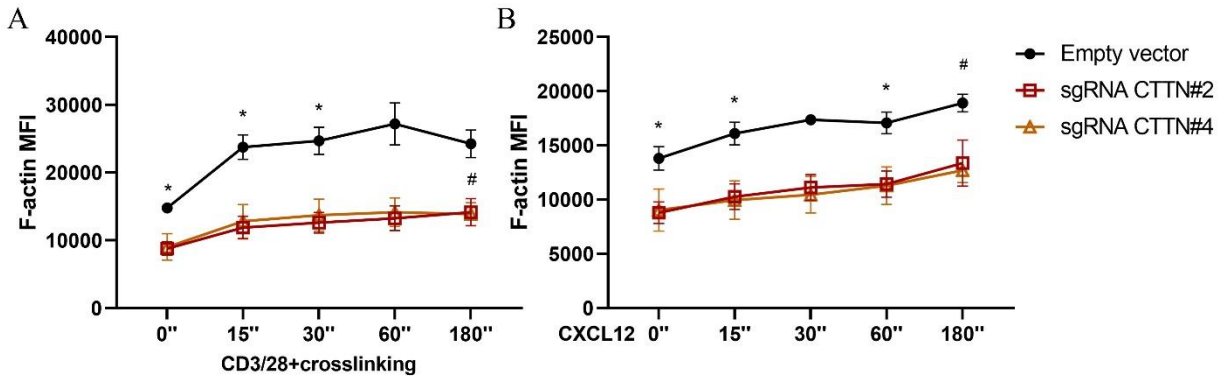


Figure 32. Cortactin-depleted Jurkat cells show reduced F-actin content in basal conditions and impaired actin polymerization upon TCR and CXCR4 engagement. Cortactin-depleted and control Jurkat cells were treated with either anti-CD3/28 antibodies and then crosslinked using a goat anti-mouse antibody (A) or with CXCL12 (right) for the indicated time points to induce TCR or CXCR4 stimulation, respectively. Cells were then immediately fixed at the indicated times and F-actin was stained using phalloidin. Samples were acquired using a BD FACS Canto II instrument. Data were analyzed by FlowJo X software. Data are presented as mean fluorescence intensity (MFI) \pm SEM. n=3-4. Significance was determined using two-way ANOVA. * $p \leq 0.05$, ** $p \leq 0.01$. *Empty vs CTTN#2; #Empty vs CTTN#4.

6.8 T cell subsets in the lymph nodes, peripheral blood, spleen and in the thymus of *Cttn*^{-/-} and *Cttn*^{+/+} mice are similar

Given the results we observed in the human cells, we aimed to further analyze the pathophysiological relevance of cortactin in T cell biology. To this end, we analyzed cortactin expression in primary mouse T cells and functional changes in cortactin-deficient T cells isolated from *Cttn*^{-/-} mice. We have previously shown that these mice display increased endothelial permeability and reduced leukocyte recruitment due to impaired GTPase signaling and ICAM-1 clustering²⁷². In addition, these mice have not shown any abnormalities in total number of leukocytes²⁷², however, a thorough characterization of T cell subpopulations and functions has never been done. Therefore, we performed a comprehensive analysis of T cell subsets and APCs in the thymus, peripheral blood and secondary lymphoid organs of *Cttn*^{+/+} and *Cttn*^{-/-} mice.

Importantly, we found that *Cttn*^{+/+} cells indeed expressed the cortactin mRNA, whereas *Cttn*^{-/-} T cells did not (**Figure 33**). We next analyzed the populations of T cell progenitors in the thymus and observed similar numbers of the thymocyte populations including CD4⁻CD8⁻ (DN), CD4⁺CD8⁺ (DP) and CD4⁺ or CD8⁺ single positive (SP) populations (**Figure 34**). Moreover, analysis of total T cell (TCR β ⁺), B cell (CD19⁺) and monocyte (CD14⁺) numbers by flow cytometry revealed no significant differences in the spleen, LNs or peripheral blood (**Figure 35**). Thus, hematopoiesis in general is not affected by the absence of cortactin.

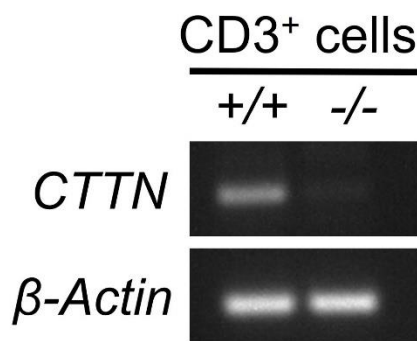


Figure 33. Expression of cortactin mRNA in CD3⁺ cells isolated from spleen of *Cttn*^{+/+} and *Cttn*^{-/-} littermates. cDNA obtained from total RNA of CD3⁺ cells isolated from the spleens of *Cttn*^{+/+} and *Cttn*^{-/-} were analyzed by end-point PCR for the presence of *CTTN* (150 bp) mRNA using specific primers (sequences are shown at Table 8). β -actin (197 bp) was using as loading control. PCR products were analyzed in a 2.0% agarose gel. A representative image from 3 independent cDNA preparations is shown.

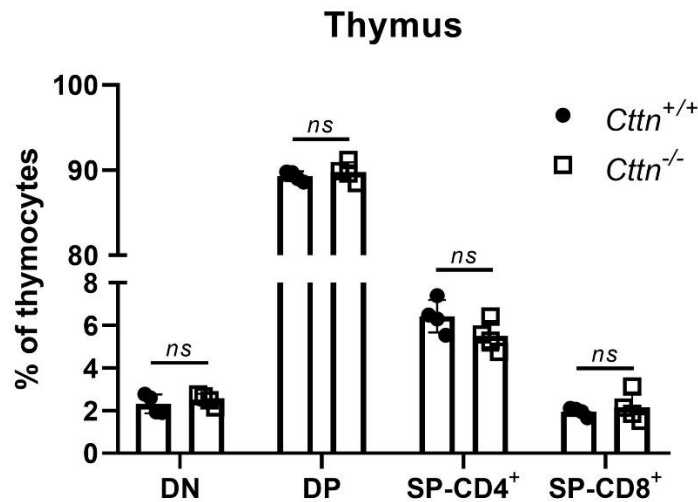


Figure 34. Thymocyte subpopulations are similar in the *Cttn*^{-/-} mice. The thymus was harvested from *Cttn*^{+/+} and *Cttn*^{-/-} mice, and thymocytes were obtained by mechanical disaggregation. Cells were then stained extracellularly with anti-CD4 and anti-CD8 antibodies and then fixed. Samples were acquired using a BD FACS Canto II instrument. Data were analyzed by FlowJo X software and are represented as percentage of total cells \pm SD; n=4. Statistical analysis was performed by two-way ANOVA using Graph Pad. ns, not significant.

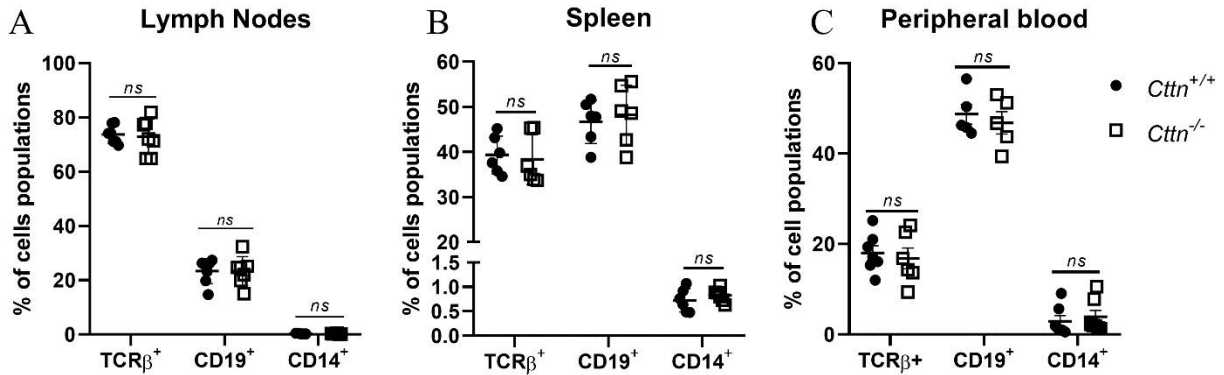


Figure 35. Analysis of B cell, T cell and monocyte populations in the LNs, spleen and peripheral blood of the *Cttm*^{-/-} mice. The LNs (inguinal, brachial, axillar and submaxillary), spleen and peripheral blood were harvested from *Cttm*^{+/+} and *Cttm*^{-/-} littermates, and cell suspensions were obtained by mechanical disaggregation. Cells were stained extracellularly with anti-TCRβ, anti-CD19 or anti-CD14. Samples were acquired using a BD FACS Canto II cytometer. Data from LN (A), spleen (B) and peripheral blood (C) were analyzed by FlowJo X software and are represented as percentage of positive cells ± SD. n=6. Statistical analysis was determined by two-way ANOVA using Graph Pad. ns, not significant.

6.9 Homing of *Cttm*^{-/-} CD4⁺ and CD8⁺ T lymphocytes to SLOs is reduced due to defective CXCR4 responses

Since we observed that total T cells number were not affected in SLOs or peripheral blood, we decided to evaluate whether T cell subsets, i.e., CD4⁺ T helper cells and cytotoxic CD8⁺ T cells presented any changes. Using these markers, flow cytometric analysis revealed a significantly reduced number of CD4⁺, but not CD8⁺ T cells in the LNs of *Cttm*^{-/-} mice, although similar numbers were observed in the spleen and peripheral blood (**Figure 36**). Thus, CD4⁺ cells might display defects in the homing to LNs, but not to the spleen.

High levels of the CXCR4-ligand, CXCL12, have been detected in the LN²⁷⁹. Moreover, cortactin has been shown to regulate the expression of surface CXCR4 in a mouse model of leukemic T cells²³². Therefore, we analyzed surface expression of CXCR4 in T cells from *Cttm*^{-/-} mice. However, we found similar levels of CXCR4 on the surface of either resting CD4⁺ and CD8⁺ *Cttm*^{-/-} T cells compared to *Cttm*^{+/+} T cells (**Figure 37**), and this finding was independent of the activation

state, although a slight tendency towards a higher expression of CXCR4 was observed in CD4⁺ *Cttn*^{-/-} T cells.

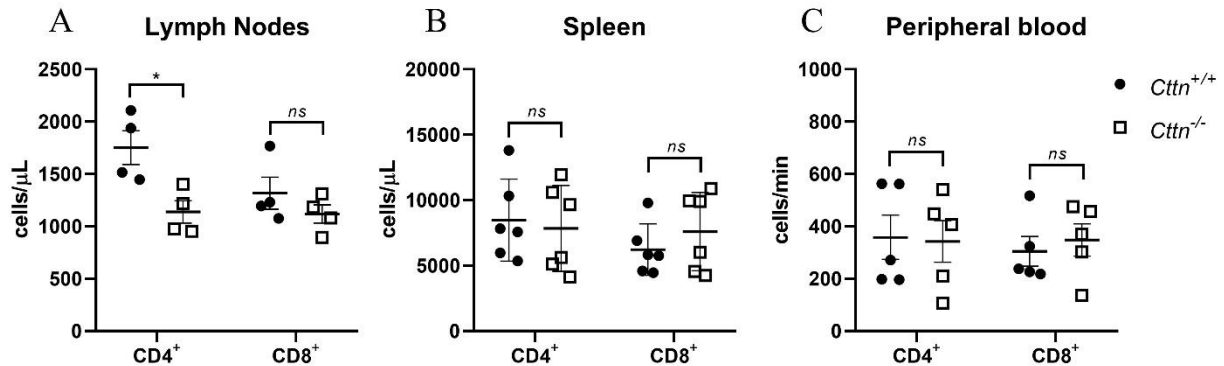


Figure 36. CD4⁺ cell population is reduced and CD8⁺ is increased in the LNs and spleen of *Cttn*^{-/-} mice. Single cell suspensions free from erythrocytes were prepared from the LN, spleen and peripheral blood from *Cttn*^{+/+} and *Cttn*^{-/-} littermates. Cells were stained extracellularly with anti-CD4 and anti-CD8 antibodies. Samples were acquired using a BD FACS Canto II. Data were analyzed by FlowJo X software. Total numbers for LN and spleen were obtained by calculating the number of cell equivalent to the percentage of positive cells for CD4 and CD8. Total counts for PB were calculated by counting the number of CD4⁺ and CD8⁺ events and normalizing by time. Data from LN (A) and spleen (B) are represented as cells/μL ± SD. Data from peripheral blood (C) are represented as cells/min ± SD. n=4-6. Statistical analysis was determined by two-way ANOVA using Graph Pad. *p≤0.05. ns, not significant.

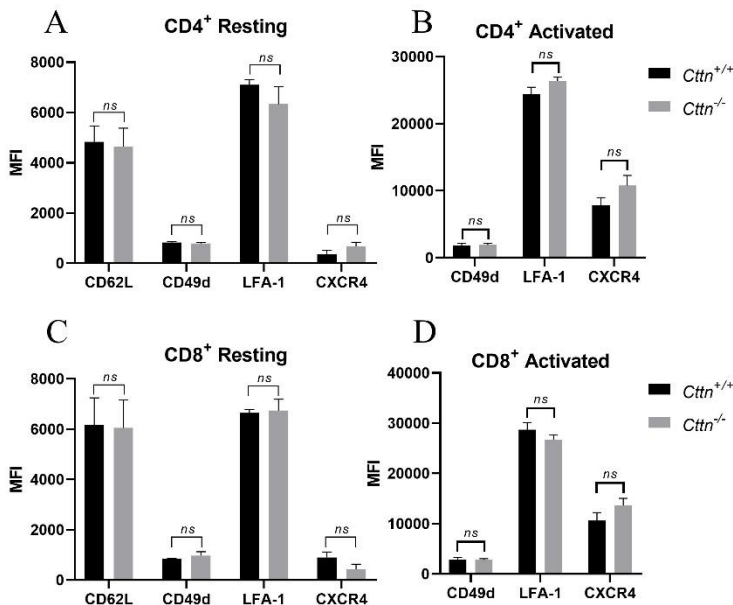


Figure 37. Characterization of the surface expression of adhesion molecules in *Cttn*^{-/-} T cells. CD3⁺ cells isolated from the spleen were left untreated (resting) (CD4⁺ in A & CD8⁺ in C) or activated with plate-bound anti-CD3/28 antibodies for 72 h (CD4⁺ B & CD4⁺ D) and stained for the indicated markers. Samples were acquired using a BD FACS Canto II instrument. Data were analyzed by FlowJo X software. Data are represented as mean fluorescence intensity ± SEM. n=4-5. Significance was determined by one-way ANOVA using Graph Pad. ns, not significant.

Furthermore, we also analyzed the expression of adhesion molecules essential for T cell homing and migration such as CD62L, LFA-1 and VLA-4, but no differences were observed in the expression of these molecules between resting or activated CD4⁺ or CD8⁺ from *Cttn*^{+/+} vs *Cttn*^{-/-} mice (**Figure 37**). Our data show that cortactin deficiency does not affect the expression of these proteins, however, whether they function properly, *e.g.* LFA-1 and VLA-4 integrin activation, or CXCR4-mediated signaling remains to be tested.

Next, we analyzed migration *in vitro* using transwell filters and CXCL12 as chemoattractant. First, we observed that without any stimulation, around 5% of resting CD3⁺ cells from both *Cttn*^{+/+} and *Cttn*^{-/-} mice randomly migrated to the bottom chamber (**Figure 38**).

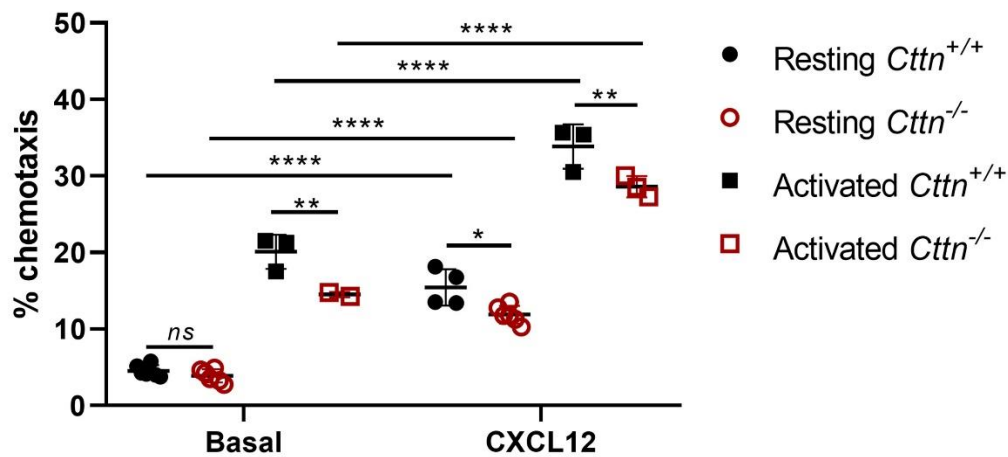


Figure 38. *Cttn*^{-/-} T cells migrate less towards CXCL12. CD3⁺ resting or activated with plate-bound anti-CD3/28 antibodies for 72 h were placed in the top chamber of a transwell filter. Filters were then placed in wells containing media supplemented with 100 ng/mL CXCL12 and incubated for 6 h. Afterwards, cells in the bottom chamber were stained with trypan blue and counted using a Neubauer chamber. The percentage of chemotaxis was calculated by dividing the number of cells in the bottom chamber between the total number of cells added on the transwell filter. Data are represented as mean percentage of chemotaxis \pm SD. n=3-5. Significance was determined using two-way ANOVA using Graph Pad. * $p \leq 0.05$, ** $p \leq 0.01$, *** $p \leq 0.001$. ns, not significant.

In the presence of CXCL12, resting *Cttn*^{+/+} CD3⁺ cells migrated significantly more towards the CXCL12 gradient compared to resting *Cttn*^{-/-} CD3⁺ cells. On the other hand, random migration of activated T cells was significantly higher than in resting cells. However, in the absence of CXCL12, random migration of activated *Cttn*^{+/+} CD3⁺ cells was significantly higher than activated

Cttn^{-/-} CD3⁺ cells, thus suggesting that *Cttn*^{-/-} CD3⁺ cells might display impaired motility. Furthermore, a higher percentage of activated *Cttn*^{+/+} CD3⁺ cells migrated towards the CXCL12 gradient compared to activated *Cttn*^{-/-} CD3⁺ cells. Of note, migration of both *Cttn*^{+/+} and *Cttn*^{-/-} activated cells was significantly higher compared to their resting counterparts. Taken together, these results highlight cortactin as a potential important regulator of CXCR4-mediated T cell migration and homing to secondary lymphoid organs.

6.10 TCR-mediated proliferation and CXCR4-mediated TCR-costimulation are impaired in *Cttn*^{-/-} T cells

Given that after activation cortactin switches to the expression of the full-length isoform, that is the most efficient in regulating actin dynamics, and that T cell activation is tightly regulated by the actin cytoskeleton, we hypothesized that cortactin might contribute to T cell functions downstream of activation. To address this, we analyzed proliferation of T cells upon activation using two models: 1) Mixed-lymphocyte reaction (MLR) using T cell-A20 co-cultures, and 2) polyclonal stimulation using anti-CD3/28 antibodies. A20 is a B cell lymphoma cell line established from Balb/c mice (H-k2^d), whereas our *Cttn*^{-/-} mice was initially generated in SV29 mice, but then backcrossed to C57BL/6J strain (H-k2^b). When co-cultured, the haplotype mismatch generates an allogeneic T cell response that induces IS formation and T cell activation and proliferation. Moreover, cells can be labeled with a fluorescent vital dye, and the number of divisions (rounds of proliferation) and dividing cells (proliferating cells) can be traced, as the fluorescence intensity then divides by half with each proliferation round. Using these combined approaches, we observed that the number of proliferating cells was significantly lower in *Cttn*^{-/-} T cells as measured by flow cytometry (**Figure 39**).

Moreover, the MLR assay generates both CD4⁺ and CD8⁺ effector cells that produce IFN γ and TNF α , and Granzyme B and IFN γ , respectively. We observed that *Cttn*^{+/+} and *Cttn*^{-/-} CD4⁺ T cells produced similar amounts of IFN γ and TNF α (**Figure 40**). Also, expression of Granzyme B and IFN γ in *Cttn*^{+/+} and *Cttn*^{-/-} CD8⁺ T cells was comparable. Hence, cortactin might be dispensable for the expression of these cytokines during differentiation of effector T cells in this model, but whether these proteins are secreted at similar levels remains to be tested.

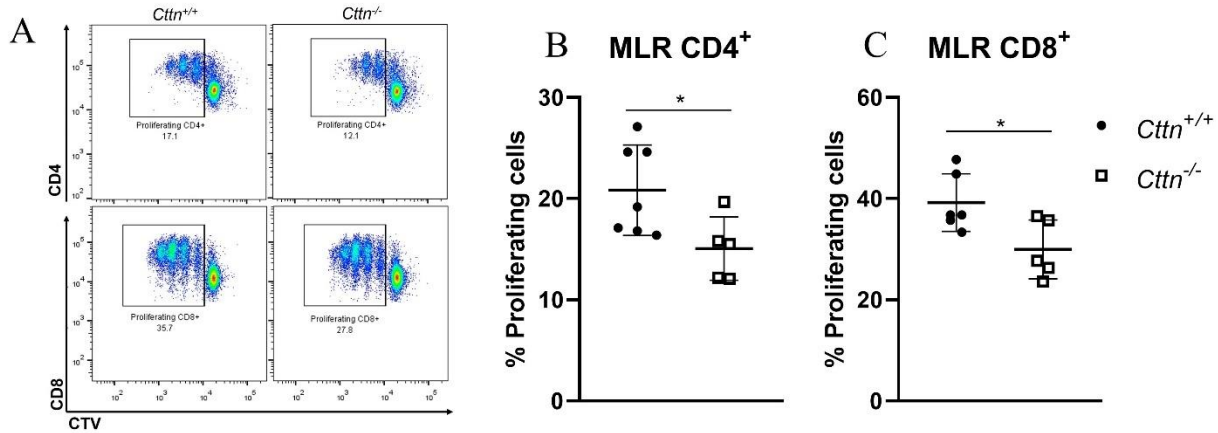


Figure 39. *Ctnn*^{-/-} T cells show impaired proliferation upon TCR stimulation. CTV-stained CD3⁺ cells were co-cultured with MMC-treated A20 cells to induce proliferation by allogenic stimulation. A) Representative dot plots of T cell proliferation showing CD4/CD8 in the Y axis and CTV signal in the X axis. B and C) Quantification of the percentage of proliferating cells from the plots shown in A). Samples were acquired using a BD FACS Canto II instrument. Data were analyzed by FlowJo X software. Data are represented as mean percentage of proliferating cells ± SD; n=5-6. Significance was determined by unpaired Student's-T test using Graph Pad. *p<0.05. CTV, CellTrace™ Violet; MLR, mixed-lymphocyte reaction; MMC, mitomycin-C.

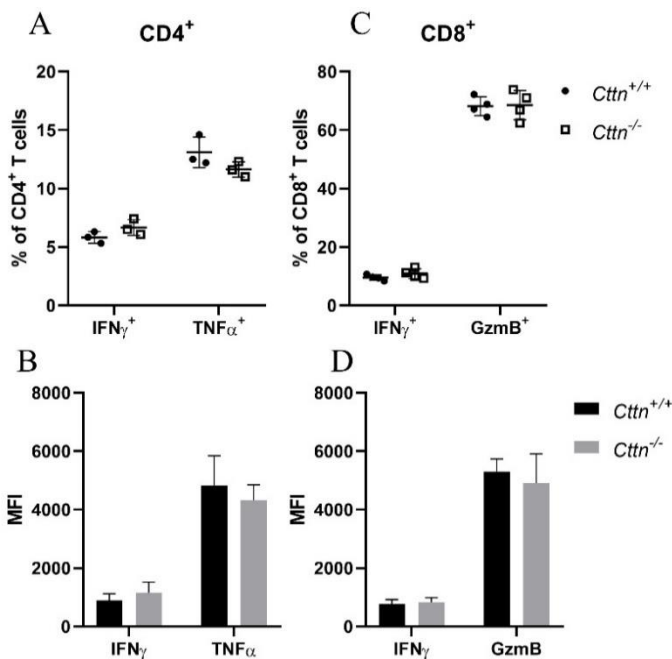


Figure 40. *Ctnn*^{-/-} T effector cells generated with the MLR assay display normal production of cytokines and Granzyme B. Effector cells from the MLR Assay were treated with Brefeldin A for 6 hours to enhance intracellular cytokine staining by inhibiting protein transport. Intracellular cytokines were analyzed by flow cytometry using a BD FACS Canto II instrument. Data was analyzed by FlowJo X software. Data are shown as percentage of positive cells (A & C) and the mean fluorescence intensity (B & D) ± SD; n=3. Significance was determined by one-way ANOVA using Graph Pad. GzmB, granzyme B.

It has been reported that CXCR4 is able to co-stimulate TCR signaling in T cells by inducing enhanced production of AP-1 target genes such as IL-2, IL-10 and CD69²⁷⁸. Given that we

observed defective responses in CXCR4-mediated migration, we analyzed whether the co-stimulatory activity of CXCR4 was also impaired. To this end, we stimulated T cells with anti-CD3/CD28 in the presence or absence of 100 ng/mL CXCL12 and analyzed expression of IL-2, CD25 and CD69, as well as proliferation. We found no significant differences in the production of IL-2, CD25 or CD69 between *Cttn*^{+/+} and *Cttn*^{-/-} T cells, in neither CD4⁺ nor CD8⁺ populations (Figure 41).

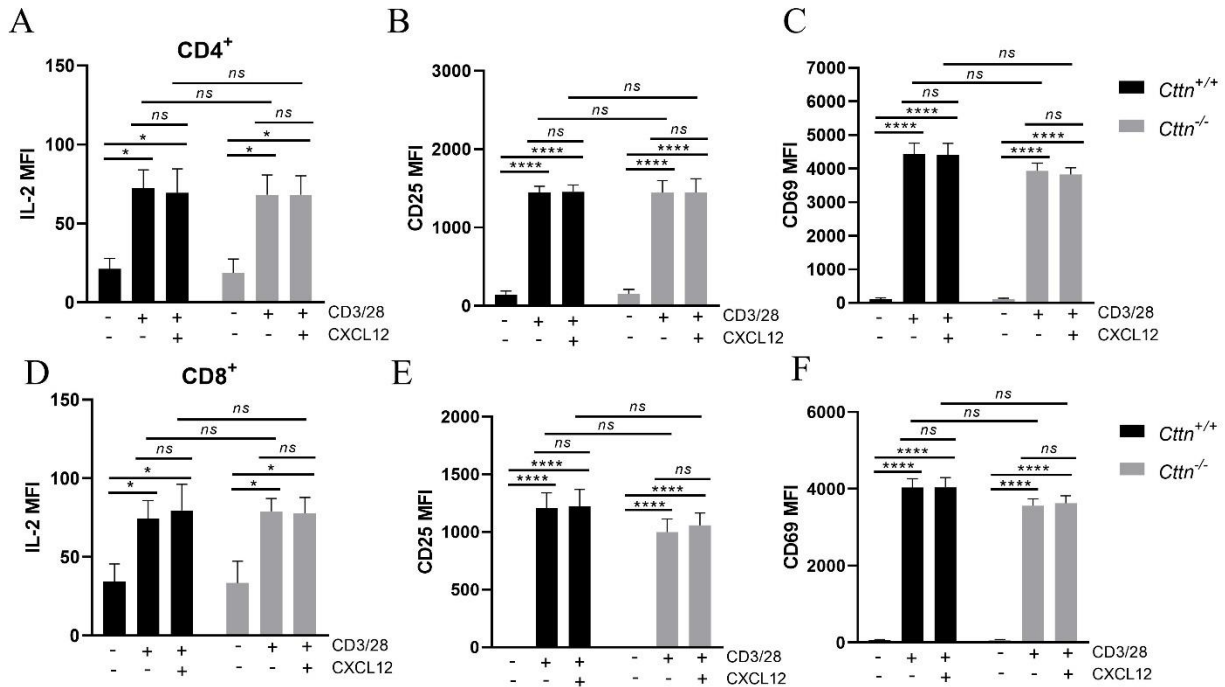


Figure 41. *Cttn*^{-/-} T cells induce similar upregulation of IL-2, CD25 and CD69 upon TCR engagement. CD3⁺ cells isolated from the spleen were seeded onto anti-CD3/28-coated plates in the presence or absence of CXCL12 and incubated for 24h. Intracellular expression of IL-2 (A&D) and extracellular expression of CD25 (B&E) and CD69 (C&F) were analyzed by flow cytometry using a BD FACS Canto II instrument. Data was analyzed by FlowJo X software. Data are represented as mean fluorescence intensity (MFI) ± SEM. n=5. Significance was determined using by two-way ANOVA using Graph Pad. *p≤0.05, **p≤0.01, ***p≤0.001, ****p≤0.0001, ns: not significant.

On the other hand, using anti-CD3/CD28 antibodies to induce proliferation, we did not detect any difference in the percentage of proliferating T cells. However, a slight non-significant tendency towards a reduced proliferation was observed in both CD4⁺ and CD8⁺ *Cttn*^{-/-} T cells (Figure 42), similar to what we previously observed with the MLR assays, suggesting that this kind of stimulus

is perhaps not strong enough to detect the defect in proliferation as we saw using the MLR assay. Importantly, when we co-stimulated with CXCL12 we observed an increased proliferation upon TCR engagement only in *Cttn*^{+/+}, but not in *Cttn*^{-/-} T cells, consistent with the defective CXCR4 signaling observed in the migration assays. Of note, this effect seemed to be specific for CD4⁺ T cells, although there was also a non-specific tendency towards lower proliferation in *Cttn*^{-/-} CD8⁺ T cells (**Figure 42**). Together, these results highlight a novel role for cortactin in TCR/CXCR4-costimulated proliferation.

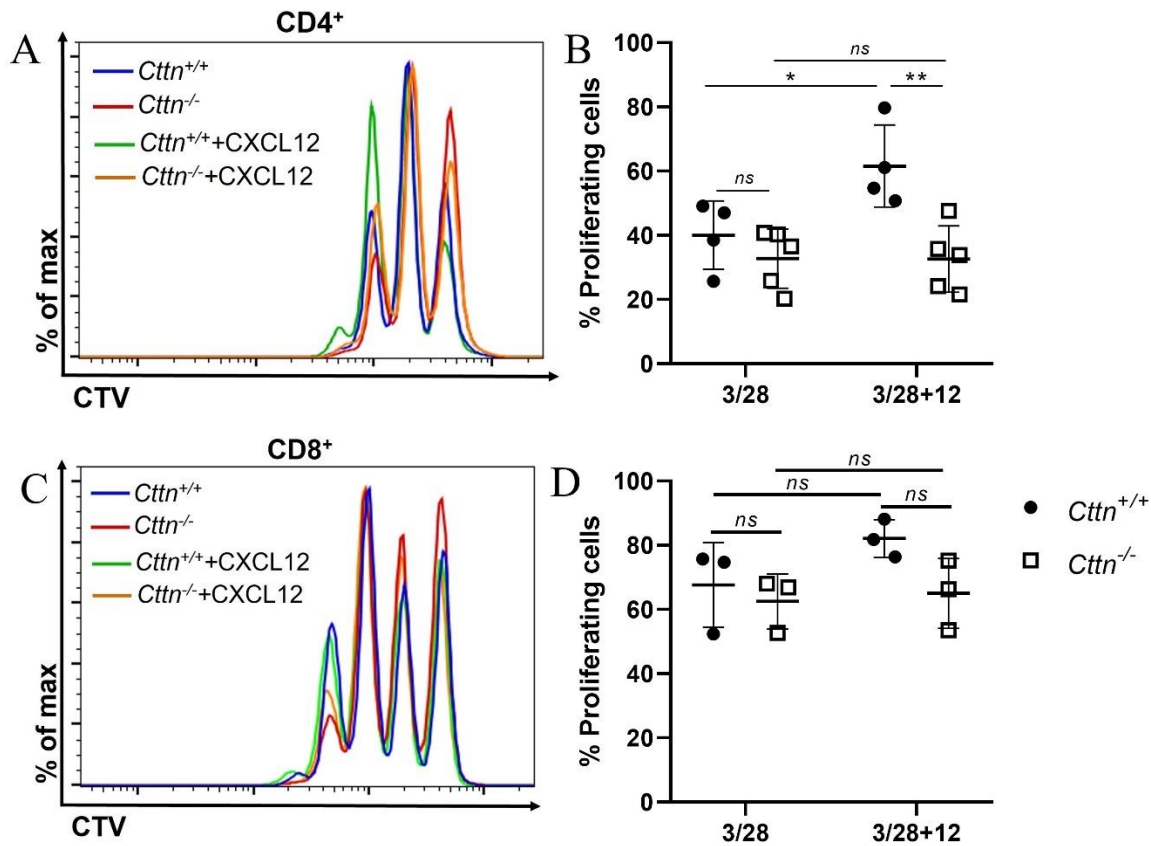


Figure 42. *Cttn*^{-/-} T cells fail to induce CXCR4-costimulation. CTV-stained CD3⁺ cells were seeded onto anti-CD3/28 coated plates in the presence or absence of 100 ng/mL CXCL12 and incubated for 72 h. Representative histograms of CTV intensity (A&C) and quantification of the percentage of proliferating CD4⁺ (B) and CD8⁺ (D) cells. Samples were acquired using a BD FACS Canto II instrument. Data was analyzed by FlowJo X software. Data are represented as mean percentage of proliferating cells ± SD; n=3-5. Significance was determined by two-way ANOVA using Graph Pad. *p≤0.05, **p≤0.01. ns, not significant. CTV, CellTrace™ Violet.

6.11 *Cttn*^{-/-} T cells fail to properly polarize F-actin to the IS

Considering the observed recruitment of cortactin to the IS, and the defect in TCR-mediated proliferation of *Cttn*^{-/-} T cells, we next asked whether cortactin-deficiency is affecting the formation of the IS. To answer this, we determined whether *Cttn*^{-/-} T cells were able to conjugate at similar rates, and whether the synapses were assembled properly. To address conjugation rates, we incubated *Cttn*^{+/+} and *Cttn*^{-/-} T cells with A20 cells for 1 h at 37°C to induce synapse formation. Then, CD3 and F-actin were stained, and the number of conjugates were analyzed by fluorescence microscopy. We found that *Cttn*^{-/-} T cells conjugated significantly less with A20 cells than *Cttn*^{+/+} under these conditions (**Figure 43**), suggesting that cortactin deficiency in T cells induces abnormal TCR responses.

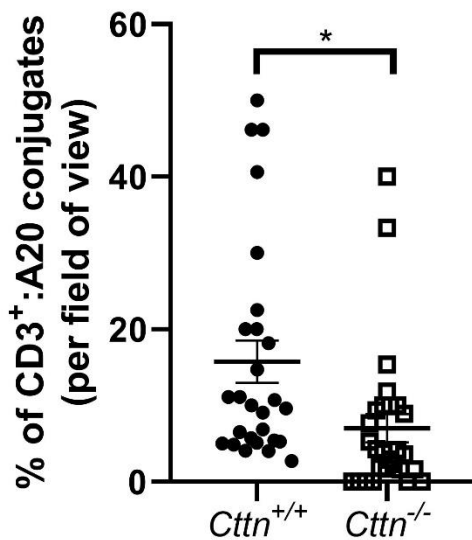


Figure 43. *Cttn*^{-/-} T cells show reduced number of conjugates with A20 cells. CD3⁺ cells from C57BL/6J mice were co-incubated with A20 cells to induce IS formation. Images were taken using a Axioscope A1 Zeiss microscope with a 40x objective. Analysis of conjugates was performed using Image J software by manually counting the number of CD3⁺ that were conjugated with A20 cells and divided by the total number of CD3⁺ cells in the field. Ten random fields were analyzed per sample in three independent assays. Statistical analysis was performed by Student's T-test using Graph Pad. n=3. *p≤0.05.

Given that IS formation depends on LFA-1 binding to ICAM-1 on APCs, we next evaluated whether *Cttn*^{-/-} T cells conjugation defect was due to impaired TCR-mediated LFA-1 activation. To answer this question, we induced the activation of LFA-1 via TCR stimulation and adhesion to ICAM-1 *in vitro*. We observed that unstimulated *Cttn*^{+/+} and *Cttn*^{-/-} T cells can bind to ICAM-1 at similar rates (**Figure 44**). Moreover, we observed that upon TCR stimulation using either PMA or CD3 antibody, a significantly higher percentage of *Cttn*^{+/+} and *Cttn*^{-/-} T cells compared to unstimulated cells adhered to ICAM-1-coated plates. However, we only observed a slight non-

tendency towards a lower frequency of adherent *Cttn*^{-/-} T cells stimulated with CD3 that did not reach statistical significance (**Figure 44**).

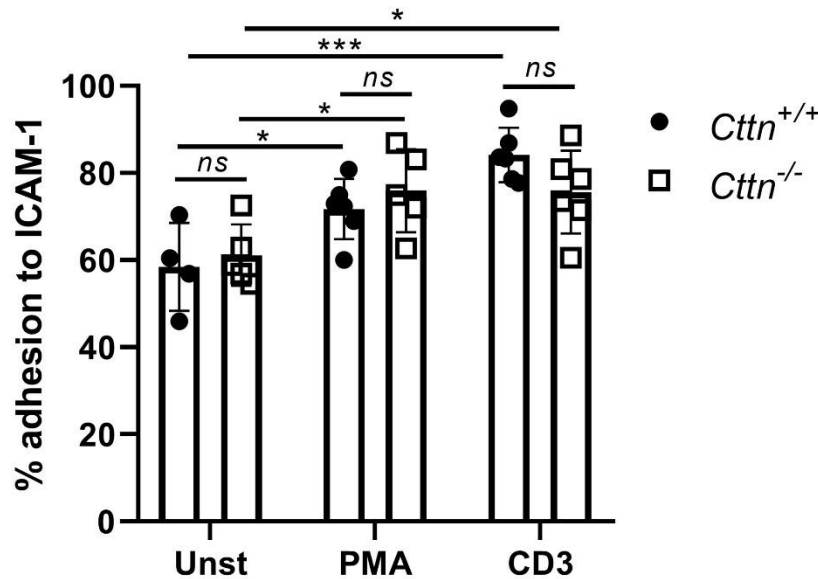


Figure 44. TCR-mediated LFA-1 activation is similar in *Cttn*^{-/-} T cells. CFDA-prestained CD3⁺ cells were seeded onto ICAM-1-Fc coated plates and then left untreated or stimulated with 50 ng/mL PMA or 5 µg/mL CD3 to induce LFA-1 activation and adhesion. Non-adherent cells were washed off and fluorescence of adherent cells was measured by absorbance at 520 nm using a Tecan spectrophotometer. Data are represented as mean percentage of adherent cells ± SD; n=4-6. Significance was determined between unstimulated and PMA and CD3 treated cells by two-way ANOVA using Graph Pad. *p≤0.05, ***p≤0.001, ns: not significant. CFDA, Carboxifluorescein diacetate.

We then analyzed the quality of the IS by means of F-actin and CD3 recruitment to the site of cell-cell contact. A detailed analysis using ImageJ software showed a more prominent enrichment of F-actin and CD3 signals at the IS in *Cttn*^{+/+} T cells compared to *Cttn*^{-/-} T cells (**Figure 45**). Moreover, using ImageJ we quantified the signal intensity of F-actin in non-conjugated and conjugated T cells. We observed that basal F-actin signal intensity, that was lower in cortactin-depleted Jurkat cells, was similar between non-conjugated *Cttn*^{+/+} and *Cttn*^{-/-} T cells, with a similar distribution at the cell periphery. However, quantification of F-actin signal intensity at the IS revealed a significantly stronger F-actin signal intensity in *Cttn*^{+/+} T cells. These results demonstrate an abnormal formation of the IS in *Cttn*^{-/-} T cells due to impaired actin dynamics, most likely de novo F-actin formation upon TCR engagement, which may also explain the reduced

proliferation observed in *Cttn*^{-/-} T cells that is dependent on proper actin dynamics but independent of IL-2. Taken together, our results demonstrate for the first time a critical role of cortactin in the regulation of actin dynamics at the IS upon TCR stimulation.

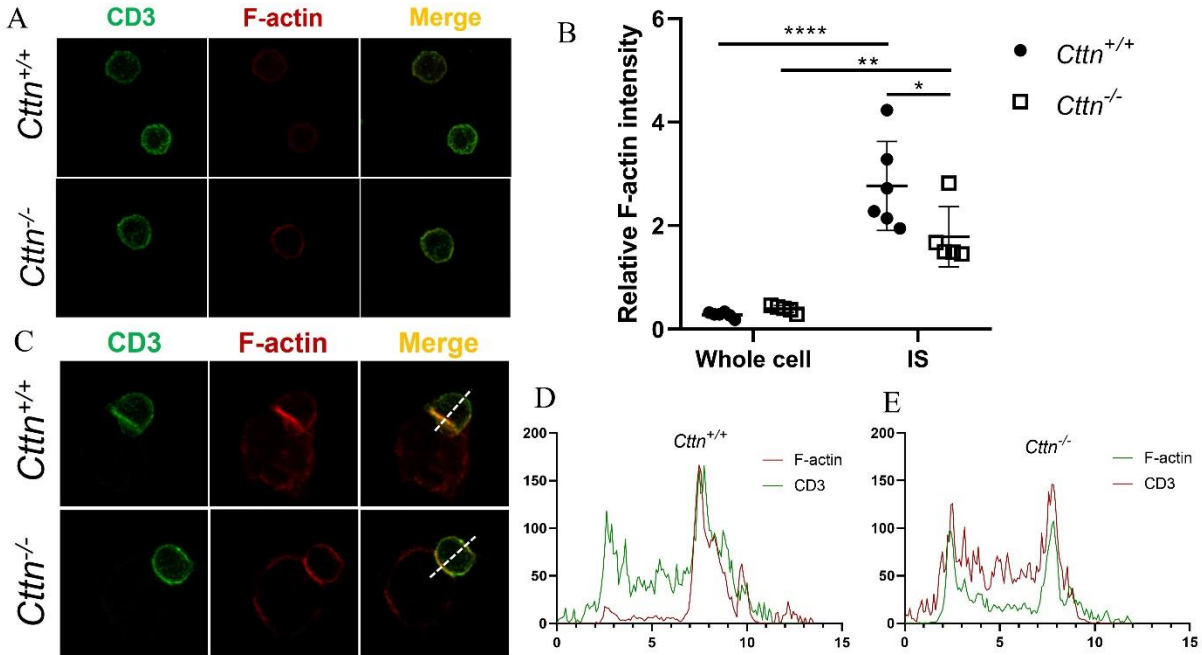


Figure 45. *Cttn*^{-/-} T cells show impaired F-actin polarization at the IS. CD3⁺ cells from C57BL/6J mice were co-incubated with A20 cells to induce immunological synapse formation. Polarization of CD3 and F-actin was analyzed by confocal microscopy. A) Representative images of un conjugated CD3⁺ cells. B) Quantification of F-actin signal in un conjugated cells (whole cell) showed in panel A or signal at the IS of conjugated cells showed in panel C. C) Representative images of CD3⁺:A20 cell conjugates. D&E) Representative histograms of fluorescence intensity distribution from dashed lines in panel. Images were taken using a Leica SP8 confocal microscope with a 63x objective and a 2x digital zoom. Analysis of F-actin polarization was performed using ImageJ software by calculating the signal intensity into the region of interest (ROI) covering the cells or the IS zone. Subsequently, the signal was normalized to the ROI area. Statistical analysis was performed by two-way ANOVA using Graph Pad. n=3.

6.12 Cortactin controls BM organoid colonization and infiltration into the CNS in a xenograft model of T-ALL

Having shown an important role of cortactin for T cell migration, we then wanted to investigate the pathophysiological relevance of our findings. Previous work from our team has established that high cortactin expression endows B-ALL cells with an enhanced migratory capacity *in vitro* and *in vivo*. Moreover, high expression of cortactin in B-ALL patients was associated with steroid treatment failure, infiltration and relapse²³³. Therefore, we hypothesized that cortactin is also involved in T-ALL pathogenesis. Our finding of cortactin overexpression in leukemic T cells supports this idea (**Figure 16**). This prompted us to analyze how cortactin-depletion would affect T-ALL development *in vivo*. To this end, we performed xenografts of control and cortactin-depleted Jurkat cells in immunodeficient NSG mice and analyzed disease progression and organ infiltration. First, we observed that wild-type Jurkat cells mostly infiltrated the BM and to a lesser extent the CNS (**Figure 46**).

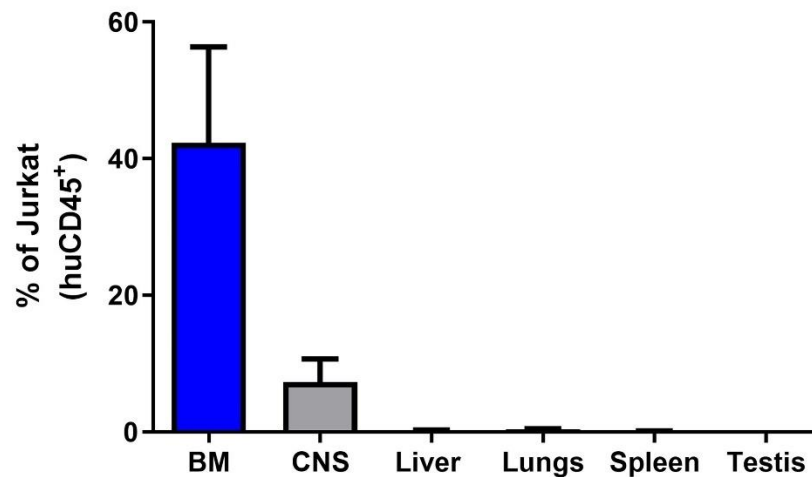


Figure 46. Jurkat cells infiltrate mostly the BM and the CNS. Jurkat cells were injected intravenously into NSG mice to induce leukemia. After the development of symptoms, mice were sacrificed, organs harvested and analyzed by Flow cytometry for the presence of human CD45⁺ cells. Samples were acquired using a BD FACS Canto II instrument. Data were analyzed by FlowJo X software. Data are presented as percentage of human CD45⁺ cells in total cells \pm SD; n=4.

Moreover, infiltration to other organs commonly involved during T-ALL such as the liver, lungs, spleen, and testis was low to absent in our xenograft model. Importantly, cortactin-depleted Jurkat cells infiltrated the BM significantly less (**Figure 47A**), and we found a reduction in leukemic burden in the peripheral blood (**Figure 47B**). Of note, infiltration into the CNS was completely prevented by the loss of cortactin in leukemic T cells (**Figure 47C**). Thus, our results highlight cortactin as a potential biomarker for the risk of organ infiltration and a potentially promising target for pharmacological inhibition to prevent BM and CNS infiltration in relapsing patients.

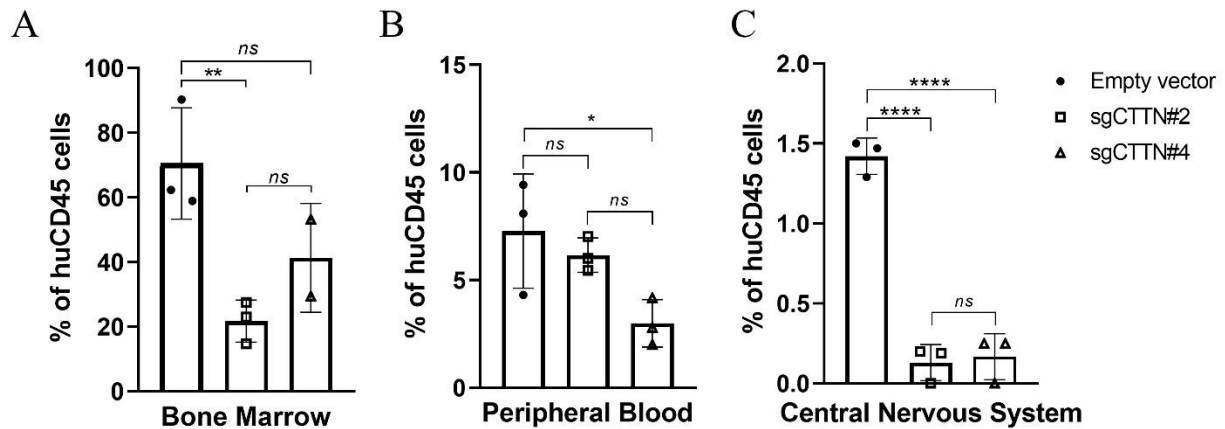


Figure 47. Infiltration of the CNS and BM is reduced in cortactin-depleted Jurkat cells. Control or cortactin-depleted Jurkat cells were injected intravenously into NSG mice to induce leukemia. After the development of symptoms, mice were sacrificed, blood, BM and the CNS were harvested and analyzed by flow cytometry for the presence of human CD45⁺ cells. Data of BM (A), peripheral blood (B) and CNS (C) are presented as percentage of human CD45⁺ cells in total cells \pm SD; n=3. Samples were acquired using a BD FACS Canto II instrument. Data were analyzed by FlowJo X software. Statistical analysis was performed by one-way ANOVA using Graph Pad. * $p \leq 0.05$, ** $p \leq 0.01$, **** $p < 0.0001$. ns, not significant.

7. DISCUSSION

Cortactin has long been considered absent in most hematopoietic cells, however, recent evidence demonstrated that cortactin is not only expressed in several types of hematopoietic cells, but that it also has a functional relevance²¹⁵. For example, in macrophages and dendritic cells, cortactin is important for migration and phagocytic activity^{228–230}. On the other hand, cortactin is also important in megakaryocytes for proper proplatelet formation²²⁷, and in platelets to induce aggregation²²⁶. Expression of cortactin was also detected in B and T cells²³¹. Moreover, cortactin was found to localize at the IS in T cell conjugates²⁴², however, the potential role for cortactin was not explored in that study. In our project, we functionally characterized the relevance of cortactin expression for the activation and migration of human and mouse T cells. We demonstrate that cortactin is recruited to the IS and essential for proper TCR- and CXCR4-induced F-actin polymerization, TCR-mediated IL-2 production and T cell proliferation. Moreover, we show that cortactin-deficient T cells display impaired CXCR4-mediated migration, and that loss of cortactin expression in leukemic T cells reduces the leukemic burden in peripheral blood and BM, and virtually abolished CNS infiltration in immunodeficient mice, thus confirming a pathological relevance of cortactin overexpression in leukemic T cells.

Cortactin expression in T cells has been controversial in the literature. Presence of cortactin protein was previously documented in human normal T cells and Jurkat cells by western blot and immunofluorescence microscopy, respectively^{231,242}. However, a different group failed to find the mRNA of cortactin in Jurkat or murine T cells isolated from the LNs¹⁹⁰. Here, we have conclusively demonstrated the presence of the cortactin protein in primary human and mouse T cells, as well as in several leukemic T cell lines, such as Jurkat and Molt-3. While cortactin expression in primary cells was low under basal conditions (**Figure 16**), it was highly upregulated upon TCR stimulation (**Figures 22** and **23**). As expected, this phenomenon was more strongly detected when stimulating T cells with PMA and ionomycin (**Figure 22**), as these stimuli bypass the TCR receptor complex and directly activate the downstream effector PLC γ 1 thus inducing calcium influx leading to vigorous TCR signals²⁸⁰. Interestingly, primary human T cells down-regulated HS1 expression in parallel to cortactin up-regulation, thus highlighting the possibility of cortactin having more prominent functions in activated than in resting T cells. Of note, it has been described that one splice variant of HS1 lacking the 3rd repeat of the actin-binding domain is

responsible for BCR-mediated apoptosis²⁸¹. Thus, it is tempting to speculate that HS1 downregulation occurs as an antiapoptotic mechanism upon TCR engagement. Moreover, we could also confirm the expression of cortactin mRNA and protein in mouse T cells (**Figure 21 and 33**). Of note, we detected that the SV1 cortactin isoform of 70 kDa was expressed in most T cell lines under basal conditions. This SV1 variant lacks exon 11 that encodes for the 6th repeat in the tandem repeat region. It is likely that Gomez *et al.* did not detect cortactin mRNA because the primers they used might have been designed against this specific site, which will be only present in the full-length cortactin variant that is expressed in most other cells.

Surprisingly, TCR stimulation in mouse primary T cells did not induce overexpression of cortactin, but instead a switch in the expression of the SV1 isoform to the full-length WT isoform of cortactin, with HS1 levels remaining unchanged. This differential isoform expression could be enhancing cortactin functions in mouse T cells, since it has been reported that the full-length cortactin isoform is better at inducing actin polymerization through the Arp2/3 complex, binds more firmly to F-actin; and cells overexpressing the WT isoform are able to migrate more efficiently compared to the same cells overexpressing the SV1 or SV2 isoforms²¹⁶. Therefore, both up-regulation of cortactin expression and the isoform switch to WT cortactin might be a functionally comparable mechanism in human and murine T cells to enhance T cell activation.

In accordance with the previously reported finding that cortactin gets recruited to the IS together with WASP and F-actin in Jurkat cells conjugated to SEE-pulsed Raji cells²⁴², we also detected cortactin recruitment to the IS in human and mouse primary T cells and Jurkat cells (**Figures 19-21**) using anti-CD3/28 beads or APCs and anti-CD3 stimulation; thus, confirming that cortactin is important during IS formation and T cell activation. However, we observed that induction of IS formation by CD3 stimulation (**Figure 19B**) was less effective to induce recruitment of F-actin and cortactin to the IS compared to the anti-CD3/28 beads or allogenic APC conjugates (**Figure 19C, 20 and 21B**). Ledderose *et al.* showed that the numbers of formed conjugates were too low using the anti-CD3 stimulation method, as only about 1% of cells conjugated when using mouse primary T cells and monocytes²⁸². Such low numbers of conjugates might be due to the fact that anti-CD3 stimulation transiently activates the integrin LFA-1 that interacts with ICAM-1 expressed on APCs, leading to a weakly assembled IS that can easily dissolve. Thus, anti-CD3

stimulation is not the best method for analyzing IS assembly, and conjugation using APC should be preferred in future experiments.

Since we observed that cortactin was recruited to the IS, we speculated that cortactin might be necessary for IS formation. Analyzing cortactin-depleted Jurkat cells co-cultivated with Raji B cells, we observed numbers of conjugates similar to control cells (**Figure 28**). Consistent with this, the surface expression of different co-stimulatory molecules that control IS formation such as CD3 and LFA-1 (**Figure 26**) were expressed at similar levels. However, whether the activation of the high affinity state of LFA-1 was compromised in cortactin-depleted Jurkat cells remains to be experimentally tested. In sharp contrast, *Cttn*^{-/-} mouse CD3⁺ T cells displayed a reduced ability to form conjugates with B-cell lymphoma A20 cells (**Figure 43**). Of note, this impaired conjugate formation was not due to defective TCR-mediated LFA-1 activation (**Figure 44**) because both cell types showed similar ICAM-1 binding capacities. These results demonstrate a novel role for cortactin IS formation at least in mouse T cell. It is worth mentioning that our assays analyzing human and mouse T cell conjugate formation followed different experimental approaches. In the case of Jurkat cells, conjugation with Raji cells was induced using anti-CD3 stimulation, that as mentioned above, only yielded very low conjugate numbers with unstable IS²⁸². On the other hand, mouse CD3⁺ cells were conjugated with A20 cells by means of allogeneic stimulation, *i.e.*, a MHC mismatch, which is a potent inducer of T cell responses. Thus, it is likely that IS formation in cortactin-depleted Jurkat cells is also impaired but might not have been obvious due to the weak conjugation procedure. It will therefore be important to repeat such experiments using different approaches to induce IS formation.

One of the first consequences of TCR engagement is the rapid polymerization of actin at the site of cell-cell contact formed between a T cell and an APC²⁸³. Moreover, the relevance of the cortactin homolog HS1 in T cell activation has been already demonstrated, as HS1-deficient T cells displayed impaired accumulation of F-actin at the IS, as well as reduced Ca⁺⁺ influx and diminished IL-2 gene transcription¹⁹⁰. Since cortactin and HS1 share a similar domain structure, we speculated that both proteins could be performing similar functions. Here, we have detected by flow cytometry that cortactin-depleted Jurkat cells presented diminished basal levels of F-actin and failed to induce actin polymerization upon TCR stimulation (**Figure 32**). Furthermore, we demonstrated that, although T cells isolated from *Cttn*^{-/-} mice presented similar levels of F-actin

than *Cttm*^{+/+} T cells under basal conditions (**Figure 45**), *Cttm*^{-/-} T cells displayed diminished actin polymerization at the site of cell-cell contact with APCs (**Figure 45**). As a matter of fact, cortactin deficiency in primary T cells resembled the absence of HS1 in T cells, therefore suggesting that both HS1 and cortactin might work in concert to properly control actin assembly at the IS in activated T cells. We are aware of the complexity of the regulation of the actin dynamics at the IS, as multiple proteins modulate this phenomenon, however, double-KO models of cortactin and HS1 might be useful to better understand whether cortactin and HS1 potentiate each other's functions or whether they act via independent mechanisms.

Proper reorganization of the actin cytoskeleton is important for multiple aspects of T cell function, including transmitting TCR signals to downstream effectors¹⁰⁶. Upon TCR engagement, rapid phosphorylation of different important T cell intracellular mediators such as ZAP-70, PLC γ 1 and ERK is induced¹²³. Although we detected defects in actin polymerization in cortactin-deficient T cells, we did not observe differences in the rapid phosphorylation of ERK upon TCR engagement using anti-CD3/28 antibodies (**Figure 30**). The MAPK pathway, of which ERK is an important effector, regulates the activity of the transcription factor AP-1 that, together with the TFs NFAT and NF- κ B, are essential for IL-2 transcription, a potent inducer of T cell proliferation and the generation of effector and memory T cells¹²⁸. Although early events of ERK phosphorylation were unaffected, we detected that upregulation of IL-2 mRNA was reduced in cortactin-depleted Jurkat cells upon TCR engagement (**Figure 29**), thus suggesting that maybe other components of the MAPK pathway are affected that need to be investigated in the future. By contrast, primary mouse *Cttm*^{-/-} T cells upregulated IL-2 production in a fashion similar to *Cttm*^{+/+} T cells (**Figure 41**). The reason for the different findings in human and mouse T cells remains elusive, but different early phosphorylation events in the MAPK pathway in response to T cell activation in mouse *Cttm*^{-/-} T cells could be the underlying mechanism. Additionally, differences in IL-2 upregulation might also result from different activation states. Jurkat is an hyperactivated leukemic T cell line characterized by constitutively active TCR signaling due to ZAP-70 overexpression²⁵⁸ leading to ERK phosphorylation and calcium influx²⁸⁴, whereas most T cells under basal conditions do not display TCR signaling unless stimulated. It has been shown that ERK activation is favored in naïve T cells upon TCR stimulation, whereas antigen-experienced (such as effector/memory) T cells rely on the activation of another protein of the MAPK pathway, namely p38, that activates preferentially the TF NFAT and IL2 expression²⁸⁵. Thus, it is possible that reduced p38 activation, but not ERK, in

cortactin-depleted Jurkat cells leads to defective activation of NFAT hence accounting for the reduced IL-2 expression. Meanwhile, ERK might play more prominent roles in the activation of resting murine T cells, since we detected normal upregulation of IL-2 observed in mouse T cells, although whether ERK is activated normally in *Cttn*^{-/-} T cells needs to be addressed. In this context, it is also important to mention that the analysis of the expression of IFN γ and TNF α in *Cttn*^{-/-} T cells, whose expression is regulated by NF- κ B and NFAT²⁸⁶, respectively, revealed no differences in *Cttn*^{-/-} T cells and *Cttn*^{+/+} T cells (**Figure 40**). However, whether the transcriptional activity of NFAT, NF- κ B or AP-1 is really affected by the absence of cortactin, and whether mouse and human T cells would show different transcriptional activities is currently unknown and should be investigated using cortactin-deficient T cells transfected with luciferase reporter plasmids containing the target sequences of these transcription factors. With such experiments, differences in the activation of these TFs in response to the absence of cortactin can be detected allowing for a prediction of target genes.

Signals from the TCR are also crucial for T cell proliferation²⁸⁷, which is in part regulated by the expression of IL-2 and its receptor CD25 in the stimulated T cell^{288,289}. Since IL-2 production was not impaired in *Cttn*^{-/-} T cells, we expected a similar rate of proliferation in these cells upon TCR engagement. As a matter of fact, proliferation of T cells induced by polyclonal stimulation with anti-CD3/28 antibodies was similar in *Cttn*^{+/+} and *Cttn*^{-/-} T cells (**Figures 42**). Nonetheless, we detected that allogeneic stimulation using A20 cells resulted in a reduced number of proliferating *Cttn*^{-/-} T cells, both CD4⁺ and CD8⁺ (**Figure 39**), in agreement with the reduced number of CD3⁺:A20 conjugates observed (**Figure 43**) and the defective F-actin recruitment to the IS (**Figure 45**). These results highlight a functional relevance of cortactin for TCR-mediated proliferation and T cell activation. The differences observed in proliferation using both methods are likely owed to the nature of the stimuli as discussed above. When using anti-CD3/28 antibodies, TCR stimulation occurs only through CD3, and co-stimulation by CD28, which is, according to our data, sufficient for T cell activation, but not for inducing all downstream signaling. Other co-stimulatory ligands on APCs such for T cell receptors including CD2, CD5, CD30, 4-1BB, OX-40, ICOS and LFA-1¹²³, are obviously required to trigger the full physiological response of T cells during activation, and highlight the relevance of cortactin for full T cell activation.

CXCL12 is another important co-stimulatory molecule for T cells as it enhances the activation of the TF AP-1 leading to increased expression of IL-2, IL-10 and CD25²⁷⁸. In fact, by using CXCL12, the ligand for CXCR4, to co-stimulate together with anti-CD3/28, we observed a significantly higher number of proliferating *Cttn*^{+/+} T cells than *Cttn*^{-/-} T cells (**Figure 42**). However, IL-2 production and CD25 expression were not enhanced by CXCL12 costimulation in our model (**Figure 41**). These results further highlight the functional differences of the stimuli used for TCR engagement; a phenomenon that has to be considered when analyzing T cell activation. Of note, the observed CXCR4-mediated TCR-costimulation was specific for CD4⁺ cells, thus revealing a potential different functional role of cortactin in different T cell subsets that should be further investigated in the future. Together, these results suggest that the absence of cortactin impacts on both TCR-mediated proliferation and CXCR4-mediated signaling.

CXCR4 is expressed in most T cell subsets, and its stimulation results in the activation of integrins, chemotaxis and gene expression^{290,291}. Moreover, cortactin expression is controlled by calcineurin and glioma-associated oncogene homolog (GLI), that in turn regulates the trafficking and surface expression of CXCR4 in leukemic T cells^{232,292}. However, in both our models of human and mouse cortactin-depleted T cells, CXCR4 surface levels were similar to control cells under basal conditions, (**Figure 27** and **37**) suggesting that CXCR4 surface levels in Jurkat and mouse CD3⁺ T cells do not depend exclusively on cortactin. For example, an association between CXCR4 and the TCR has been detected in primary and leukemic T cells upon TCR- or CXCR4-engagement^{278,293,294}. As a matter of fact, the T-ALL cell line DND4 used in the work by Tosello *et al.*, do not express the TCR, although it is not clear whether the mouse T-ALL generated by Passaro *et al.*, express the TCR. Thus, it is plausible that CXCR4 is translocated to the T cell surface by a mechanism dependent on cortactin and the TCR, whereas in T-ALL cell lines deficient on the TCR this trafficking depends solely on cortactin. Moreover, whether CXCR4 dynamics upon CXCL12 stimulation, such as endocytosis or receptor recycling are affected in our cells needs to be addressed.

Nevertheless, when we analyzed the migration of these cells towards a CXCL12 gradient, both human and mouse T cells lacking cortactin expression showed a significantly reduced number of migrating cells (**Figure 31** and **38**). Since migration is highly dependent on the actin cytoskeleton,

this reduced motility can likely be explained by the reduced initial values of F-actin in cortactin-deficient cells (**Figure 32**). As a matter of fact, cortactin-depleted Jurkat cells showed impaired induction of actin polymerization upon CXCL12 (**Figure 32**), therefore explaining in part the reduced chemotactic capacity. Although we have not tested this in mouse *Cttm*^{-/-} T cells, it is tempting to speculate that CXCR4-induced actin polymerization is also defective in these cells. Nevertheless, whether the defective CXCR4-mediated migration is completely dependent on the induction of F-actin polymerization needs to be corroborated using actin depolymerizing agents in cortactin-deficient T cells. Of note, chemotaxis of mouse T cells was performed using total CD3⁺ cells, which contain both CD4⁺ and CD8⁺ cells. Since we observed a defect in proliferation after CXCR4-mediated TCR-costimulation only in CD4⁺ cells, but not CD8⁺ cells, we speculate that CD4⁺ cells may account for the diminished migration, however, it remains to be analyzed whether CD8⁺ cells might also have defective responses to CXCR4. In summary, our results demonstrate that cortactin is an important downstream effector of F-actin polymerization upon CXCR4 stimulation in T cells, rather than controlling initial CXCR4 surface expression.

Several studies have demonstrated that cortactin overexpression in solid tumors is associated with metastasis and an overall worse prognosis for these patients^{208,215,217}. Furthermore, cortactin expression was also detected in leukemias, such as B-cell chronic lymphocytic leukemia (B-CLL), B-cell ALL (B-ALL)^{231,233} and mouse T-ALL²³². Of note, we have detected expression of much higher levels of cortactin in the T-ALL cell lines Jurkat and Molt-3 compared to normal T cells (**Figure 16**). In accordance, high expression of cortactin mRNA was detected by quantitative PCR in T-ALL samples compared to non-leukemic patients²⁹⁵. On the other hand, cortactin expression was associated to increased matrix metalloprotease-9 secretion, motility and invasion in B-CLL²³⁴; and B-ALL cells with higher expression of cortactin displayed enhanced migration capacity *in vitro* and *in vivo*²³³. Furthermore, cortactin expression in T-ALL controlled the trafficking of CXCR4, thus regulating migration and homing of leukemic T cells to the BM^{232,292}; and high expression of cortactin mRNA in T-ALL patients was positively correlated with an increased blast count in peripheral blood, higher risk of CNS involvement and overall worse prognosis²⁹⁵. Using cortactin-depleted Jurkat cells in xenograft assays, we observed that mice developed a milder disease, as leukemia burden in BM and peripheral blood was reduced, compared to control Jurkat

cells (**Figure 47**). Of note, a reduction of leukemic cells in peripheral blood is consistent with diminished leukemic burden in the BM, as leukemic T cells must engraft first in the BM before starting to proliferate and then exit to peripheral blood. The reduced leukemic cells in the BM might be explained by either a defect in the homing to the BM or diminished proliferation/increased apoptosis. We demonstrated that proliferation and apoptosis of cortactin-depleted and control Jurkat cells were similar under basal conditions *in vitro* (**Figure 26**) suggesting that it is rather the homing defect accounting for the reduced leukemic burden. However, we do not discard that in environments such as the BM that is rich in CXCL12, these cortactin-depleted Jurkat cells would display diminished survival. As a matter of fact, besides controlling chemotaxis and migration in T-ALL, the CXCL12/CXCR4 axis controls the survival and proliferation of T-ALL cells in the BM *in vivo*²³². Thus, an impaired response of cortactin-depleted Jurkat cells to CXCL12 in the BM may also lead to reduced proliferation or increased apoptosis in the BM *in vivo*. It will therefore be interesting to analyze the BM microenvironment and niche tropism in cortactin-deficient vs WT mice.

T-ALL cells also display a tropism for the CNS, a feature that negatively impinges in the prognosis of T-ALL patients²⁵⁴. We have also demonstrated that cortactin-depleted Jurkat cells lose the ability to infiltrate the CNS (**Figure 47C**), a similar defect than the one observed using cortactin-deficient B-ALL cells²³³. Interestingly, in another report CNS infiltration was dependent first on the colonization of the skull BM from where then the meninges and subsequently the CSF were invaded. Skull BM homing by T-ALL cells in turn was governed by the expression of CXCR4 in T-ALL cells, but not CCR6 or CCR7²⁵⁴. Therefore, it seems that leukemic T-cells do not migrate across the brain-blood-barrier, but rather access to the meninges via the skull BM²⁵⁴. The reduced leukemic burden in the BM of mice injected with cortactin-depleted Jurkat cells thus might also explain the low to absent infiltration of cortactin-depleted Jurkat cells to the CNS. However, whether the same phenomenon occurs in our model needs to be proven experimentally.

Moreover, high expression of HS1 mRNA was also found in T-ALL samples from patients that positively correlated with CNS infiltration and BM relapse²⁹⁵. However, we have detected comparably low expression of HS1 in the T-ALL cells we analyzed compared to normal T cells (**Figure 16**). Interestingly, HS1 was not upregulated as a compensatory effect by the absence of cortactin (**Figure 25**), and since we observed a very prominent defect in T-ALL development by

cortactin depletion, we speculate that HS1 might not be as important as cortactin for organ infiltration by Jurkat cells. Taken together, our results demonstrate that cortactin is a key factor regulating the migration of leukemic T cells, potentially by modulating signaling events downstream of the CXCR4/CXCL12 axis including F-actin polymerization.

8. CONCLUSION

The expression of cortactin was conclusively demonstrated in different human and mouse T cells in this work. Moreover, we found that cortactin was recruited to the IS where it was essential for actin dynamics upon TCR engagement, CXCR4-mediated TCR co-stimulation and proper T cell activation. On the other hand, cortactin played a critical role for CXCR4-dependent migration of T cells *in vitro* and *in vivo* likely through the regulation of actin dynamics. However, a causal relationship still needs to be conclusively demonstrated. Finally, we demonstrated the pathological relevance of cortactin in T-ALL, as cortactin-deficient T cells failed to colonize the BM and infiltrate the CNS. Together, our results highlight cortactin as an important regulator of T cell functions and T-ALL aggressiveness. Cortactin may thus be an interesting novel pharmacological target for autoimmune diseases or T-ALL.

9. PERSPECTIVES

- I. To determine the downstream effectors that connect TCR signaling with cortactin activation.
- II. To establish the causal relationship between defective actin remodeling and migration in the absence of cortactin.
- III. To analyze by intravital microscopy the homing of *Cttn*^{-/-} T cells to the LNs
- IV. To evaluate whether impaired synapse formation equally affects the effector functions of helper (CD4⁺) and cytotoxic (CD8⁺) cells and/or other T cell subsets.

10. REFERENCES

1. Bonilla, F. A. & Oettgen, H. C. Adaptive immunity. doi:10.1016/j.jaci.2009.09.017.
2. Budd, R. C. & Fortner, K. A. T Lymphocytes. *Kelley's Textb. Rheumatol.* 174–190 (2013) doi:10.1016/B978-1-4377-1738-9.00013-X.
3. Luckheeram, R. V., Zhou, R., Verma, A. D. & Xia, B. CD4⁺T cells: differentiation and functions. *Clin. Dev. Immunol.* **2012**, (2012).
4. Yui, M. A. & Rothenberg, E. V. Developmental gene networks: a triathlon on the course to T cell identity. *Nat. Publ. Gr.* (2014) doi:10.1038/nri3702.
5. Ciofani, M. & Zúñiga-Pflücker, J. C. The thymus as an inductive site for T lymphopoiesis. *Annu. Rev. Cell Dev. Biol.* **23**, 463–493 (2007).
6. Boes, K. M. & Durham, A. C. Bone Marrow, Blood Cells, and the Lymphoid/Lymphatic System. *Pathol. Basis Vet. Dis. Expert Consult* 724-804.e2 (2017) doi:10.1016/B978-0-323-35775-3.00013-8.
7. Savino, W., Smaniotto, S. & Dardenne, M. Hematopoiesis. *Advances in Experimental Medicine and Biology* vol. 567 167–185 (2005).
8. Famili, F., Wiekmeijer, A. S. & Staal, F. J. The development of T cells from stem cells in mice and humans. *Futur. Sci. OA* **3**, (2017).
9. Rieger, M. A. & Schroeder, T. Hematopoiesis. *Cold Spring Harb. Perspect. Biol.* **4**, (2012).
10. Spangrude, G. J., Heimfeld, S. & Weissman, I. L. Purification and characterization of mouse hematopoietic stem cells. *Science* **241**, 58–62 (1988).
11. Uchida, N. & Weissman, I. L. Searching for hematopoietic stem cells: evidence that Thy-1.1lo Lin- Sca-1+ cells are the only stem cells in C57BL/Ka-Thy-1.1 bone marrow. *J. Exp. Med.* **175**, 175–184 (1992).
12. Morrison, S. J. & Weissman, I. L. The long-term repopulating subset of hematopoietic stem cells is deterministic and isolatable by phenotype. *Immunity* **1**, 661–673 (1994).
13. Van Galen, P. *et al.* Reduced lymphoid lineage priming promotes human hematopoietic stem cell expansion. *Cell Stem Cell* **14**, 94–106 (2014).
14. Notta, F. *et al.* Distinct routes of lineage development reshape the human blood hierarchy across ontogeny. *Science* **351**, (2016).
15. Bigas, A., Martin, D. I. K. & Milner, L. A. Notch1 and Notch2 inhibit myeloid differentiation in response to different cytokines. *Mol. Cell. Biol.* **18**, 2324–2333 (1998).
16. Allman, D., Punt, J. A., Izon, D. J., Aster, J. C. & Pear, W. S. An invitation to T and more: notch signaling in lymphopoiesis. *Cell* **109 Suppl**, S1 (2002).
17. Lam, L. T., Ronchini, C., Norton, J., Capobianco, A. J. & Bresnick, E. H. Suppression of erythroid but not megakaryocytic differentiation of human K562 erythroleukemic cells by notch-1. *J. Biol. Chem.* **275**, 19676–19684 (2000).
18. Krause, D. S. Regulation of hematopoietic stem cell fate. *Oncogene* **21**, 3262–3269 (2002).
19. Månsson, R. *et al.* Molecular evidence for hierarchical transcriptional lineage priming in fetal and adult stem cells and multipotent progenitors. *Immunity* **26**, 407–419 (2007).
20. Sitnicka, E. *et al.* Key role of flt3 ligand in regulation of the common lymphoid progenitor but not in maintenance of the hematopoietic stem cell pool. *Immunity* **17**, 463–472 (2002).
21. Allman, D. *et al.* Thymopoiesis independent of common lymphoid progenitors. *Nat. Immunol.* **4**, 168–174 (2003).
22. Spits, H. *et al.* Innate lymphoid cells--a proposal for uniform nomenclature. *Nat. Rev. Immunol.* **13**, 145–149 (2013).
23. Yokota, Y. *et al.* Development of peripheral lymphoid organs and natural killer cells depends on the helix-loop-helix inhibitor Id2. *Nature* **397**, 702–706 (1999).
24. Thomas, D., Vadas, M. & Lopez, A. Regulation of haematopoiesis by growth factors - emerging insights and therapies. *Expert Opin. Biol. Ther.* **4**, 869–879 (2004).
25. Rothenberg, E. V., Moore, J. E. & Yui, M. A. Launching the T-cell-lineage developmental programme. *Nature Reviews Immunology* vol. 8 9–21 (2008).
26. Lind, E. F., Prockop, S. E., Porritt, H. E. & Petrie, H. T. Mapping precursor movement through the postnatal thymus reveals specific microenvironments supporting defined stages of early lymphoid development. *J. Exp. Med.* **194**, 127–134 (2001).
27. Bhandoola, A. & Sambandam, A. Parabiotic mice From stem cell to T cell: one route or many? *Nat. Rev.*

- Immunol.* **6**, 117–126 (2006).
28. Shortman, K. & Wu, L. Early T Lymphocyte Progenitors. <https://doi.org/10.1146/annurev.immunol.14.1.29> **14**, 29–47 (2003).
 29. Arinobu, Y. *et al.* Reciprocal activation of GATA-1 and PU.1 marks initial specification of hematopoietic stem cells into myeloerythroid and myelolymphoid lineages. *Cell Stem Cell* **1**, 416–427 (2007).
 30. Yoshida, T., Yao-Ming Ng, S., Zuniga-Pflucker, J. C. & Georgopoulos, K. Early hematopoietic lineage restrictions directed by Ikaros. *Nat. Immunol.* **7**, 382–391 (2006).
 31. Adolfsson, J. *et al.* Identification of Flt3⁺ lympho-myeloid stem cells lacking erythro-megakaryocytic potential a revised road map for adult blood lineage commitment. *Cell* **121**, 295–306 (2005).
 32. Weerkamp, F. *et al.* Human thymus contains multipotent progenitors with T/B lymphoid, myeloid, and erythroid lineage potential. *Blood* **107**, 3131–3137 (2006).
 33. Han, W., Ye, Q. & Moore, M. A. S. A soluble form of human Delta-like-1 inhibits differentiation of hematopoietic progenitor cells. *Blood* **95**, 1616–1625 (2000).
 34. Jaleco, A. C. *et al.* Differential effects of Notch ligands Delta-1 and Jagged-1 in human lymphoid differentiation. *J. Exp. Med.* **194**, 991–1001 (2001).
 35. Spits, H. Development of $\alpha\beta$ T cells in the human thymus. *Nat. Rev. Immunol.* **2002 210** **2**, 760–772 (2002).
 36. Germain, R. N. t-cell development and the CD4-CD8 lineage decision. *Nat. Rev. Immunol.* **2**, 309–322 (2002).
 37. Van Rijssel, J. *et al.* The Rho-GEF Trio regulates a novel pro-inflammatory pathway through the transcription factor Ets2. *Biol. Open* **2**, 569–579 (2013).
 38. Weber, B. N. *et al.* A critical role for TCF-1 in T-lineage specification and differentiation. *Nature* **476**, 63–69 (2011).
 39. Gifford, C. A. & Meissner, A. Epigenetic obstacles encountered by transcription factors: reprogramming against all odds. *Curr. Opin. Genet. Dev.* **22**, 409–415 (2012).
 40. Willert, K. & Jones, K. A. Wnt signaling: is the party in the nucleus? *Genes Dev.* **20**, 1394–1404 (2006).
 41. Yang, Q., Jeremiah Bell, J. & Bhandoola, A. T-cell lineage determination. *Immunol. Rev.* **238**, 12–22 (2010).
 42. Rothenberg, E. V. T cell lineage commitment: identity and renunciation. *J. Immunol.* **186**, 6649–6655 (2011).
 43. Seo, W. & Taniuchi, I. Mini-Review Transcriptional regulation of early T-cell development in the thymus. *Eur. J. Immunol* **46**, 531–538 (2016).
 44. Zhang, J. A., Mortazavi, A., Williams, B. A., Wold, B. J. & Rothenberg, E. V. Dynamic transformations of genome-wide epigenetic marking and transcriptional control establish T cell identity. *Cell* **149**, 467–482 (2012).
 45. Mingueneau, M. *et al.* The transcriptional landscape of $\alpha\beta$ T cell differentiation. *Nat. Immunol.* **14**, 619–632 (2013).
 46. Petrie, H. T. & Zúñiga-Pflücker, J. C. Zoned out: functional mapping of stromal signaling microenvironments in the thymus. *Annu. Rev. Immunol.* **25**, 649–679 (2007).
 47. Capone, M., Hockett, R. D. & Zlotnik, A. Kinetics of T cell receptor beta, gamma, and delta rearrangements during adult thymic development: T cell receptor rearrangements are present in CD44(+)CD25(+) Pro-T thymocytes. *Proc. Natl. Acad. Sci. U. S. A.* **95**, 12522–12527 (1998).
 48. Godfrey, D. I., Kennedy, J., Mombaerts, P., Tonegawa, S. & Zlotnik, A. Onset of TCR-beta gene rearrangement and role of TCR-beta expression during CD3-CD4-CD8- thymocyte differentiation. *J. Immunol.* **152**, (1994).
 49. Livák, F., Tourigny, M., Schatz, D. G. & Petrie, H. T. Characterization of TCR Gene Rearrangements During Adult Murine T Cell Development. *J. Immunol.* **162**, (1999).
 50. Dutta, A., Zhao, B. & Love, P. E. New insights into TCR β -selection. *Trends Immunol.* **42**, 735–750 (2021).
 51. Dudley, E. C., Petrie, H. T., Shah, L. M., Owen, M. J. & Hayday, A. C. T cell receptor beta chain gene rearrangement and selection during thymocyte development in adult mice. *Immunity* **1**, 83–93 (1994).
 52. Klein, L., Kyewski, B., Allen, P. M. & Hogquist, K. A. Positive and negative selection of the T cell repertoire: what thymocytes see (and don't see). (2014) doi:10.1038/nri3667.
 53. Kisielow, P. & Von Boehmer, H. Development and selection of T cells: facts and puzzles. *Adv. Immunol.* **58**, 87–209 (1995).
 54. Surh, C. D. & Sprent, J. Pillars Article: T-Cell Apoptosis Detected In Situ during Positive and Negative Selection in the Thymus. *Nature*. 1994. 372: 100-103. *J. Immunol.* **201**, 7–10 (2018).

55. Drayton, D. L., Liao, S., Mounzer, R. H. & Ruddle, N. H. Lymphoid organ development: from ontogeny to neogenesis. *Nat. Immunol.* **7**, 344–353 (2006).
56. Sigmundsdottir, H. & Butcher, E. C. Environmental cues, dendritic cells and the programming of tissue-selective lymphocyte trafficking. *Nat. Immunol.* **9**, 981–987 (2008).
57. Takeda, A., Sasaki, N. & Miyasaka, M. The molecular cues regulating immune cell trafficking. *Proc. Jpn. Acad. Ser. B. Phys. Biol. Sci.* **93**, 183–195 (2017).
58. Lee, M. *et al.* Transcriptional programs of lymphoid tissue capillary and high endothelium reveal control mechanisms for lymphocyte homing. *Nat. Immunol.* (2014) doi:10.1038/ni.2983.
59. Marsal, J. & Agace, W. W. Targeting T-cell migration in inflammatory bowel disease. *J. Intern. Med.* **272**, 411–429 (2012).
60. Schnoor, M., Alcaide, P., Voisin, M. B. & Van Buul, J. D. Crossing the Vascular Wall: Common and Unique Mechanisms Exploited by Different Leukocyte Subsets during Extravasation. *Mediators Inflamm.* **2015**, (2015).
61. Mackay, C. R., Marston, W. L. & Dudler, L. Naive and memory T cells show distinct pathways of lymphocyte recirculation. *J. Exp. Med.* **171**, 801–817 (1990).
62. Campbell, J. J. *et al.* Chemokines and the arrest of lymphocytes rolling under flow conditions. *Science* (80-). (1998) doi:10.1126/science.279.5349.381.
63. Manes, T. D. & Pober, J. S. Antigen Presentation by Human Microvascular Endothelial Cells Triggers ICAM-1-Dependent Transendothelial Protrusion by, and Fractalkine-Dependent Transendothelial Migration of, Effector Memory CD4+ T Cells. *J. Immunol.* **180**, 8386–8392 (2008).
64. Engelhardt, B. Molecular mechanisms involved in T cell migration across the blood-brain barrier. *J. Neural Transm.* **113**, 477–485 (2006).
65. Stein, J. V. *et al.* L-selectin-mediated leukocyte adhesion in vivo: microvillous distribution determines tethering efficiency, but not rolling velocity. *J. Exp. Med.* **189**, 37–49 (1999).
66. Brown, M. J. *et al.* Chemokine stimulation of human peripheral blood T lymphocytes induces rapid dephosphorylation of ERM proteins, which facilitates loss of microvilli and polarization. *Blood* **102**, 3890–3899 (2003).
67. Majstoravich, S. *et al.* Lymphocyte microvilli are dynamic, actin-dependent structures that do not require Wiskott-Aldrich syndrome protein (WASp) for their morphology. (2004) doi:10.1182/blood-2004-02-0437.
68. Hammer, D. A. & Apte, S. M. Simulation of cell rolling and adhesion on surfaces in shear flow: general results and analysis of selectin-mediated neutrophil adhesion. *Biophys. J.* **63**, 35–57 (1992).
69. Lawrence, M. B. & Springer, T. A. Leukocytes roll on a selectin at physiologic flow rates: distinction from and prerequisite for adhesion through integrins. *Cell* **65**, 859–873 (1991).
70. Briskin, M. J., McEvoy, L. M. & Butcher, E. C. MADCAM-1 has homology to immunoglobulin and mucin-like adhesion receptors and to IgA1. *Nature* **363**, 461–464 (1993).
71. Berlin, C. *et al.* alpha 4 integrins mediate lymphocyte attachment and rolling under physiologic flow. *Cell* **80**, 413–422 (1995).
72. Vestweber, D. How leukocytes cross the vascular endothelium. *Nat. Rev. Immunol.* **15**, 692–704 (2015).
73. Atarashi, K., Hirata, T., Matsumoto, M., Kanemitsu, N. & Miyasaka, M. Rolling of Th1 Cells via P-Selectin Glycoprotein Ligand-1 Stimulates LFA-1-Mediated Cell Binding to ICAM-1. *J. Immunol.* **174**, 1424–1432 (2005).
74. Timmerman, I., Daniel, A. E., Kroon, J. & Van Buul, J. D. Leukocytes Crossing the Endothelium: A Matter of Communication. *Int. Rev. Cell Mol. Biol.* **322**, 281–329 (2016).
75. Madri, J. & Graesser, D. Cell migration in the immune system: the evolving inter-related roles of adhesion molecules and proteinases. *Dev. Immunol.* **7**, 103–116 (2000).
76. Springer, T. A. & Dustin, M. L. Integrin inside-out signaling and the immunological synapse. *Curr. Opin. Cell Biol.* **24**, 107–115 (2012).
77. Cook-Mills, J. M. Active participation of endothelial cells in inflammation. *J. Leukoc. Biol.* **77**, 487–495 (2004).
78. Miyasaka, M. & Tanaka, T. Lymphocyte trafficking across high endothelial venules: dogmas and enigmas. *Nat. Rev. Immunol.* **4**, 360–370 (2004).
79. Förster, R. *et al.* CCR7 coordinates the primary immune response by establishing functional microenvironments in secondary lymphoid organs. *Cell* **99**, 23–33 (1999).
80. Nakano, H. *et al.* Genetic defect in T lymphocyte-specific homing into peripheral lymph nodes. *Eur. J. Immunol.* (1997) doi:10.1002/eji.1830270132.

81. Laffon, A. *et al.* Upregulated expression and function of VLA-4 fibronectin receptors on human activated T cells in rheumatoid arthritis. *J Clin Invest* **88**, 546–552 (1991).
82. Bönig, H. & Kim, Y. Targeted Therapy of Acute Myeloid Leukemia. 637–654 (2015) doi:10.1007/978-1-4939-1393-0.
83. Chigaev, A., Wu, Y., Williams, D. B., Smagley, Y. & Sklar, L. A. Discovery of Very Late Antigen-4 (VLA-4, $\alpha 4\beta 1$ integrin) allosteric antagonists. *J. Biol. Chem.* **286**, 5455–5463 (2011).
84. Hyun, Y.-M., Chung, H.-L., McGrath, J. L., Waugh, R. E. & Kim, M. Activated Integrin VLA-4 Localizes to the Lamellipodia and Mediates T Cell Migration on VCAM-1. *J. Immunol.* **183**, 359–369 (2009).
85. Walling, B. L. & Kim, M. LFA-1 in T Cell Migration and Differentiation. *Front. Immunol.* **9**, (2018).
86. Krummel, M. F., Bartumeus, F. & Gérard, A. T cell migration, search strategies and mechanisms. *Nat. Rev. Immunol.* **16**, 193–201 (2016).
87. Bajénoff, M. *et al.* Stromal Cell Networks Regulate Lymphocyte Entry, Migration, and Territoriality in Lymph Nodes. *Immunity* (2006) doi:10.1016/j.immuni.2006.10.011.
88. Carman, C. V. *et al.* Transcellular diapedesis is initiated by invasive podosomes. *Immunity* **26**, 784–797 (2007).
89. Carman, C. V. Mechanisms for transcellular diapedesis: probing and pathfinding by ‘invadosome-like protrusions’. *J. Cell Sci.* **122**, 3025–3035 (2009).
90. Shulman, Z. *et al.* Lymphocyte crawling and transendothelial migration require chemokine triggering of high-affinity LFA-1 integrin. *Immunity* **30**, 384–396 (2009).
91. Gérard, A., Van Der Kammen, R. A., Janssen, H., Ellenbroek, S. I. & Collard, J. G. The Rac activator Tiam1 controls efficient T-cell trafficking and route of transendothelial migration. *Blood* **113**, 6138–6147 (2009).
92. Linder, S. Invadosomes at a glance. *J. Cell Sci.* **122**, 3009–3013 (2009).
93. Marelli-Berg, F., Carman, C. V & Martinelli, R. T Lymphocyte-endothelial interactions: emerging Understanding of Trafficking and Antigen-Specific immunity. **6**, (2015).
94. Martinelli, R. *et al.* Probing the biomechanical contribution of the endothelium to lymphocyte migration: diapedesis by the path of least resistance. *J. Cell Sci.* **127**, 3720–3734 (2014).
95. Sumagin, R. & Sarelius, I. H. Intercellular adhesion molecule-1 enrichment near tricellular endothelial junctions is preferentially associated with leukocyte transmigration and signals for reorganization of these junctions to accommodate leukocyte passage. *J. Immunol.* **184**, 5242–5252 (2010).
96. Woodfin, A. *et al.* The junctional adhesion molecule JAM-C regulates polarized transendothelial migration of neutrophils in vivo. *Nat. Immunol.* **12**, 761–769 (2011).
97. Abadier, M. *et al.* Cell surface levels of endothelial ICAM-1 influence the transcellular or paracellular T-cell diapedesis across the blood-brain barrier. *Eur. J. Immunol.* **45**, 1043–1058 (2015).
98. Wimmer, I. *et al.* PECAM-1 Stabilizes Blood-Brain Barrier Integrity and Favors Paracellular T-Cell Diapedesis Across the Blood-Brain Barrier During Neuroinflammation. *Front. Immunol.* **10**, (2019).
99. Muller, W. A. Mechanisms of Leukocyte Transendothelial Migration. *Annu. Rev. Pathol. Mech. Dis.* (2011) doi:10.1146/annurev-pathol-011110-130224.
100. Millán, J. *et al.* Lymphocyte transcellular migration occurs through recruitment of endothelial ICAM-1 to caveola- and F-actin-rich domains. *Nat. Cell Biol.* **2006** **8**, 113–123 (2006).
101. Mempel, T. R., Henrickson, S. E. & Von Andrian, U. H. T-cell priming by dendritic cells in lymph nodes occurs in three distinct phases. *Nature* **427**, 154–159 (2004).
102. Goldrath, A. W., Bogatzki, L. Y. & Bevan, M. J. Naive T cells transiently acquire a memory-like phenotype during homeostasis-driven proliferation. *J. Exp. Med.* **192**, 557–564 (2000).
103. Min, B. *et al.* Neonates support lymphopenia-induced proliferation. *Immunity* **18**, 131–140 (2003).
104. Dustin, M. L. T-cell activation through immunological synapses and kinapses. *Immunol. Rev.* **221**, 77–89 (2008).
105. Rudolph, M. G., Stanfield, R. L. & Wilson, I. A. How TCRs bind MHCs, peptides, and coreceptors. *Annu. Rev. Immunol.* **24**, 419–466 (2006).
106. Burkhardt, J. K., Carrizosa, E. & Shaffer, M. H. The Actin Cytoskeleton in T Cell Activation. *Annu. Rev. Immunol.* (2008) doi:10.1146/annurev.immunol.26.021607.090347.
107. Huppa, J. B. & Davis, M. M. T-cell-antigen recognition and the immunological synapse. *Nat. Rev. Immunol.* **3**, 973–983 (2003).
108. Irvine, D. J., Purbhoo, M. A., Krosgaard, M. & Davis, M. M. Direct observation of ligand recognition by T cells. *Nature* **419**, 845–849 (2002).

109. Monks, C. R. F., Freiberg, B. A., Kupfer, H., Sciaky, N. & Kupfer, A. Three-dimensional segregation of supramolecular activation clusters in T cells. *Nature* **395**, 82–86 (1998).
110. Alarcón, B., Mestre, D. & Martínez-Martín, N. The immunological synapse: a cause or consequence of T-cell receptor triggering? *Immunology* **133**, 420–425 (2011).
111. Čemerski, S. & Shaw, A. Immune synapses in T-cell activation. *Curr. Opin. Immunol.* **18**, 298–304 (2006).
112. Saito, T. & Yokosuka, T. Immunological synapse and microclusters: the site for recognition and activation of T cells. *Curr. Opin. Immunol.* **18**, 305–313 (2006).
113. Dustin, M. L. A dynamic view of the immunological synapse. *Semin. Immunol.* **17**, 400–410 (2005).
114. Stinchcombe, J. C., Majorovits, E., Bossi, G., Fuller, S. & Griffiths, G. M. Centrosome polarization delivers secretory granules to the immunological synapse. *Nature* **443**, 462–465 (2006).
115. Bunnell, S. C. *et al.* T cell receptor ligation induces the formation of dynamically regulated signaling assemblies. *J. Cell Biol.* **158**, 1263–1275 (2002).
116. Koretzky, G. A., Abtahian, F. & Silverman, M. A. SLP76 and SLP65: complex regulation of signalling in lymphocytes and beyond. *Nat. Rev. Immunol.* **6**, 67–78 (2006).
117. Zhang, W. *et al.* Essential role of LAT in T cell development. *Immunity* **10**, 323–332 (1999).
118. Sommers, C. L., Samelson, L. E. & Love, P. E. LAT: a T lymphocyte adapter protein that couples the antigen receptor to downstream signaling pathways. *Bioessays* **26**, 61–67 (2004).
119. Liu, S. K., Fang, N., Koretzky, G. A. & McGlade, C. J. The hematopoietic-specific adaptor protein gads functions in T-cell signaling via interactions with the SLP-76 and LAT adaptors. *Curr. Biol.* **9**, 67–75 (1999).
120. Reynolds, L. F. *et al.* Vav1 transduces T cell receptor signals to the activation of the Ras/ERK pathway via LAT, Sos, and RasGRP1. *J. Biol. Chem.* **279**, 18239–18246 (2004).
121. Reynolds, L. F. *et al.* Vav1 transduces T cell receptor signals to the activation of phospholipase C-gamma1 via phosphoinositide 3-kinase-dependent and -independent pathways. *J. Exp. Med.* **195**, 1103–1114 (2002).
122. Dombroski, D. *et al.* Kinase-independent functions for Itk in TCR-induced regulation of Vav and the actin cytoskeleton. *J. Immunol.* **174**, 1385–1392 (2005).
123. Smith-Garvin, J. E., Koretzky, G. A. & Jordan, M. S. T cell activation. *Annu. Rev. Immunol.* **27**, 591–619 (2009).
124. Wang, J., Shannon, M. F. & Young, I. G. A role for Ets1, synergizing with AP-1 and GATA-3 in the regulation of IL-5 transcription in mouse Th2 lymphocytes. *Int. Immunol.* **18**, 313–323 (2006).
125. Bremer, S., Vethe, N. T. & Bergan, S. Monitoring Calcineurin Inhibitors Response Based on NFAT-Regulated Gene Expression. in *Personalized Immunosuppression in Transplantation: Role of Biomarker Monitoring and Therapeutic Drug Monitoring* 259–290 (Elsevier, 2016). doi:10.1016/B978-0-12-800885-0.00011-4.
126. Sun, Z. *et al.* PKC-theta is required for TCR-induced NF-kappaB activation in mature but not immature T lymphocytes. *Nature* **404**, 402–407 (2000).
127. Crabtree, G. R. & Olson, E. N. NFAT signaling: choreographing the social lives of cells. *Cell* **109 Suppl**, (2002).
128. Malek, T. R. The biology of interleukin-2. *Annu. Rev. Immunol.* **26**, 453–479 (2008).
129. Ross, S. H. & Cantrell, D. A. Signaling and Function of Interleukin-2 in T Lymphocytes. *Annu. Rev. Immunol.* **36**, 411 (2018).
130. Janas, M. L., Groves, P., Kienzle, N. & Kelso, A. IL-2 regulates perforin and granzyme gene expression in CD8+ T cells independently of its effects on survival and proliferation. *J. Immunol.* **175**, 8003–8010 (2005).
131. Kasahara, T., Hooks, J. J., Dougherty, S. F. & Oppenheim, J. J. Interleukin 2-mediated immune interferon (IFN-gamma) production by human T cells and T cell subsets. *J. Immunol.* **130**, (1983).
132. Hinrichs, C. S. *et al.* IL-2 and IL-21 confer opposing differentiation programs to CD8+ T cells for adoptive immunotherapy. *Blood* **111**, 5326–5333 (2008).
133. Reem, G. H. & Yeh, N. H. Interleukin 2 regulates expression of its receptor and synthesis of gamma interferon by human T lymphocytes. *Science* **225**, 429–430 (1984).
134. Zhu, J. T Helper Cell Differentiation, Heterogeneity, and Plasticity. *Cold Spring Harb. Perspect. Biol.* **10**, (2018).
135. Medzhitov, R. *et al.* Highlights of 10 years of immunology in Nature Reviews Immunology. *Nat. Rev. Immunol.* **2011 1110** **11**, 693–702 (2011).
136. Murray, H. W., Rubin, B. Y., Carriero, S. M., Harris, A. M. & Jaffee, E. A. Human mononuclear phagocyte antiprotazoal mechanisms: oxygen-dependent vs oxygen-independent activity against intracellular

- Toxoplasma gondii. *J. Immunol.* **134**, (1985).
137. Kim, H. P., Imbert, J. & Leonard, W. J. Both integrated and differential regulation of components of the IL-2/IL-2 receptor system. *Cytokine Growth Factor Rev.* **17**, 349–366 (2006).
 138. Szabo, S. J., Sullivan, B. M., Peng, S. L. & Glimcher, L. H. Molecular mechanisms regulating Th1 immune responses. *Annu. Rev. Immunol.* **21**, 713–758 (2003).
 139. Zhu, L., Cho, E., Zhao, G., Roh, M. I. R. & Zheng, Z. The Pathogenic Effect of Cortactin Tyrosine Phosphorylation in Cutaneous Squamous Cell Carcinoma. **400**, 393–400 (2019).
 140. Dardalhon, V., Korn, T., Kuchroo, V. K. & Anderson, A. C. Role of Th1 and Th17 cells in organ-specific autoimmunity. (2008) doi:10.1016/j.jaut.2008.04.017.
 141. Lazarevic, V. *et al.* T-bet represses T(H)17 differentiation by preventing Runx1-mediated activation of the gene encoding ROR γ t. *Nat. Immunol.* **12**, 96–104 (2011).
 142. Lugo-Villarino, G., Maldonado-López, R., Possemato, R., Peñaranda, C. & Glimcher, L. H. T-bet is required for optimal production of IFN-gamma and antigen-specific T cell activation by dendritic cells. *Proc. Natl. Acad. Sci. U. S. A.* **100**, 7749–7754 (2003).
 143. Afkarian, M. *et al.* T-bet is a STAT1-induced regulator for IL-12R expression in naïve CD4⁺ T cells. *Nat. Immunol.* **3**, 549–557 (2002).
 144. Sokol, C. L. *et al.* Basophils function as antigen-presenting cells for an allergen-induced T helper type 2 response. *Nat. Immunol.* **10**, 713–720 (2009).
 145. Prete, G. Del. Human Th1 and Th2 lymphocytes: their role in the pathophysiology of atopy. *Allergy* **47**, 450–455 (1992).
 146. Steinke, J. W. & Borish, L. Th2 cytokines and asthma — Interleukin-4: its role in the pathogenesis of asthma, and targeting it for asthma treatment with interleukin-4 receptor antagonists. *Respir. Res.* **2**, 66 (2001).
 147. Doucet, C. *et al.* IL-4 and IL-13 specifically increase adhesion molecule and inflammatory cytokine expression in human lung fibroblasts. *Int. Immunol.* **10**, 1421–1433 (1998).
 148. Martinez-Moczygemba, M. & Huston, D. P. Biology of common beta receptor-signaling cytokines: IL-3, IL-5, and GM-CSF. *J. Allergy Clin. Immunol.* **112**, 653–665 (2003).
 149. Couper, K. N., Blount, D. G. & Riley, E. M. IL-10: the master regulator of immunity to infection. *J. Immunol.* **180**, 5771–5777 (2008).
 150. Wynn, T. A. IL-13 effector functions. *Annu. Rev. Immunol.* **21**, 425–456 (2003).
 151. Fort, M. M. *et al.* IL-25 induces IL-4, IL-5, and IL-13 and Th2-associated pathologies in vivo. *Immunity* **15**, 985–995 (2001).
 152. Kaplan, M. H., Schindler, U., Smiley, S. T. & Grusby, M. J. Stat6 is required for mediating responses to IL-4 and for the development of Th2 cells. *Immunity* **4**, 313–319 (1996).
 153. Glimcher, L. H. & Murphy, K. M. Lineage commitment in the immune system: the T helper lymphocyte grows up. *Genes Dev.* **14**, 1693–1711 (2000).
 154. Zhu, J., Guo, L., Watson, C. J., Hu-Li, J. & Paul, W. E. Stat6 is necessary and sufficient for IL-4's role in Th2 differentiation and cell expansion. *J. Immunol.* **166**, 7276–7281 (2001).
 155. Veldhoen, M. *et al.* Transforming growth factor-beta 'reprograms' the differentiation of T helper 2 cells and promotes an interleukin 9-producing subset. *Nat. Immunol.* **9**, 1341–1346 (2008).
 156. Angkasekwinai, P. Th9 Cells in Allergic Disease. *Curr. Allergy Asthma Rep.* **19**, (2019).
 157. Ouyang, W., Kolls, J. K. & Zheng, Y. The Biological Functions of T Helper 17 Cell Effector Cytokines in Inflammation. *Immunity* **28**, 454–467 (2008).
 158. Korn, T., Bettelli, E., Oukka, M. & Kuchroo, V. K. IL-17 and Th17 cells. *Annu. Rev. Immunol.* **27**, 485–517 (2009).
 159. Ivanov, I. I. *et al.* The orphan nuclear receptor ROR γ directs the differentiation program of proinflammatory IL-17⁺ T helper cells. *Cell* **126**, 1121–1133 (2006).
 160. Moseley, T. A., Haudenschild, D. R., Rose, L. & Reddi, A. H. Interleukin-17 family and IL-17 receptors. *Cytokine Growth Factor Rev.* **14**, 155–174 (2003).
 161. Chen, W. J. *et al.* Conversion of peripheral CD4⁺CD25⁻ naive T cells to CD4⁺CD25⁺ regulatory T cells by TGF-beta induction of transcription factor Foxp3. *J. Exp. Med.* **198**, 1875–1886 (2003).
 162. Sakaguchi, S. *et al.* Foxp3⁺ CD25⁺ CD4⁺ natural regulatory T cells in dominant self-tolerance and autoimmune disease. *Immunol. Rev.* **212**, 8–27 (2006).
 163. Zhu, J., Yamane, H. & Paul, W. E. Differentiation of effector CD4 T cell populations (*). *Annu. Rev. Immunol.* **28**, 445–489 (2010).

164. Bilate, A. M. & Lafaille, J. J. Induced CD4+Foxp3+ regulatory T cells in immune tolerance. *Annu. Rev. Immunol.* **30**, 733–758 (2012).
165. Li, M. O., Wan, Y. Y. & Flavell, R. A. T cell-produced transforming growth factor-beta1 controls T cell tolerance and regulates Th1- and Th17-cell differentiation. *Immunity* **26**, 579–591 (2007).
166. Kriegel, M. A., Li, M. O., Sanjabi, S., Wan, Y. Y. & Flavell, R. A. Transforming growth factor-beta: recent advances on its role in immune tolerance. *Curr. Rheumatol. Rep.* **8**, 138–144 (2006).
167. Yoshimura, A. & Muto, G. TGF- β function in immune suppression. *Curr. Top. Microbiol. Immunol.* **350**, 127–147 (2011).
168. Vinuesa, C. G., Tangye, S. G., Moser, B. & Mackay, C. R. Follicular B helper T cells in antibody responses and autoimmunity. *Nat. Rev. Immunol.* **5**, 853–865 (2005).
169. Breitfeld, D. *et al.* Follicular B helper T cells express CXC chemokine receptor 5, localize to B cell follicles, and support immunoglobulin production. *J. Exp. Med.* **192**, 1545–1551 (2000).
170. Fazilleau, N., Mark, L., McHeyzer-Williams, L. J. & McHeyzer-Williams, M. G. Follicular helper T cells: lineage and location. *Immunity* **30**, 324–335 (2009).
171. Vogelzang, A. *et al.* A Fundamental Role for Interleukin-21 in the Generation of T Follicular Helper Cells. *Immunity* **29**, 127–137 (2008).
172. Nurieva, R. I. *et al.* Generation of T follicular helper cells is mediated by interleukin-21 but independent of T helper 1, 2, or 17 cell lineages. *Immunity* **29**, 138–149 (2008).
173. Bossaller, L. *et al.* ICOS deficiency is associated with a severe reduction of CXCR5+CD4 germinal center Th cells. *J. Immunol.* **177**, 4927–4932 (2006).
174. Billadeau, D. D., Nolz, J. C. & Gomez, T. S. Regulation of T-cell activation by the cytoskeleton. *Nature Reviews Immunology* (2007) doi:10.1038/nri2021.
175. Tskvitaria-Fuller, I., Rozelle, A. L., Yin, H. L. & Wülfing, C. Regulation of sustained actin dynamics by the TCR and costimulation as a mechanism of receptor localization. *J. Immunol.* **171**, 2287–2295 (2003).
176. Krummel, M. F., Sjaastad, M. D., Wulfing, C. W. & Davis, M. M. Differential clustering of CD4 and CD3zeta during T cell recognition. *Science* **289**, 1349–1352 (2000).
177. Valitutti, S., Dessing, M., Aktories, K., Gallati, H. & Lanzavecchia, A. Sustained signaling leading to T cell activation results from prolonged T cell receptor occupancy. Role of T cell actin cytoskeleton. *J. Exp. Med.* **181**, 577–584 (1995).
178. Bunnell, S. C., Kapoor, V., Tribble, R. P., Zhang, W. & Samelson, L. E. Dynamic actin polymerization drives T cell receptor-induced spreading: a role for the signal transduction adaptor LAT. *Immunity* **14**, 315–329 (2001).
179. Cullinan, P., Sperling, A. I. & Burkhardt, J. K. The distal pole complex: a novel membrane domain distal to the immunological synapse. *Immunol. Rev.* **189**, 111–122 (2002).
180. Vicente-Manzanares, M. & Sánchez-Madrid, F. Role of the cytoskeleton during leukocyte responses. *Nat. Rev. Immunol.* **4**, 110–122 (2004).
181. Tybulewicz, V. L. J. Vav-family proteins in T-cell signalling. *Curr. Opin. Immunol.* **17**, 267–274 (2005).
182. Billadeau, D. D. & Burkhardt, J. K. Regulation of cytoskeletal dynamics at the immune synapse: new stars join the actin troupe. *Traffic* **7**, 1451–1460 (2006).
183. Zeng, R. *et al.* SLP-76 coordinates Nck-dependent Wiskott-Aldrich syndrome protein recruitment with Vav-1/Cdc42-dependent Wiskott-Aldrich syndrome protein activation at the T cell-APC contact site. *J. Immunol.* **171**, 1360–1368 (2003).
184. Volkman, B. F., Prehoda, K. E., Scott, J. A., Peterson, F. C. & Lim, W. A. Structure of the N-WASP EVH1 domain-WIP complex: insight into the molecular basis of Wiskott-Aldrich Syndrome. *Cell* **111**, 565–576 (2002).
185. De La Fuente, M. A. *et al.* WIP is a chaperone for Wiskott-Aldrich syndrome protein (WASP). *Proc. Natl. Acad. Sci. U. S. A.* **104**, 926–931 (2007).
186. Badour, K., Zhang, J. & Siminovitch, K. A. The Wiskott-Aldrich syndrome protein: forging the link between actin and cell activation. *Immunol. Rev.* **192**, 98–112 (2003).
187. Antón, I. M. *et al.* WIP deficiency reveals a differential role for WIP and the actin cytoskeleton in T and B cell activation. *Immunity* **16**, 193–204 (2002).
188. Zipfel, P. A. *et al.* Role for the Abi/wave protein complex in T cell receptor-mediated proliferation and cytoskeletal remodeling. *Curr. Biol.* **16**, 35–46 (2006).
189. Billadeau, D. D. *et al.* The WAVE2 complex regulates actin cytoskeletal reorganization and CRAC-mediated calcium entry during T cell activation. *Nat. Rev. Immunol.* **16**, 24–34 (2006).

190. Gomez, T. S. *et al.* HS1 Functions as an Essential Actin-Regulatory Adaptor Protein at the Immune Synapse. *Immunity* (2006) doi:10.1016/j.immuni.2006.03.022.
191. Rivas, F. V., O'Keefe, J. P., Alegre, M.-L. & Gajewski, T. F. Actin cytoskeleton regulates calcium dynamics and NFAT nuclear duration. *Mol. Cell. Biol.* **24**, 1628–1639 (2004).
192. Holsinger, L. J. *et al.* Defects in actin-cap formation in Vav-deficient mice implicate an actin requirement for lymphocyte signal transduction. *Curr. Biol.* **8**, 563–573 (1998).
193. Föger, N., Rangell, L., Danilenko, D. M. & Chan, A. C. Requirement for coronin 1 in T lymphocyte trafficking and cellular homeostasis. *Science* **313**, 839–842 (2006).
194. Eibert, S. M. *et al.* Cofilin peptide homologs interfere with immunological synapse formation and T cell activation. *Proc. Natl. Acad. Sci. U. S. A.* **101**, 1957–1962 (2004).
195. Krummel, M. F. & Macara, I. Maintenance and modulation of T cell polarity. *Nat. Immunol.* **7**, 1143–1149 (2006).
196. Angel Del Pozo, M., Vicente-Manzanares, M., Tejedor, R., Serrador, J. M. & Sánchez-Madrid, F. S. Rho GTPases control migration and polarization of adhesion molecules and cytoskeletal ERM components in T lymphocytes. doi:10.1002/(SICI)1521-4141(199911)29:11.
197. D'Souza-Schorey, C., Boettner, B. & Van Aelst, L. Rac regulates integrin-mediated spreading and increased adhesion of T lymphocytes. *Mol. Cell. Biol.* **18**, 3936–3946 (1998).
198. Haddad, E. *et al.* The interaction between Cdc42 and WASP is required for SDF-1-induced T-lymphocyte chemotaxis. *Blood* **97**, 33–38 (2001).
199. Snapper, S. B. *et al.* WASP deficiency leads to global defects of directed leukocyte migration in vitro and in vivo. *J. Leukoc. Biol.* **77**, 993–998 (2005).
200. Yan, C. *et al.* WAVE2 deficiency reveals distinct roles in embryogenesis and Rac-mediated actin-based motility. *EMBO J.* **22**, 3602–3612 (2003).
201. Laudanna, C., Campbell, J. J. & Butcher, E. C. Role of Rho in chemoattractant-activated leukocyte adhesion through integrins. *Science* **271**, 981–983 (1996).
202. Constantin, G. *et al.* Chemokines trigger immediate beta2 integrin affinity and mobility changes: differential regulation and roles in lymphocyte arrest under flow. *Immunity* **13**, 759–769 (2000).
203. Jacobelli, J., Chmura, S. A., Buxton, D. B., Davis, M. M. & Krummel, M. F. A single class II myosin modulates T cell motility and stopping, but not synapse formation. *Nat. Immunol.* **5**, 531–538 (2004).
204. Bustelo, X. R. Understanding Rho/Rac biology in T-cells using animal models. *Bioessays* **24**, 602–612 (2002).
205. Bardi, G., Niggli, V. & Loetscher, P. Rho kinase is required for CCR7-mediated polarization and chemotaxis of T lymphocytes. *FEBS Lett.* **542**, 79–83 (2003).
206. Lee, J. H. *et al.* Roles of p-ERM and Rho-ROCK signaling in lymphocyte polarity and uropod formation. *J. Cell Biol.* **167**, 327–337 (2004).
207. Wu, H., Reynolds, A. B., Kanner, S. B., Vines, R. R. & Parsons, J. T. Identification and characterization of a novel cytoskeleton-associated pp60src substrate. *Mol. Cell. Biol.* (1991) doi:10.1128/MCB.11.10.5113.
208. Schnoor, M., Stradal, T. E. & Rottner, K. Cortactin: Cell Functions of A Multifaceted Actin-Binding Protein. *Trends in Cell Biology* (2017) doi:10.1016/j.tcb.2017.10.009.
209. Li, A., Zhang, L., Zhang, X., Jin, W. & Ren, Y. Expression and clinical significance of cortactin protein in ovarian neoplasms. *Clin. Transl. Oncol.* **18**, 220–227 (2016).
210. Hiura, K., Lim, S. -S, Little, S. P., Lin, S. & Sato, M. Differentiation dependent expression of tensin and cortactin in chicken osteoclasts. *Cell Motil. Cytoskeleton* (1995) doi:10.1002/cm.970300405.
211. Mizutani, K. *et al.* Essential role of neural Wiskott-Aldrich syndrome protein in podosome formation and degradation of extracellular matrix in src-transformed fibroblasts. *Cancer Res.* (2002).
212. Castro-Ochoa, K. F., Guerrero-Fonseca, I. M. & Schnoor, M. Hematopoietic cell-specific lyn substrate (HCLS1 or HS1): A versatile actin-binding protein in leukocytes. *Journal of Leukocyte Biology* (2019) doi:10.1002/JLB.MR0618-212R.
213. Weaver, A. M. *et al.* Cortactin promotes and stabilizes Arp2/3-induced actin filament network formation. *Curr. Biol.* (2001) doi:10.1016/S0960-9822(01)00098-7.
214. Schuurin, E., Verhoeven, E., Mooi, W. J. & Michalides, R. J. Identification and cloning of two overexpressed genes, U21B31/PRAD1 and EMS1, within the amplified chromosome 11q13 region in human carcinomas. *Oncogene* (1992).
215. Castellanos-Martínez, R., Jiménez-Camacho, K. E. & Schnoor, M. Cortactin Expression in Hematopoietic Cells: Implications for Hematological Malignancies. *Am. J. Pathol.* **190**, 958–967 (2020).

216. van Rossum, A. G. S. H. *et al.* Alternative Splicing of the Actin Binding Domain of Human Cortactin Affects Cell Migration. *J. Biol. Chem.* **278**, 45672–45679 (2003).
217. Yin, M., Ma, W. & An, L. Cortactin in cancer cell migration and invasion. *Oncotarget* **8**, 88232–88243 (2017).
218. Tehrani, S., Tomasevic, N., Weed, S., Sakowicz, R. & Cooper, J. A. Src phosphorylation of cortactin enhances actin assembly. *Proc. Natl. Acad. Sci. U. S. A.* (2007) doi:10.1073/pnas.0701077104.
219. Wang, W., Liu, Y. & Liao, K. Tyrosine phosphorylation of cortactin by the FAK-Src complex at focal adhesions regulates cell motility. *BMC Cell Biol.* **12**, 49 (2011).
220. Yang, L., Kowalski, J. R., Zhan, X., Thomas, S. M. & Lusciuskas, F. W. Endothelial cell cortactin phosphorylation by Src contributes to polymorphonuclear leukocyte transmigration in vitro. *Circ. Res.* **98**, 394–402 (2006).
221. Luo, C. *et al.* CXCL12 induces tyrosine phosphorylation of cortactin, which plays a role in CXC chemokine receptor 4-mediated extracellular signal-regulated kinase activation and chemotaxis. *J. Biol. Chem.* **281**, 30081–30093 (2006).
222. Zhang, X. *et al.* HDAC6 Modulates Cell Motility by Altering the Acetylation Level of Cortactin. *Mol. Cell* (2007) doi:10.1016/j.molcel.2007.05.033.
223. Zhang, Y. *et al.* Deacetylation of cortactin by SIRT1 promotes cell migration. *Oncogene* (2009) doi:10.1038/onc.2008.388.
224. Weed, S. A. & Parsons, J. T. Cortactin: Coupling membrane dynamics to cortical actin assembly. *Oncogene* (2001) doi:10.1038/sj.onc.1204783.
225. van Rossum, A. G. S. H., Schuurings-Scholtes, E., van Buuren-van Seggelen, V., Kluin, P. M. & Schuurings, E. Comparative genome analysis of cortactin and HS1: The significance of the F-actin binding repeat domain. *BMC Genomics* **6**, 1–14 (2005).
226. Ozawa, K., Kashiwada, K., Takahashi, M. & Sobue, K. Translocation of Cortactin (p80/85) to the Actin-Based Cytoskeleton during Thrombin Receptor-Mediated Platelet Activation. *Exp. Cell Res.* (1995) doi:10.1006/excr.1995.1367.
227. Messaoudi, K. *et al.* Critical role of the HDAC6-cortactin axis in human megakaryocyte maturation leading to a proplatelet-formation defect. *Nat. Commun.* (2017) doi:10.1038/s41467-017-01690-2.
228. Chou, H. C. *et al.* WIP Regulates the Stability and Localization of WASP to Podosomes in Migrating Dendritic Cells. *Curr. Biol.* (2006) doi:10.1016/j.cub.2006.10.037.
229. Van Audenhove, I., Debeuf, N., Boucherie, C. & Gettemans, J. Fascin actin bundling controls podosome turnover and disassembly while cortactin is involved in podosome assembly by its SH3 domain in THP-1 macrophages and dendritic cells. *Biochim. Biophys. Acta - Mol. Cell Res.* (2015) doi:10.1016/j.bbamcr.2015.01.003.
230. Yan, B. *et al.* Histone deacetylase 6 modulates macrophage infiltration during inflammation. *Theranostics* (2018) doi:10.7150/thno.25317.
231. Gattazzo, C. *et al.* Cortactin, another player in the Lyn signaling pathway, is over-expressed and alternatively spliced in leukemic cells from patients with B-cell chronic lymphocytic leukemia. *Haematologica* **99**, 1069–1077 (2014).
232. Passaro, D. *et al.* CXCR4 Is Required for Leukemia-Initiating Cell Activity in T Cell Acute Lymphoblastic Leukemia. *Cancer Cell* **27**, 769–779 (2015).
233. Velázquez-Avila, M. *et al.* High cortactin expression in B-cell acute lymphoblastic leukemia is associated with increased transendothelial migration and bone marrow relapse. *Leukemia* (2018) doi:10.1038/s41375-018-0333-4.
234. Martini, V. *et al.* Cortactin, a Lyn substrate, is a checkpoint molecule at the intersection of BCR and CXCR4 signalling pathway in chronic lymphocytic leukaemia cells. *Br. J. Haematol.* **178**, 81–93 (2017).
235. Taniuchi, I. *et al.* Antigen-receptor induced clonal expansion and deletion of lymphocytes are impaired in mice lacking HS1 protein, a substrate of the antigen-receptor-coupled tyrosine kinases. *EMBO J.* (1995) doi:10.1002/j.1460-2075.1995.tb00036.x.
236. Carrizosa, E. *et al.* Hematopoietic lineage cell-specific protein 1 is recruited to the immunological synapse by IL-2-inducible T cell kinase and regulates phospholipase C γ 1 Microcluster dynamics during T cell spreading. *J. Immunol.* **183**, 7352–7361 (2009).
237. Fung-Leung, W.-P. *et al.* T Cell Subset and Stimulation Strength-Dependent Modulation of T Cell Activation by Kv1.3 Blockers. (2017) doi:10.1371/journal.pone.0170102.
238. DeCoursey, T. E., Chandy, K. G., Gupta, S. & Cahalan, M. D. Voltage-gated K⁺ channels in human T

- lymphocytes: a role in mitogenesis? *Nature* **307**, 465–468 (1984).
239. Lin, C. S. *et al.* Voltage-gated potassium channels regulate calcium-dependent pathways involved in human T lymphocyte activation. *J. Exp. Med.* **177**, 637–645 (1993).
240. Hajdu, P. *et al.* The C-terminus SH3-binding domain of Kv1.3 is required for the actin-mediated immobilization of the channel via cortactin. *Mol. Biol. Cell* **26**, 1640–1651 (2015).
241. Lettau, M., Kabelitz, D. & Janssen, O. SDF1 α -induced interaction of the adapter proteins Nck and HS1 facilitates actin polymerization and migration in T cells. *Eur. J. Immunol.* **45**, 551–561 (2015).
242. Martinez-Quiles, N., Ho, H.-Y. H., Kirschner, M. W., Ramesh, N. & Geha, R. S. Erk/Src Phosphorylation of Cortactin Acts as a Switch On-Switch Off Mechanism That Controls Its Ability To Activate N-WASP. *Mol. Cell. Biol.* (2004) doi:10.1128/MCB.24.12.5269-5280.2004.
243. Deng, X. *et al.* Wnt 5a and CCL25 promote adult T-cell acute lymphoblastic leukemia cell migration, invasion and metastasis. *Oncotarget* **8**, 39033–39047 (2017).
244. Coustan-Smith, E. *et al.* Early T-Cell Precursor Leukemia: A Subtype of Very High-Risk Acute Lymphoblastic Leukemia Identified in Two Independent Cohorts. *Lancet The* **10**, 147–156 (2010).
245. Goldberg, J. M. *et al.* Childhood T-cell acute lymphoblastic leukemia: The Dana-Farber Cancer Institute Acute Lymphoblastic Leukemia Consortium experience. *J. Clin. Oncol.* **21**, 3616–3622 (2003).
246. Attarbaschi, A. *et al.* Mediastinal mass in childhood T-cell acute lymphoblastic leukemia: Significance and therapy response. *Med. Pediatr. Oncol.* **39**, 558–565 (2002).
247. Tremblay, M., Tremblay, C. S., Herblot, S., Tremblay, S. & Aplan, P. D. Modeling T-cell acute lymphoblastic leukemia induced by the SCL Modeling T-cell acute lymphoblastic leukemia induced by the SCL and LMO1 oncogenes. *Genes Dev.* 1093–1105 (2010) doi:10.1101/gad.1897910.
248. Pear, W. S. Exclusive development of T cell neoplasms in mice transplanted with bone marrow expressing activated Notch alleles. *J. Exp. Med.* **183**, 2283–2291 (1996).
249. Girardi, T., Vicente, C., Cools, J. & Keersmaecker, K. De. Europe PMC Funders Group The genetics and molecular biology of T-ALL. **129**, 1113–1123 (2017).
250. Van Vlierberghe, P., Ferrando, A., Vlierberghe, P. Van & Ferrando, A. The molecular es basis of T cell acute lymphoblastic leukemia. *J. Clin. Invest.* (2012) doi:10.1172/JCI61269.3398.
251. Trinquand, A. *et al.* Toward a NOTCH1/FBXW7/RAS/PTEN-based oncogenetic risk classification of adult T-Cell acute lymphoblastic leukemia: A group for research in adult acute lymphoblastic leukemia study. *J. Clin. Oncol.* **31**, 4333–4342 (2013).
252. Belver, L. & Ferrando, A. The genetics and mechanisms of T cell acute lymphoblastic leukaemia. *Nat. Rev. Cancer* **16**, 494–507 (2016).
253. Padi, S. K. R. *et al.* Targeting the PIM protein kinases for the treatment of a T-cell acute lymphoblastic leukemia subset. *Oncotarget* **8**, 30199–30216 (2017).
254. Jost, T. R. *et al.* Role of CXCR4-mediated bone marrow colonization in CNS infiltration by T cell acute lymphoblastic leukemia. *J. Leukoc. Biol.* **99**, 1077–1087 (2016).
255. Hashiguchi, T. *et al.* Adult T-cell leukemia (ATL) cells which express neural cell adhesion molecule (NCAM) and infiltrate into the central nervous system. *Intern. Med.* **41**, 34–38 (2002).
256. Ishikawa, T. *et al.* E-selectin and vascular cell adhesion molecule-1 mediate adult T-cell leukemia cell adhesion to endothelial cells. *Blood* **82**, 1590–1598 (1993).
257. Pitt, L. A. *et al.* CXCL12-Producing Vascular Endothelial Niches Control Acute T Cell Leukemia Maintenance. *Cancer Cell* **27**, 755–768 (2015).
258. Alsadeq, A. *et al.* The role of ZAP70 kinase in acute lymphoblastic leukemia infiltration into the central nervous system. *Haematologica* **102**, 346–355 (2017).
259. Melo, R. D. C. C. *et al.* CXCR7 is highly expressed in acute lymphoblastic leukemia and potentiates CXCR4 response to CXCL12. *PLoS One* **9**, 1–12 (2014).
260. Buonamici, S. *et al.* CCR7 signalling as an essential regulator of CNS infiltration in T-cell leukaemia. *Nature* **459**, 1000–1004 (2009).
261. Wang, H. *et al.* ZAP-70: an essential kinase in T-cell signaling. *Cold Spring Harbor perspectives in biology* (2010) doi:10.1101/cshperspect.a002279.
262. Medyouf, H. *et al.* Targeting calcineurin activation as a therapeutic strategy for T-cell acute lymphoblastic leukemia. *Nat. Med.* **13**, 736–741 (2007).
263. Pham, L. V., Tamayo, A. T., Yoshimura, L. C., Lin-Lee, Y. C. & Ford, R. J. Constitutive NF-kappaB and NFAT activation in aggressive B-cell lymphomas synergistically activates the CD154 gene and maintains lymphoma cell survival. *Blood* **106**, 3940–3947 (2005).

264. Marafiot, T. *et al.* The NFATc1 transcription factor is widely expressed in white cells and translocates from the cytoplasm to the nucleus in a subset of human lymphomas. *Br. J. Haematol.* **128**, 333–342 (2005).
265. Akimzhanov, A. *et al.* Epigenetic changes and suppression of the nuclear factor of activated T cell 1 (NFATC1) promoter in human lymphomas with defects in immunoreceptor signaling. *Am. J. Pathol.* **172**, 215–224 (2008).
266. Müller, M. R. & Rao, A. NFAT, immunity and cancer: a transcription factor comes of age. *Nat. Rev. Immunol.* **10**, 645–656 (2010).
267. Neilson, J. R., Winslow, M. M., Hur, E. M. & Crabtree, G. R. Calcineurin B1 is essential for positive but not negative selection during thymocyte development. *Immunity* **20**, 255–266 (2004).
268. Gachet, S. *et al.* Leukemia-initiating cell activity requires calcineurin in T-cell acute lymphoblastic leukemia. *Leukemia* **27**, 2289–2300 (2013).
269. MacGrath, S. M. & Koleske, A. J. Cortactin in cell migration and cancer at a glance. *J. Cell Sci.* **125**, 1621–1626 (2012).
270. de Bock, C. E. & Cools, J. T-ALL: Home Is where the CXCL12 Is. *Cancer Cell* **27**, 745–746 (2015).
271. de Barros, A. P. D. N. *et al.* Osteoblasts and Bone Marrow Mesenchymal Stromal Cells Control Hematopoietic Stem Cell Migration and Proliferation in 3D In Vitro Model. *PLoS One* **5**, e9093 (2010).
272. Schnour, M. *et al.* Cortactin deficiency is associated with reduced neutrophil recruitment but increased vascular permeability in vivo. *J. Exp. Med.* (2011) doi:10.1084/jem.20101920.
273. Sosa-Costa, A. *et al.* Lateral mobility and nanoscale spatial arrangement of chemokine-activated $\alpha 4 \beta 1$ integrins on T cells. *J. Biol. Chem.* **291**, 21053–21062 (2016).
274. Singh, V., Erb, U. & Zöller, M. Cooperativity of CD44 and CD49d in leukemia cell homing, migration, and survival offers a means for therapeutic attack. *J. Immunol.* **191**, 5304–5316 (2013).
275. Soodgupta, D. *et al.* Ex Vivo and In Vivo Evaluation of Overexpressed VLA-4 in Multiple Myeloma Using LLP2A Imaging Agents. *J. Nucl. Med.* **57**, 640–645 (2016).
276. Shalapour, S. *et al.* High VLA-4 expression is associated with adverse outcome and distinct gene expression changes in childhood B-cell precursor acute lymphoblastic leukemia at first relapse. *Haematologica* **96**, 1627–1635 (2011).
277. Berrazouane, S., Doucet, A., Boisvert, M., Barabé, F. & Aoudjit, F. VLA-4 Induces Chemoresistance of T Cell Acute Lymphoblastic Leukemia Cells via PYK2-Mediated Drug Efflux. *Cancers (Basel)*. **13**, (2021).
278. Kumar, A. *et al.* CXCR4 Physically Associates with the T Cell Receptor to Signal in T Cells. *Immunity* **25**, 213–224 (2006).
279. Müller, A. *et al.* Involvement of chemokine receptors in breast cancer metastasis. *Nature* **410**, 50–56 (2001).
280. Ai, W., Li, H., Song, N., Li, L. & Chen, H. Optimal Method to Stimulate Cytokine Production and Its Use in Immunotoxicity Assessment. *Int. J. Environ. Res. Public Health* **10**, 3834 (2013).
281. Sawabe, T. *et al.* Aberrant HS1 molecule in a patient with systemic lupus erythematosus. *Genes Immun.* **4**, 122–131 (2003).
282. Ledderose, C., Bromberger, S., Slubowski, C. J., Sueyoshi, K. & Junger, W. G. Frontline Science: P2Y11 receptors support T cell activation by directing mitochondrial trafficking to the immune synapse. *J. Leukoc. Biol.* **109**, 497–508 (2021).
283. Ryser, J. E., Rungger-Brändle, E., Chaponnier, C., Gabbiani, G. & Vassalli, P. The area of attachment of cytotoxic T lymphocytes to their target cells shows high motility and polarization of actin, but not myosin. *J. Immunol.* **128**, (1982).
284. Williams, B. L. *et al.* Phosphorylation of Tyr319 in ZAP-70 is required for T-cell antigen receptor-dependent phospholipase C-gamma1 and Ras activation. *EMBO J.* **18**, 1832 (1999).
285. Adachi, K. & Davisa, M. M. T-cell receptor ligation induces distinct signaling pathways in naive vs. antigen-experienced T cells. *Proc. Natl. Acad. Sci. U. S. A.* **108**, 1549–1554 (2011).
286. Khalaf, H., Jass, J. & Olsson, P. E. Differential cytokine regulation by NF-kappaB and AP-1 in Jurkat T-cells. *BMC Immunol.* **11**, (2010).
287. Poltorak, M. *et al.* TCR activation kinetics and feedback regulation in primary human T cells. *Cell Commun. Signal.* **11**, (2013).
288. Gaffen, S. L. & Liu, K. D. Overview of interleukin-2 function, production and clinical applications. *Cytokine* **28**, 109–123 (2004).
289. Lenardo, M. *et al.* Mature T lymphocyte apoptosis--immune regulation in a dynamic and unpredictable antigenic environment. *Annu. Rev. Immunol.* **17**, 221–253 (1999).
290. Thelen, M. Dancing to the tune of chemokines. *Nat. Immunol.* **2**, 129–134 (2001).

291. Suzuki, Y., Rahman, M. & Mitsuya, H. Diverse transcriptional response of CD4+ T cells to stromal cell-derived factor SDF-1: cell survival promotion and priming effects of SDF-1 on CD4+ T cells. *J. Immunol.* **167**, 3064–3073 (2001).
292. Tosello, V. *et al.* Cross-talk between GLI transcription factors and FOXC1 promotes T-cell acute lymphoblastic leukemia dissemination. *Leukemia* **35**, 984–1000 (2021).
293. Kumar, A., Kremer, K. N., Sims, O. L. & Hedin, K. E. Measuring the proximity of T-lymphocyte CXCR4 and TCR by fluorescence resonance energy transfer (FRET). *Methods Enzymol.* **460**, 379–397 (2009).
294. Kremer, K. N. *et al.* TCR-CXCR4 signaling stabilizes cytokine mRNA transcripts via a PREX1-Rac1 pathway: implications for CTCL. *Blood* **130**, 982 (2017).
295. Aref, S., Fawzy, E., Darwish, A., Aref, M. & Agdar, M. Al. Cortactin Expression is a Novel Biomarker for Risk Stratification of T-Cell Acute Lymphoblastic Leukemia. *J. Pediatr. Hematol. Oncol.* **43**, E798–E803 (2021).